Mineral Res. Expl. Bull., 144, 1-22, 2012

GEOCHEMICAL PROPERTIES AND RODINGITIZATION OF DIABASE DYKES CUTTING PERIDOTITES IN YÜKSEKOVA COMPLEX (ÖZALP, VAN - TURKEY)

Kurtuluş GÜNAY*, Ali Rıza ÇOLAKOĞLU** and Üner ÇAKIR***

ABSTRACT.- In this study, the geology of diabase dykes which cut peridotites of Yüksekova Complex (Özalp, Van, Turkey) and the effects of Ca metasomatism that caused the metamorphism of these peridotites were investigated. Within the light of mineralogical and petrographical studies and geochemical data; it was determined that diabase dykes that cut peridotites in Yüksekova Complex had shown rodingitization in various degrees due to Ca metasomatism. Depending on this metasomatism, Ca-Al-Mg rich silicates were formed. The mineralogy of rodingitized dykes with ophitic texture is composed of diopside, plagioclase, hydrogrossularite, chlorite, epidote and in minor amounts phlogopite, prehnite, apatite, calcite, opaque minerals. Metasomatism caused enrichment of Ca and depletion of SiO_2 in whole rock major oxides of dykes in tholeiitic character. So, dykes were divided into three different subgroups. The first group is formed from high grade rodingitized diabase dykes (~38.0–42.0 wt. % in SiO_2; 19.0–26.0 wt. % in CaO). The grade of rodingitization in diabase dykes forming the second group is relatively low (~42.5–43.0 wt. % in SiO_2; 14.5–15.0 wt. % in CaO). However, the effect of rodingitization has not been encountered due to results of both petrographical and geochemical analyses in diabase dykes which form the third group (~47.0–50.0 wt. % in SiO_2; 10.0–12.0 wt. % in CaO). It is considered that in rodingitized dykes of which are enriched by trace and REE (Rare Earth Element) contents, the fluids affecting the metasomatic source have developed as a result of interactions with other rocks which were enriched more in these elements. It is also contemplated that the local geology, tectonical structure of the environment and the heat, oxygen fugacity and chemical composition in fluids which would develop due to those factors are significant in this interaction.

Key words: Diabase dykes, peridotite, Ca-metasomatism, element mobility, Yüksekova Complex.

INTRODUCTION

The major oxide trace and REE (rare earth element) contents of ultramafic and mafic rocks of the oceanic lithosphere supply significant contributions in interpreting the geodynamical environments which these rocks have formed (Pearce et al., 1981; Shervais, 2001; Pearce and Stern, 2006). However, the overthrust of ophiolites onto the continent following the intraoceanic imbrication, overthrust processes and long geological evolution which these had been subjected until they took their recent position caused change over the geochemical compositions of these rocks (Coleman, 1977; Puga et al., 1999; Bach and Klein, 2009; Putnis and Austrheim, 2010).

Rodingitization is another phenomenon that causes the metamorphism of rocks of the oceanic crust. Ca rich fluids coming out of pyroxenes during the serpentinization process of peridotites can not enter the structure of serpentine mineral lattices. So; this metamorphism de-

* Maden Tetkik ve Arama Genel Müdürlüğü, Maden Etüt ve Arama Dairesi, 06800, Çankaya, Ankara, Türkiye.
** Yüzüncü Yıl Üniversitesi, Jeoloji Mühendisliği Bölümü, 65080, Kampüs, Van, Türkiye.
*** Hacettepe Üniversitesi, Jeoloji Mühendisliği Bölümü, 06800, Beytepe, Ankara, Türkiye.

velops by the Ca metasomatism which these fluids have formed together with serpentinites and other contact rocks (Frost and Beard, 2007; Koutsovitis et al., 2008; Austrheim and Prestvik, 2008). Diopside is one of the most significant minerals supplying Ca addition in fluids forming the rodingitization (Coleman, 1967; Frost and Beard, 2007). The presence of diopside, chlorite and hydrogrossularite minerals which can be defined petrographically in basaltic rocks indicate the presence of rodingitization in these rocks (Tisikouras et al., 2009). Silica activities of fluids that have been derived from the serpentinization of calcic pyroxenes to be low is considered as a reason of increasing CaO wt. % versus depleted SiO_2 wt. % (Li et al., 2008; Bach and Klein, 2009).

The effects of metasomatic events and different alteration processes can partially be revealed by the investigation of major oxide, trace element and REE behaviors. In addition, reliable petrological interpretations could only be made by dwelling on elements which have not relatively been affected during all these processes (Floyd and Winchester, 1975; Pearce and Norry, 1979; Wood, 1980; Pearce, 1982).

The purpose of this article is to investigate the geochemical properties of diabase dykes cutting peridotite deposit in ophiolitic slices located Özalp region, Van, Turkey It was also aimed at studying metamorphic processes due to rodingitization and analyzing their effects on rock chemistry comparing with dolerite and rodingite samples of Othrys ophiolite.

GENERAL GEOLOGY

Rock assemblages formed by ophiolite and ophiolitic melanges cover large areas in Anatolia (Figure 1-A). As related with the evolution of Paleotethys and Neotethys Oceans, ophiolites are generally observed in areas associated with suture zones in Anatolia which was formed from a couple of microcontinents and separated by these suture zones at different ages (Şengör and Yılmaz, 1981).

Anatolia was divided into tectonical units in east west directions as related with Tethys evolution. Whilst these tectonical units were defined as Pontides, Sakarya Continent, Anatolide-Tauride Block and Southeast Anatolian Fold Belt by Şengör and Yılmaz (1981), these units were classified by Okan and Tüysüz (1999) as Pontides, Anatolide-Tauride Block and as the Kırşehir Massif which is in between them. To which tectonic block the Eastern Anatolia belongs consists of some differences in previous studies. Okan and Tüysüz (1999) included the Eastern Anatolia and the east of Lake Van into Anatolide-Tauride Block. However, Dilek (2008) and Dilek and Furnes (2009) defined the region as Mesozoic continental margin and included it into Pontides. Çakır (2009) claimed the presence of only one Tethys Ocean in Anatolia, interpreted that the south of the Neotethyan suture zone which had passed through the southern boundary of Pontides as Arabian Promontory (this area also covers the Lake Van and its eastern part).

However, Şengör et al. (2003), Keskin (2005) and Şengör et al. (2008) defined the region where our study area is also located in as an “accretional mélange”, as the “East Anatolian Accretional Complex” (EAAC) that developed on the Neotethyan oceanic lithosphere subducting under Eurasian continent towards north in Upper Cretaceous – Oligocene periods. This complex is observed as a belt trending in NW-SE in 150-180 km width. It was also stated that EAAC which reflects the connection of pieces of continental and oceanic crusts between the Arabian and Eurasian plates got into domal shape and elevated 2 km during the collisional stage which started in Mid Eocene and even continues today

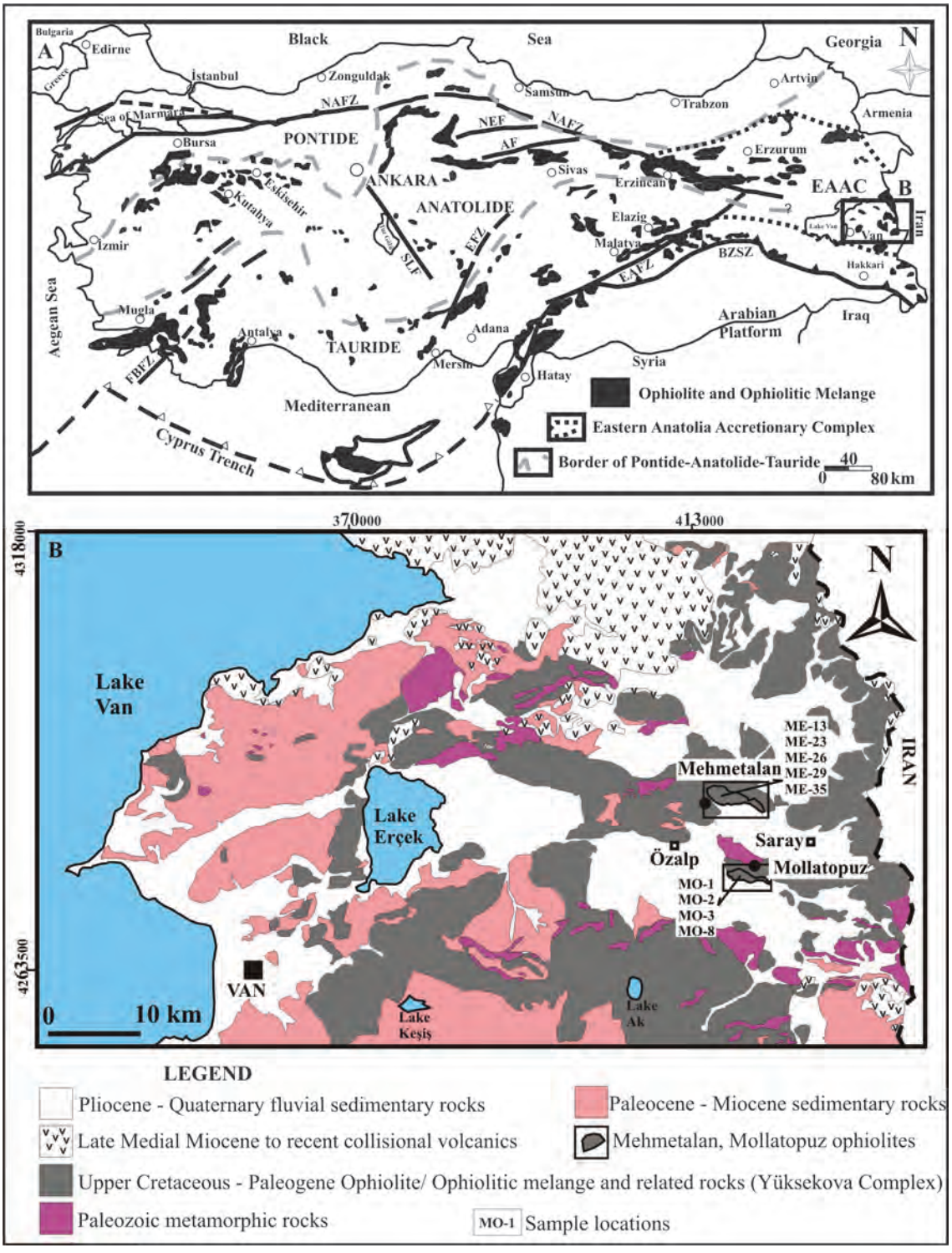

Figure 1- A Distribution of ophiolites in Anatolia (the boundary of tectonic units (Okan and Tüysüz, 1999), the distribution of ophiolites (Uçurum et al., 2006) and the boundary of dyke (Keskin, 2005); B) Geological map of the region between Eastern side of Lake Van and Iranian Border (modified from Şenel, 2002).

(Elitok and Dolmaz, 2007; Yılmaz, 1993; Bozkurt, 2001; Koçyiğit et al., 2001; Barazangi et al., 2006, Şengör et al., 2008).

The south and east of EAAC is covered by ophiolitic units deposited in Late Paleocene aged flyschoidal sequences from Upper Oligocene to Pliocene (Şengör et al. 2003) and by post Oligocene young sediments. Paleozoic aged metamorphic blocks are observed as dispersed and at different positions with these blocks. These metamorphic blocks are assessed as pieces of Anatolide-Tauride microcontinents (Göncüoğlu et al., 1997; Okay and Tüysüz, 1999). It is known that the flysch becomes younger, its surround gets shallower from Cretaceous to Oligocene and Oligocene aged units at north become an unconformable cover going from north to south through complex (Tüysüz and Erler, 1993).

However; volcanic units are observed in north and northeastern parts of the accretional complex. Ophiolitic layers located in EAAC represent pieces of the Neotethyan oceanic lithosphere that lasted from Triassic to Miocene over the region (Şengör and Yılmaz, 1981; Robertson and Dixon, 1984; Ustaömer and Robertson, 1997). Ophiolitic units of the Özalp Region are observed in the form of slices approximately in east-west directions within accretional complex (Figure 1-B). These ophiolitic units are generally represented by peridotite, gabbro and by sporadically cutting rodingitized diabase dykes.

Peridotites represented by tectonitic textured harzburgites in Özalp Ophiolites generally extend in EW directions. Diabase dykes forming the subject of the study are almost fragmented and show an approximate parallelism to the EW extension (Figure 2). Partly preserved dykes which are 1 to 2 meters in thickness and 30 to 40 meters in length are rarely observed over these regions. Isolated diabase dykes are brownish and outer surfaces are pale yellowish at rodingitized sections. These dykes over their broken fresh surfaces are seen in color tones ranging from black to gray and have porphyritic texture (Figure 2a).

Mafic dykes are more resistant than peridotites. During upwelling because of its resistance, these have caused the development of weak zones with accompanying peridotites along the contact. Boudinaged dykes are observed as surrounded by a serpentinized belt which had occasionally reached 1 meter in thickness and developed along weak zones. These dykes have more intensely serpentinized periphery than peridotites that accompany them along boudin axes (Figure 2 b, c). Along these serpentinized belts, foliations which their elongations have approximately developed parallel to the elongation of boudins are seen.

The alteration which was detected petrographically in isolated dykes (uralitization, formation of chlorite, epidote) shows that these overall dykes could be defined as diabase. Rodingitization is more effective in dykes which are observed by its boudinaged structures. These dykes have gained a schistose structure by its yellowish color tone and occasional shearing in them. It is assumed that rodingitized dykes that were situated with peridotite units had gained its boudin structure during internal shear along the period starting from the formation of accretional melange to its recent position (Cawood et al., 2009).

METHOD OF STUDY

Total of 50 samples were collected from dykes observed in ophiolitic slices cropping out at northeast and southeast of Özalp County located at east of Lake Van. After these samples had petrographically been studied, 9 thin sections were prepared to perform geochemical analyses in the Thin Section Laboratory of the Geological Engineering Department at Yüzüncü Yıl University in Van, Turkey. Major oxide, trace element and REE contents of samples prepared

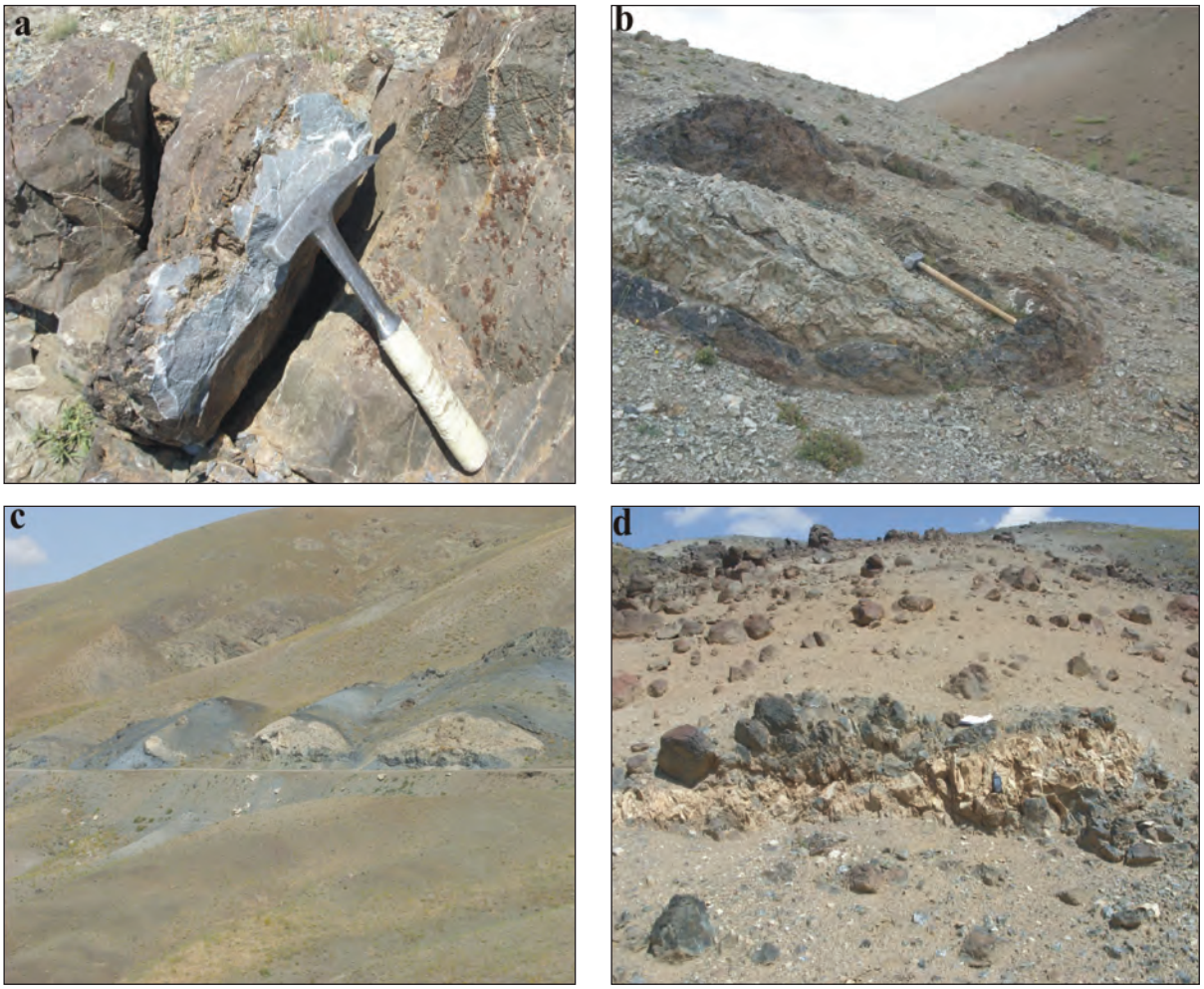

Figure 2- a) A view from fresh diabase dyke surfaces, b) diabase dyke observed in a folded structure, c) a view from diabase dykes that have gained boudin structure, d) a view of rodingitized linear diabase dyke.

were analyzed by ICP – AES / ICP – MS (Inductively Coupled Plasma – Atomic Emission Spectrometry / Mass Spectrometry) methods at ALS laboratories in Canada. In order to confirm some mineral assemblages defined at petrographical studies, XRD (X-Ray Diffraction) and mineral description analyses were also carried out for samples MO-1 and ME-23 in MTA (General Directorate of Mineral Research and Exploration) in Ankara, Turkey.

PETROGRAPHY AND MINERALOGY

Diabase dykes cutting peridotites were partially rodingitized by Ca metasomatism in ophiolitic slices of the Özalp region (Figure 3, a, b). These mafic dykes typically exhibit ophitic texture in thin sections. The rock is mainly composed of uralitized clinopyroxene (diopside), plagioclase, garnet (hydrogarnet), chlorite, epidote, phlogopite, apatite, calcite and of opaque minerals. Although most of dykes are seen as rodingitized in thin sections, partly fresh dolerite dykes were observed as well (Figure 3 c, d).

Pyroxenes among prismatic plagioclase crystals are represented by diopside and augite.

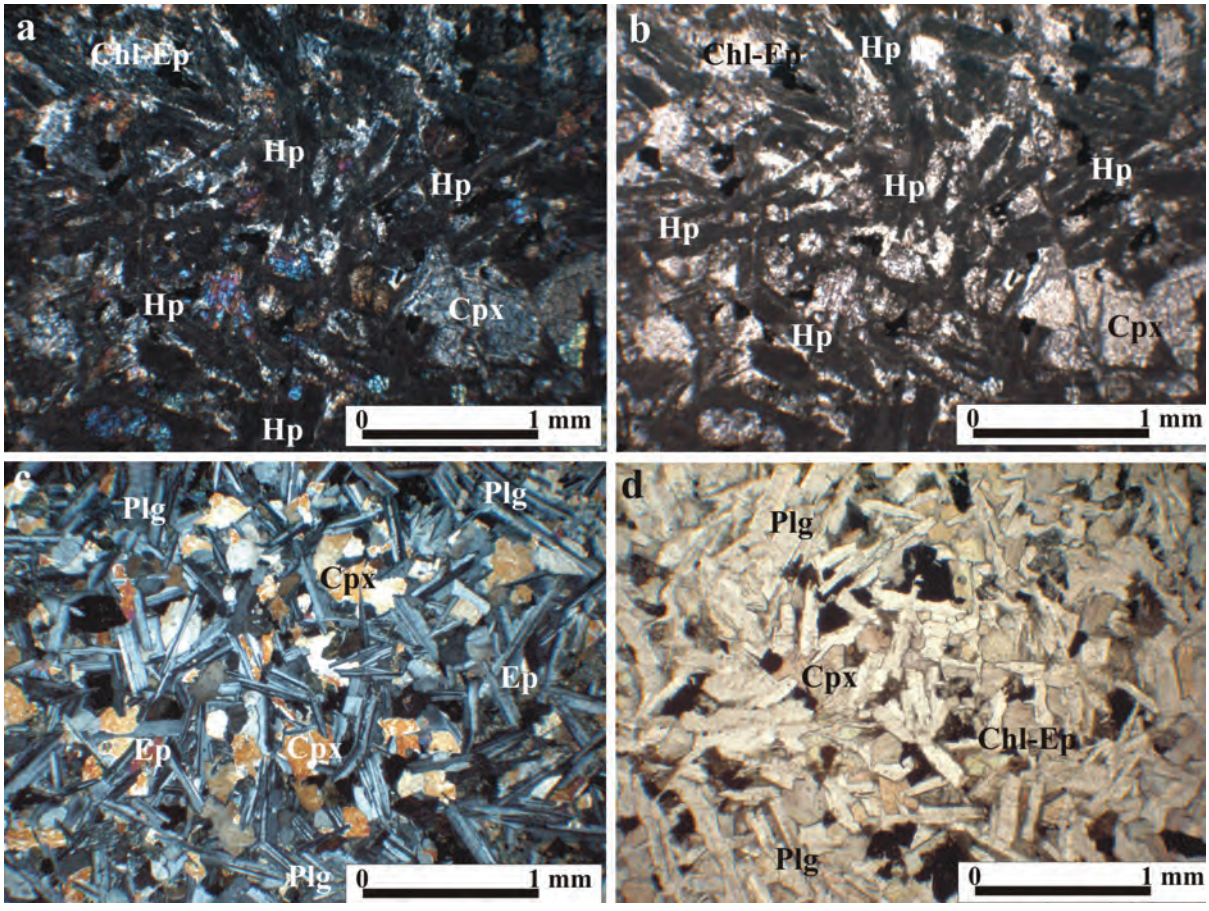

Figure 3- Thin section views of diabase dykes (a, c: crossed nikol; b, d: parallel nikol), (a-b) rodingitized diabase dykes, sample no: ME-23; (c-d) dolerite dyke sample no: MO-8, (Plg: plagioclase, Cpx: Clinopyroxene, Ep: Epidote, Hp: Hydrogrossularite, Chl-Ep: Chlorite-Epidote).

Uralitization and chloritization were frequently encountered in pyroxene phenocrystals. Hydrogarnet and sericite being formed from plagioclases form the most frequently observed metasomatism and alteration minerals. Subhedral opaque minerals were detected in all thin sections in addition to apatites found as accessory mineral. The assemblage of calcite, titanite, actinolite, chlorite and epidote which were especially observed in some thin sections are seen as an indicator of low grade hydrothermal alteration within greenschist facies (Elthon, 1979; Spear, 1981). Petrographical observations indicate that rodingitization periods developed on dykes could be classified according to the relative abundance of hydrogrossularite in thin sections.

Petrographically defined diopside, chlorite and hydrogrossularite mineral assemblages in dykes of Özalp ophiolites indicate the petrographical data of rodintigization in these dykes (Tisikouras et al., 2009). The presence of this mineral assemblage detected in petrographical studies was also verified by XRD analyses (Figure 4).

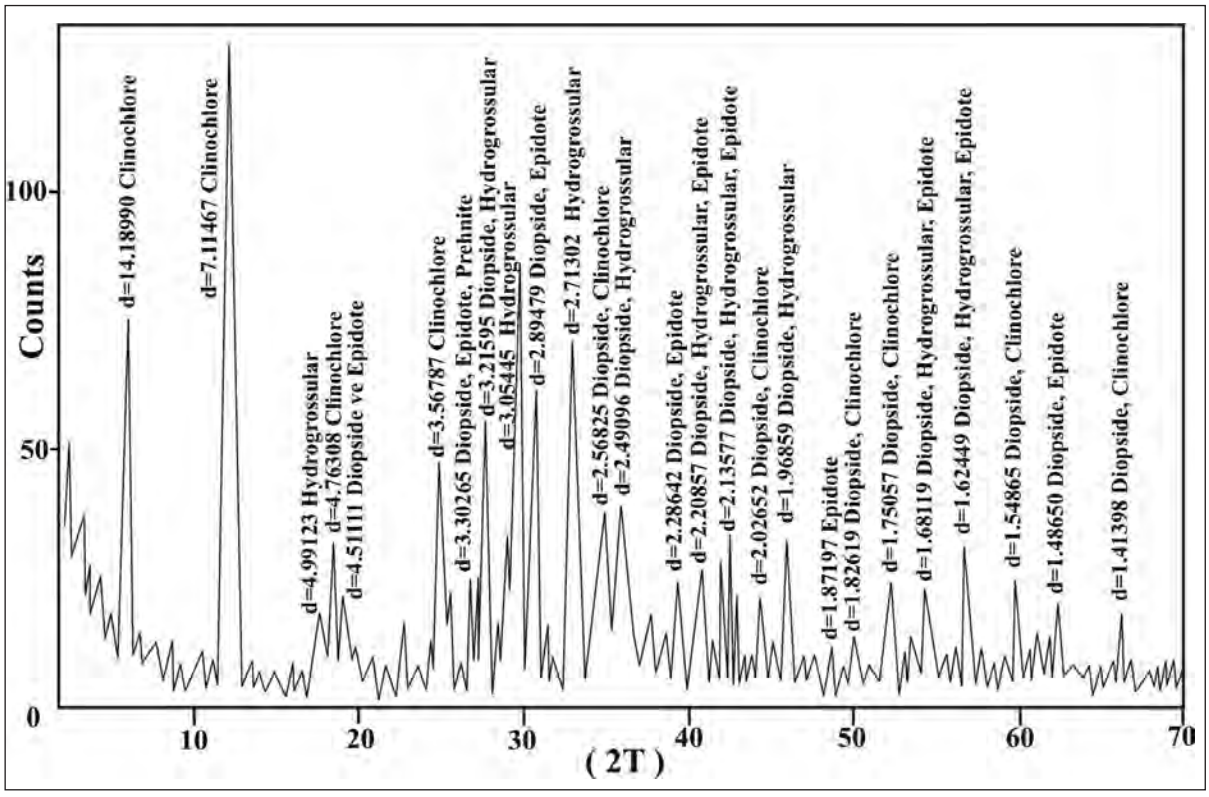

Figure 4- Simplified XRD chart of the rodingitized sample MO-1.

GEOCHEMISTRY

Results of major oxide, trace and REE analyses of dyke samples taken from Özalp ophiolites are given in table 1. In addition to samples which the effect of alteration was intensely observed, ME-29 from Mehmetalan field and MO-8 from Mollatopuz field showed an alteration effect at a lower grade than other samples. Weight loss values due to heat in these samples are 2.5 and 3.46 wt. % for ME-29 and MO-8, respectively. Weight loss values due to heat of the other samples vary between 4.25 – 6.34 wt. %. Generally; these heat weight loss values are the indicator of low grade hydrothermal alteration.

For the geochemical classification of these dykes the elements which are considered as unaffected were relatively used, because of the alteration effect detected in petrographical studies (Figure 5). Dolerite and rodingite samples of the Otrhys ophiolite seen in diagrams were used in order to emphasize on the similarities of major geochemical characteristics with the samples used in this study. Dykes fall into subalkaline basalt field in Zr/TiO_2*0.0001 vs Nb/Y diagram (Winchester and Floyd, 1977), which is reliably used in the classification of basaltic rocks that affected from alteration (Figure 5a).

Tholeiitic basalts are distinguished from alkaline basalts with their relatively low P_2O_5 content (Winchester and Floyd, 1977). Tholeiitic and alkaline basalts which exhibit the behavior of an incompatible element in magmatic differentiation

Table 1- Geochemical analysis results of dykes in Mehmetalan and Mollatopuz fields. HGRD- high grade rodingitized diabase dykes, LGRD- low grade rodingitized diabase dykes, DD- unrodingitized diabase dykes. Major and trace elements are in % and ppm, re spectively (Othrys dolerite and rodingite samples were taken from Koutsovisit et al., 2008; Tsikouras et al., 2009).

	Diabase and rodingite in the study									Dolerite and rodingite of Othrys ophiolite						
	HGRD					LGRD		DD		Dolerit			Rodenjit			
	ME-13	ME-23	MO-1	MO-2	MO-3	ME-26	ME-35	MO-8	ME-29	OD-1	OD-2	OMD-1	OR-1	OR-2	OR-3	OR-4
SiO_2	38,2	39	37,9	39,1	41,8	42,5	43,1	49,6	47,1	59,17	58,78	53,91	41,49	39,59	38,94	38,89
Al_2O_3	12,75	14,75	13,7	13,1	13,25	17,65	15,3	14,55	15,05	14,81	14,68	15,41	10,68	10,89	12,81	17,27
Fe_2O_3	9,01	9,18	8,95	9,53	9,7	8,09	9,25	10,8	11,8	10,47	9,3	8,32	7,41	10,73	9	9,62
CaO	19,3	20,2	24,8	23,2	20,4	15,05	14,6	11,6	10,2	8,46	8,01	5,74	19,53	17,21	21,93	16,38
MgO	9,03	8,5	6,19	6,43	6,2	8,36	9,13	5,34	6,98	3,35	3,73	8,13	16,22	14,73	11,19	11,52
Na_2O	3,1	1,89	1,62	1,74	2,04	2,56	2,63	2,85	3,78	1,54	2,14	5,23	0,01	0,11	0,09	0,03
K_2O	0,01	0,02	0,02	0,04	0,1	0,18	0,29	0,93	0,45	0,1	0,2	0,05	0,04	0,04		
TiO_2	0,87	0,91	1,03	1,12	1,16	0,75	0,9	0,59	1,41	0,48	0,46	0,26	0,23	1,16	0,92	0,46
MnO	0,15	0,16	0,15	0,16	0,17	0,14	0,16	0,16	0,2	0,13	0,14	0,17	0,17	0,31	0,27	0,23
P_2O_5	0,07	0,09	0,09	0,11	0,1	0,07	0,09	0,04	0,14	0,05	0,04	0,02	0,02	0,06	0,05	0,03
LOI	6,34	5,51	5,52	5,53	4,86	4,25	4,66	3,46	2,5	0,79	2,48	2,8	5,1	5,13	4,72	5,8
Total	98,9	100,5	100	100	100	99,8	101	100,5	99,8	99,35	99,96	100	100,89	100,01	99,92	100,23
Co	46,6	44,7	36,4	38,6	37,7	43,5	47,5	37,5	45,6	30	27			53	39	
Cr	420	370	210	220	200	350	400	70	190	30	20	84	1528	600	420	312
Ni	196	165	90	94	81	169	192	42	80	20	30	47	459	220	150	84
Ba	20,8	27,6	16,7	31,4	66,1	747	1135	70	689	9	16	4,5	15,1			6
Rb	1,2	1,5	0,5	1,6	2,7	3,6	6,9	11,6	9,4		4					
Sr	204	181	142,5	614	2610	579	520	270	424	78	139	157,2	3,4			20,5
Th	0,4	0,43	0,47	0,5	0,54	0,39	0,43	0,32	0,88	0,36	0,39	0,3		0,08	0,06	
Ta	0,1	0,2	0,2	0,2	0,2	0,1	0,1	0,1	0,3	0,06	0,05	0,1		0,04		0,1
Nb	2,6	2,7	3,2	3,5	3,7	2,2	2,7	1,9	4,8	1	0,9			0,6	0,5	1
Hf	1,6	1,7	1,9	2	2,2	1,4	1,7	1	2,7	0,8	0,8			1,7	1,4	0,7
Y	20,9	21,8	23,7	25,3	26,8	17,9	21,9	17,6	32,8	12	13,5	5,8	8,3	28,3	24,1	11
Zr	57	59	65	71	74	48	59	29	97	19	22	6,9	6,1	41	35	18,1
La	4,3	4,4	4,8	5,2	5,4	4,5	4,6	2,6	7,7	1,41	1,53	0,7	0,6	1,18	1,05	0,8
Ce	10,4	10,8	11,7	12,6	13,3	10,4	11	5,7	18,4	3,52	3,84	1,8	0,7	4,23	3,75	2
Pr	1,46	1,51	1,63	1,74	1,84	1,37	1,53	0,75	2,56	0,47	0,51	0,2	0,12	0,85	0,75	0,32
Nd	7,2	7,6	8,2	8,7	9,3	7	7,8	4	12,5	2,52	2,73	1,1	0,6	5,79	5,1	2
Sm	2,33	2,42	2,73	2,75	2,96	2,08	2,39	1,33	3,78	0,81	0,92	0,2	0,3	2,41	2,13	0,8
Eu	0,95	0,95	1,09	1,07	1,15	0,85	1,01	0,56	1,47	0,371	0,402	0,15	0,1	2,19	3,45	0,26
Gd	2,85	2,92	3,17	3,37	3,59	2,56	3	1,87	4,51	1,24	1,37	0,6	0,75	3,55	3,08	1,22
Tb	0,52	0,54	0,6	0,62	0,67	0,47	0,55	0,39	0,85	0,27	0,3	0,12	0,18	0,75	0,63	0,27
Dy	3,46	3,64	3,95	4,12	4,41	3,01	3,63	2,73	5,46	1,92	2,23	0,92	1,21	4,92	4,1	1,74
Ho	0,77	0,83	0,88	0,94	0,98	0,65	0,82	0,63	1,23	0,43	0,47	0,19	0,28	0,99	0,84	0,39
Er	2,28	2,43	2,7	2,8	3	2,01	2,42	2,01	3,71	1,4	1,51	0,64	0,94	2,94	2,48	1,21
Tm	0,34	0,37	0,37	0,42	0,42	0,29	0,35	0,31	0,55	0,226	0,239	0,09	0,17	0,433	0,365	0,19
Yb	2,22	2,28	2,51	2,66	2,79	1,86	2,33	2,09	3,55	1,57	1,63	0,77	1,14	2,72	2,33	1,36
Lu	0,33	0,36	0,37	0,42	0,44	0,29	0,36	0,31	0,54	0,262	0,265	0,13	0,16	0,411	0,354	0,22

by these properties can be divided into two different areas with respect to Zr. It is seen that low P_2O_5 (0.04-0.14) contents and diabase dykes of Özalp ophiolite slices fall into the Tholeiitic field (Figure 5 b). It is seen in diagrams that, dolerite and rodingite samples of Otrhys ophiolite are in tholeiitic character.

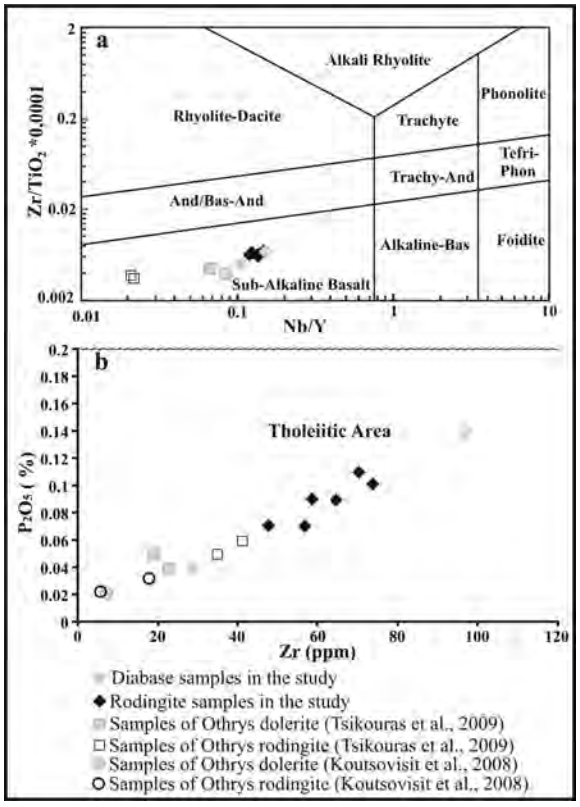

Figure 5- a) Zr/TiO_2 vs Nb/Y classification diagram (Winchester and Floyd, 1977), b) P_2O_5 / Zr classification diagram (Winchester and Floyd, 1976).

DISCUSSION

Dykes which constitute the subject of this study are tholeiitic in character and were divided into three different subgroups according to the results geochemical analyses, also in compliance with petrographical observations. The first group is the "high grade rodingitized diabase dykes" and has 41.8 – 37.9 wt. % SiO_2 and 19.3 – 25.7 wt. % CaO. The second group is the "low grade rodingitized diabase dykes" that has 42.5-43.1 wt. % SiO_2 and 14.55-15.05 wt. % CaO. However, the diabase dykes that have no effect of rodingitization constitute the third group. There was not encountered rodingitization in this group neither in petrographical nor in geochemical analysis results. Although diabase dykes forming this group have 47.1-49.6 wt. %. SiO_2, the weight % values for CaO range in between 10.2 – 11.6. On the ternary diagram, prepared by the correlation of changes on rodingitization duration and major oxide elements, it was seen that the high grade rodingitized samples cumulated in rodingitized areas (Figure 6). Unrodingitized samples cumulate farther from high grade rodingitization field than low grade rodingitized samples.

Rodingites indicate the presence of metasomatic events at low temperatures which were affected by fluids originating from the serpentinization of peridotites (Coleman, 1967; Dubinska, 1995 and 1997; Normand and Williams-Jones, 2007). The effects of these metasomatic events become evident with the enrichment of wt. % in CaO (~25.7) but a depletion in the wt. % in SiO_2 (~37.9) in whole rock geochemistry's. The increase in the CaO ratio in dykes of Özalp ophiolite requires the supply of Ca addition to the source of rodingitization. Fluids at low temperatures resulting with serpentinization are characterized by being alkaline (generally pH > 10) and enriched by Ca (Palandri and Reed, 2004). It is considered that Ca addition to metasomatic source could only be made by the serpentinization of calcic pyroxenes. Diopside is one of the most important minerals that could supply Ca addition to the source of rodintigization (http://webmineral.com/data/Diopside.shtml) with its total oxide ratio [$CaMg(Si_2O_6)$] 25.90 % CaO – 18.61 % MgO and 55.49 % SiO_2 (Coleman, 1967; Austrheim and Prestvik, 2008). Serpentinization process of diopside might occur by the reaction given below by Frost and Beard (2007).

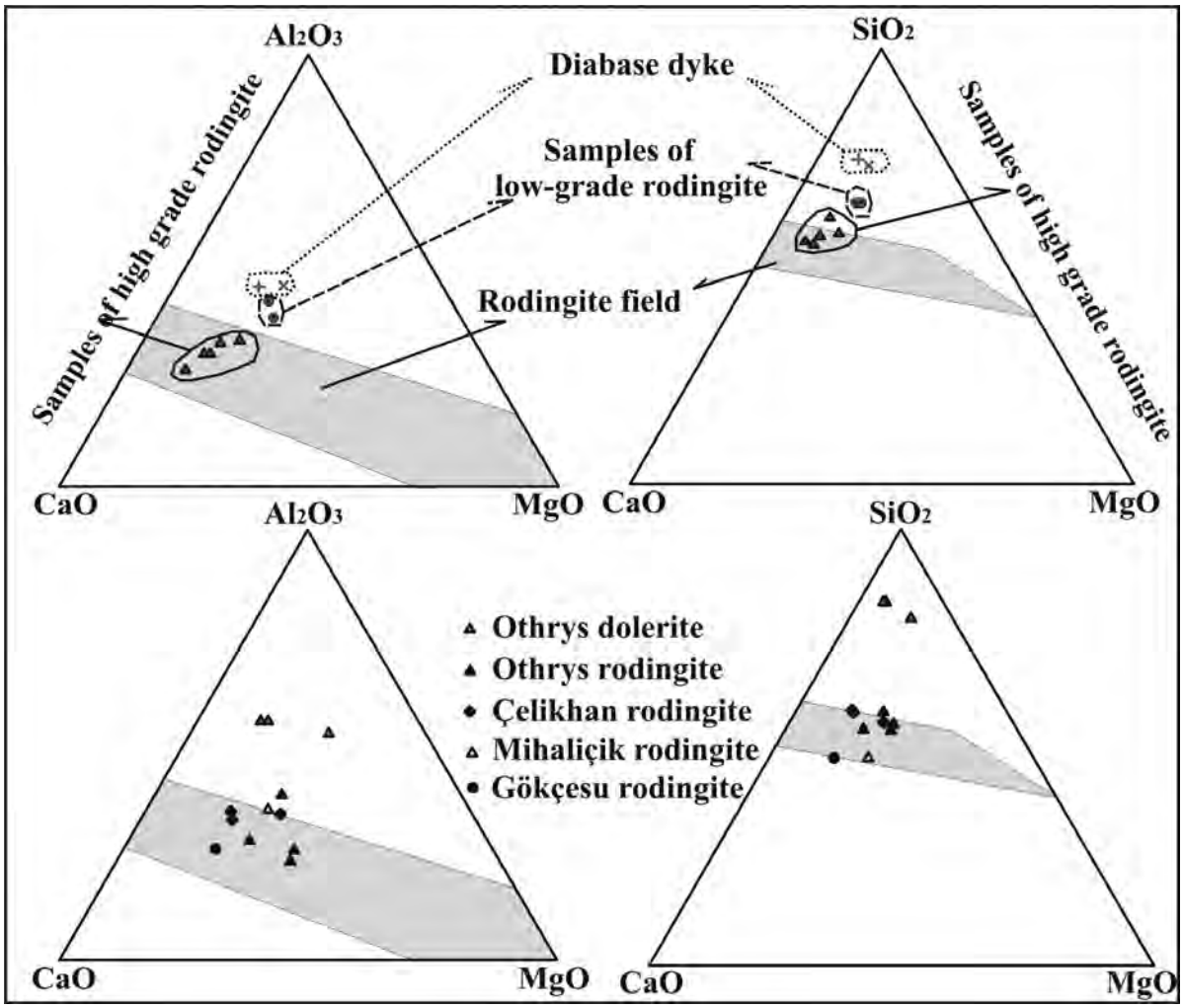

Figure 6- Ternary diagram of major oxides in which rodingitization areas are shown (each areas were taken from different authors as; rodingitization areas (Frost and Beard, 2007); Mihaliçik rodingite samples (Çoğulu and Vuagnat, 1965); Çelikhan rodingite samples (Pişkin, 1975); Gökçesu rodingite samples (Bassaget et al., 1967); Othrys dolerite and rodingite samples (Koutsovisit et al., (2008) and Tsikouras et al., (2009)).

$3CaMgSi_2O_6 + 6H^+ = Mg_3Si_2O_5(OH)_4 + 3Ca^{+2} + H_2O + 4SiO_2(aq)$

Serpentinization and the Ca^+ addition to the source in this equilibrium which developed as a reaction of diopside with H^+ in fluids are clearly seen. Moreover; as the alkalinity increases in fluids along the overall reaction, the silica activity rapidly decreases. One of the significant reactions that decrease the silica activity in fluids is the serpentinization and talc occurrence processes of Mg silicates in these environments (Frost and Beard, 2007). The Ca increase in metasomatic source supplying the rodingitization occurs with the degradation of calcic pyroxenes in serpentinization process. However; silica % values of diabase dykes which rodingitization effects were not observed are higher than low and high grade rodingitized dykes (see Table 1, Figure 7). This phenomenon is the indicator of depleted SiO_2 in the source of rodingitization. The low amount in silica activities of fluids which

derived from the serpentinization of calcic pyroxenes is interpreted as the reason of SiO_2 depletion at the source of rodingitization (Frost and Beard, 2007; Li et al., 2008; Bach and Klein, 2009). Hence; rodingitization phenomenon being realized by the Ca metasomatism in dykes of Özalp ophiolites is verified by CaO enrichment in whole rock geochemistry results. However, this case reveals the reason of the depletion of SiO_2 in dykes.

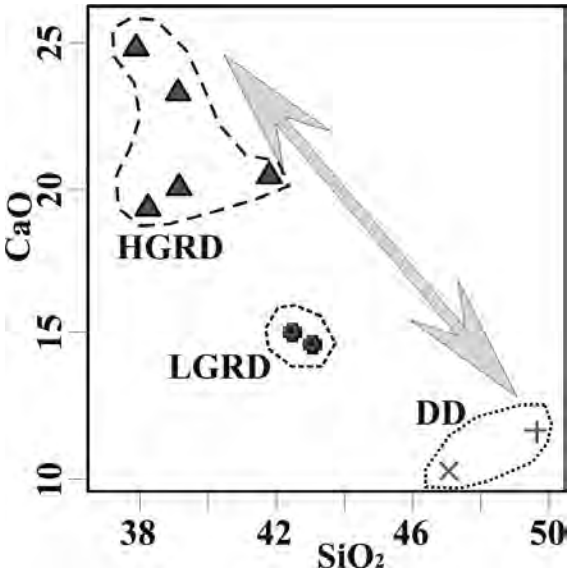

Figure 7- CaO-SiO_2 Harker diagram of the isolated diabase dykes (HGRD: high grade rodingitized dykes; LGRD: low grade rodingitized dykes; DD: unrodingitized diabase dykes).

Hydrogrossularite and chlorite which are the characteristic minerals of rodingites occur as the secondary product due to the reaction of Ca-Mg silicates with calcic plagioclases during reaction processes developed by the effect of fluids over the source of rodingitization. Typical reactions of these processes were explained below by Frost and Beard (2007).

$5CaMgSi_2O_6 + 4CaAl_2Si_2O_8 + 8H_2O = 3Ca_3Al_2Si_3O_{12} + Mg_5Al_2Si_3O_{10}(OH)_8 + 6SiO_2(aq)$

$Ca_3Al_2Si_3O_{12} + 2xH_2O = Ca_3Al_2Si_2O_8(SiO_4)_{(1-x)}(OH)_{4x} + xSiO_2(aq)$

Geochemical properties of samples indicate that all reaction pairs presented within the availability of minerals that developed as a result of rodingitization had occurred in dykes of Özalp ophiolite.

Normalized MORB multi element spider diagrams of isolated dykes were presented in figure 8. In multi element spider diagrams which is prepared by normalizing to MORB, trace element contents of dykes are seen as it had been more enriched with respect to Mid Oceanic Ridge Basalts (MORB) by Large Ion Lithophile (LIL) elements (LIL- Cs, Rb, K, Ba, Sr). As LIL elements show various distributions, the depletion in Nb is encountered despite the enrichment in Th element. However; there is observed parallel but partly depleted distribution to normalized MORB line in High Field Strength (HFS) elements in this diagram (such as; Zr, Sm, Ti, Y, Yb). It is seen that value ranges of diabase and rodingite dykes of Mehmetalan and Mollatopuz show a consistent distribution except for LIL elements. Yet;

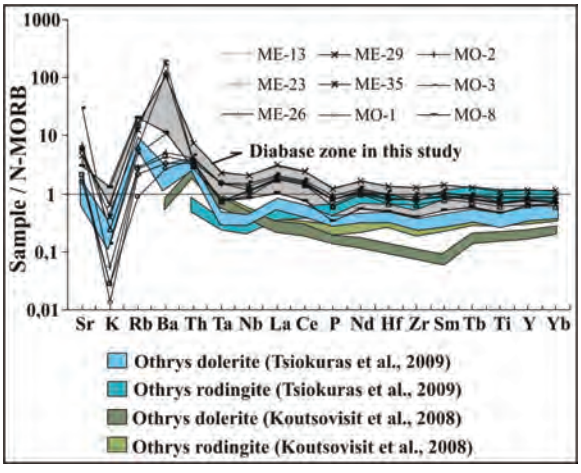

Figure 8- Multi element spider diagrams of isolated dykes normalized to MORB (normalized MORB values were taken from Sun and Mc Donough, 1989).

clear differences are observed among Othrys dolerite and rodingite samples. Despite Th depletion in Othrys rodingites, there is not observed an evident difference in Ta, Nb, La and Ce elements but enrichment in all HFS elements starting from element P. This case is also valid for the other samples taken from various sites of Othrys ophiolite (Koutsovisit et al., 2008).

Element mobility is controlled by mineralogical changes that occur during alterations. It is known that alkali elements have high mobility due to alteration processes. At time of low grade alteration and metamorphism, studies carried out on behavior of elements showed that some of them were depleted or enriched, while of some remained as stable (Cann, 1970; Coish, 1977; Humpris and Thompson, 1978). The irregular distribution of Ba, Sr, Rb, and K elements in the multi element spider diagram (normalized to MORB) of isolated dykes may reflect the effect of alteration and/or metasomatic events. It is also known that these elements are rather mobile under metamorphic conditions due to low ionic potentials (< 3) (Pearce and Cann, 1973; Pearce, 1975, 1982, 1983; Saunders et al., 1980). It is claimed that Th element are stable even under conditions of alteration, sea bottom metamorphism and greenschist metamorphism as it has high ionic potential (3<) (Pearce, 1975, 1983; Wood, 1980). In addition to the decrease from Th to Nb which shows enrichment above the normalized MORB line in isolated dolerite dykes, values beneath the line of normalized MORB in HFS elements might reflect the effect of component of subduction zone (Pearce and Stern, 2006). Ta and Nb in the spider diagram are the elements that have the highest ionic potentials (7). However, it is seen that value ranges of Ta and Nb elements have not been subjected to significant changes in dolerite and rodingite samples. There is observed a significant enrichment from Ce to Yb only in Otrhys rodingites, although they have high ionic potential (3<) compared to dolerites. It is difficult to say that this situation has developed by the effect of alkali fluids only in metasomatic source, since such a case was not observed in rodingite samples during the study. Therefore; it seems probable that the enrichment of the metasomatic source of Otrhys rodingites by fluids interacted with alkaline rocks. There is observed a similarity in REE distribution patterns between the rodingitized diabase dyke samples and unrodingitized dyke samples in REE spider diagram normalized to Chondrite (Figure 9). Especially; a slight enrichment in Light Rare Earth Elements (LREE: La, Ce, Pr, Nd, Pm, Sm) relative to Heavy Rare Earth Elements (HREE: Gd, Tb, Dy, Ho, Er, Tm, Yb, Lu) is one of most important data exhibiting the difference of magmatic source of dykes than MORB in the study. Despite that; it was seen that Otrhys dolerite samples had been enriched by HREE relative to LREE. This situation indicates that Otrhys dolerites could be derived from the partial melting of a MORB source at high temperatures at shallow depths.

Rodingitized samples in REE contents of dykes in this study take place within the value ranges of samples MO-8 and ME-29 which the effect of rodingitization effect was not observed. However, looking at REE distributions of dolerite and rodingite samples taken from different areas of Otrhys ophiolite, it is observed that REE contents of rodingite samples show a more obvious enrichment trend except for La and Ce elements compared to dolerite samples (Koutsuvisit et al., 2008; Tsikouras et al., 2009). Unless fluid/rock ratios of REEs are very high under low grade metamorphic conditions, they are accepted as immobile compared to trace elements (Michard, 1989). In addition to this, much altered rocks which were subjected to high grade metamorphism are not totally immobile, either (Humphries, 1984). The positive Eu anomaly in Otrhys rodingite samples (Tisikouras et al., 2009) indicate the degradation of feldspar minerals enriched by Eu within the presence of early differentiation fluids (Hopf, 1993). According to the results of geo-

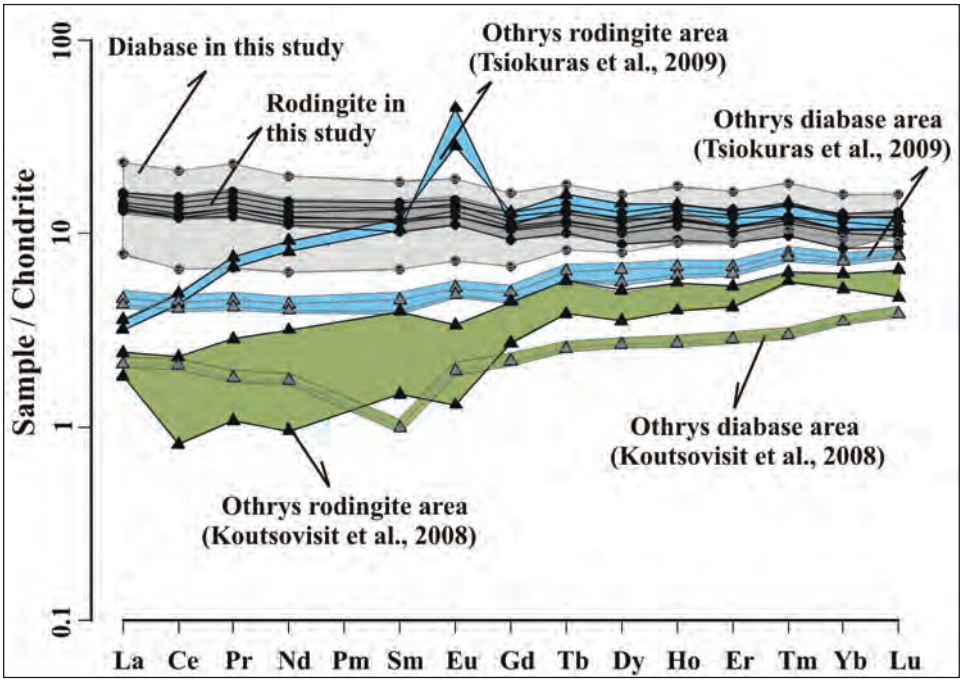

Figure 9- REE diagrams of isolated dykes normalized to Chondrite (REE normalization values were taken from Sun and McDonough (1989)).

chemical analyses, the values of Otrhys dolerites [~59 wt. % SiO_2 - ~8 wt. % CaO - ~3 wt. % MgO - ~14 wt. % Al_2O_3 (Tsiokuras et al., 2009), ~54 wt. % SiO_2 - ~5 wt. % CaO - ~8 wt. % MgO - ~15 w.t. % Al_2O_3 (Koutsovisit et al., 2008)] show differences in terms of SiO_2 according to major oxide values of samples in this study (MO-8, 49 wt. % SiO_2, ME-29, 47 wt. % SiO_2). It can be considered that differences in whole rock chemistry over the source of rodingitization within this value range are effective in post rodingitization REE distributions. However, when rodingitization degree in dykes investigated are generally considered according to SiO_2 and CaO proportions which rodingites contain, REE enrichment at approximate levels in all rodingite samples could be expected to occur. Whereas; REE contents of rodingite samples analyzed in this study exist within value ranges of original rocks. This makes us think that, metasomatic source of Otrhys rodingites were enriched by fluids which was interacted with REE enriched alkaline rocks as it was the same as in REE differentiations.

Positive correlations of elements such as; Zr, Y, Ti, Nb observed in ophiolitic mafic rocks are in compatible with olivine-clinopyroxene-plagioclase fractionation (Pearce and Norry, 1979; Pearce, 1982). This situation enables Zr element to be used as a fractionation index. In trace element Harker diagrams of isolated dykes prepared with respect to Zr show disordered trends. This situation forms an alteration effect free of fractionation. However, it can be said that trace elements that exhibit a linear trend were not affected from alteration and metasomatic events (Figure 10). Indeed; the trace element distributions of dykes which were not affected from Ca metasomatism and rodingitized dykes in these diagrams exhibit the same correlations.

Elements such as Th, Ti, Y, Yb, Nb, La, Ce and Lu are frequently used in petrogenetic interpretations especially for ophiolitic mafic rocks (Pearce and Cann, 1973; Winchester and Floyd, 1976; Pearce and Norry, 1979; Wood, 1980;

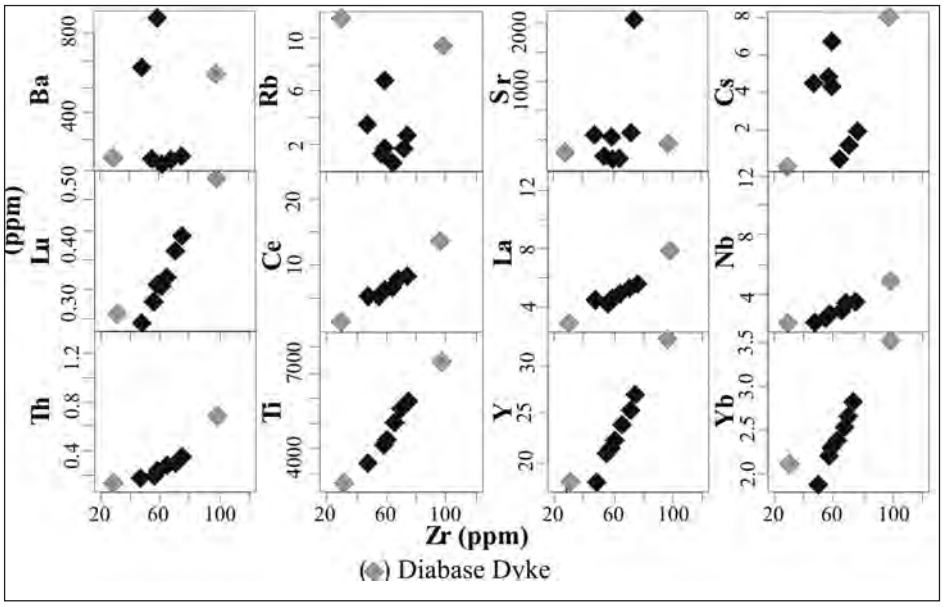

Figure 10- Trace element Harker diagrams prepared with respect to Zr.

Pearce, 1982). It shows that these elements could reliably be used even in the presence of metasomatic effects in dykes of Özalp ophiolites.

The effect of Ca metasomatism on certain major oxide elements were analyzed in the columnar graphic shown in figure 11. The correlations of samples ordered by decreasing SiO_2 values are observed starting from unrodingitized samples in this graph. The determination values (R^2) for SiO_2 (~0.9), CaO (~0.6) and MgO (~0.4) show positive correlations for rodingitization processes. However, R^2 values for Al_2O_3 (~0.05) and Fe_2O_{3T} (~0.07) give quite poor correlations in the graph shown in figure 11. This state might indicate that Al_2O_3 and Fe_2O_{3T} oxides were not relatively affected from rodingitization processes.

It is accepted that transient metals such as Cr, Ni which could enter the lattice of silicate minerals like serpentine and olivine are relatively immobile at low grade alteration (Staudigel et al., 1996). The columnar correlation diagram which was prepared to assess the behaviors of Co element, one of the transient elements together with Cr and Ni, showed that these elements were quite mobile at metasomatic source (Figure 12).

High positive determination coefficient value (R^2) for Cr (~0.9), Ni (~0.9) and Co (~0.6), ranging from samples in which rodingitized were not observed towards rodingitized samples in this diagram indicate that these transient metals were enriched at metasomatic source.

Element mobility in altered rocks with respect to their original rocks could be analyzed by Isocon analysis. Effectively shown method details of element mobility were explained by Grant (1986). Isocon method is the technique which the enrichment or depletion of elements in altered rocks with respect to original rocks could be revealed even at very minor quantitative values. Gain and loss estimations of rodingitized dykes using this method were represented in table 2. Negative values in this table indicate depletion, however positive values indicate enrichment. Average val-

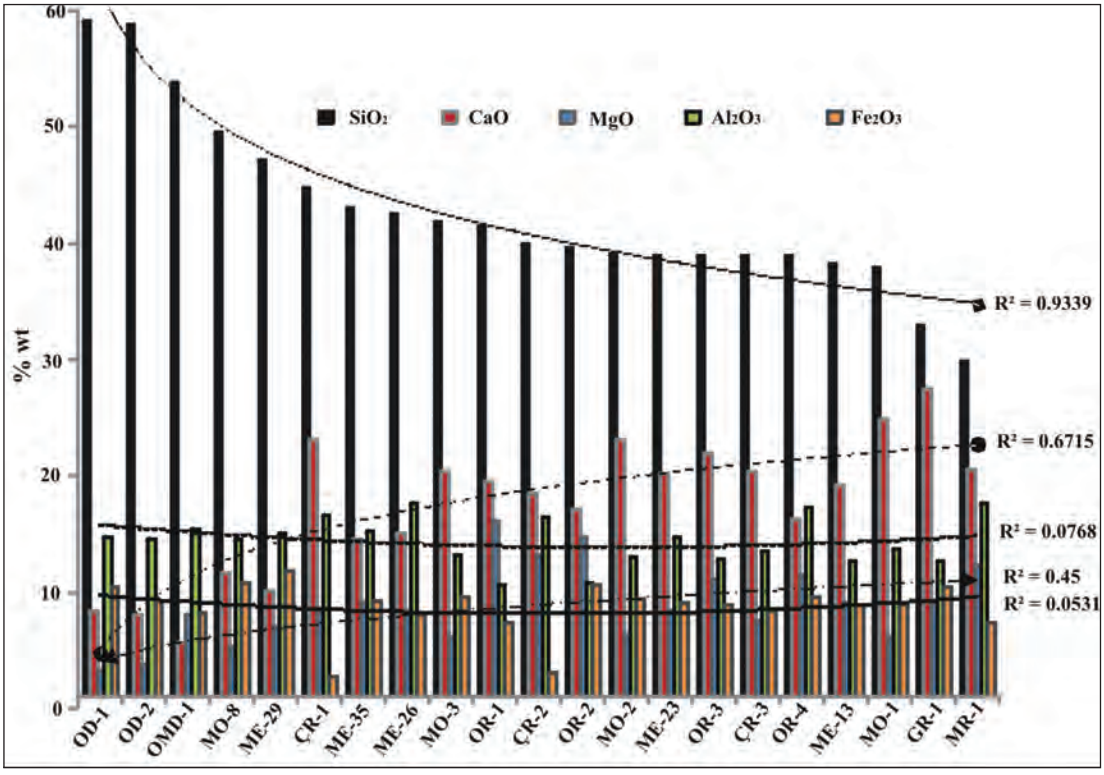

Figure 11- Columnar correlation diagram of major oxide elements. Values of each samples were taken from the related authors (OD-1, OD-2, OR-2, OR-3 (Tsiokuras et al., 2009); OMD-1, OR-1, OR-4 (Koutsovisit et al., 2008); ÇR-1, ÇR-2, ÇR-3 (Pişkin, 1975); GR-1 (Bassaget et al., 1967) and MR-1 (Çoğulu and Vuagnat, 1965).

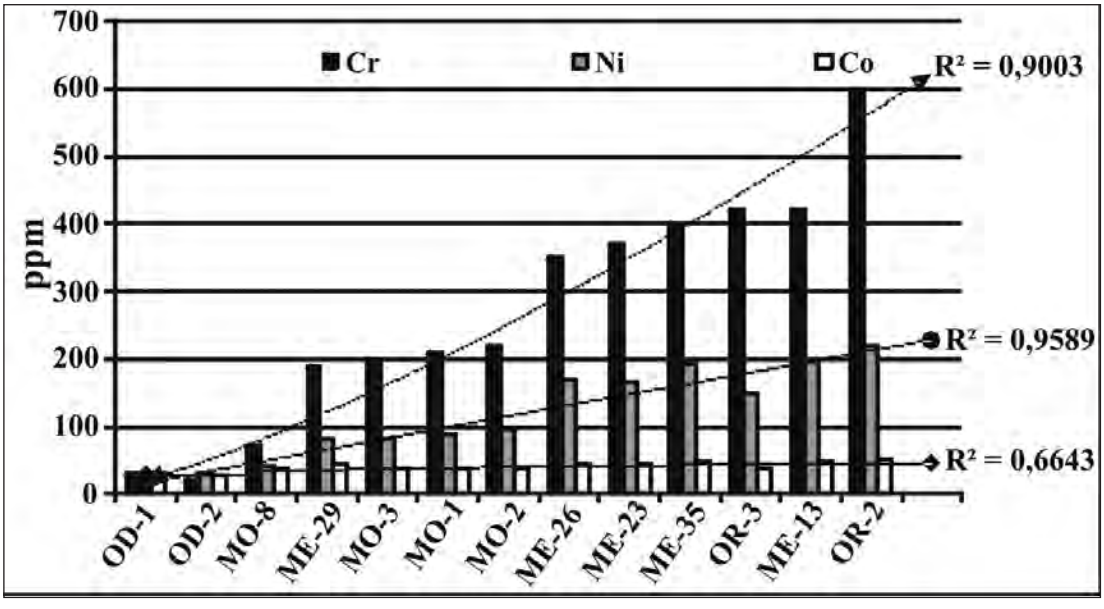

Figure 12- Columnar correlation diagram of Cr-Ni-Co elements ranging from fresh sample (OD-1) to rodingitized sample (OR-2). (See Figure 11 for sample sources).

Table 2- Gain (+) and loss (-) estimations of rodingites in terms of wt. % and ppm with respect to original rocks.

	Rodingite dyke of Van-Özalp Area							Tsiokuras et., al., 200		Koutsovisit et., al., 2008	
	ME-26	ME-35	ME-13	ME-23	MO-1	MO-2	MO-3	OR-2	OR-3	OR-1	OR-4
SiO_2	-5,85	-5,25	-10,15	-9,35	-10,45	-9,25	-6,55	-19,39	-20,04	-12,42	-15,02
Al_2O_3	2,85	0,45	-2,05	-0,05	-1,10	-1,70	-1,55	-3,86	-1,94	-4,73	1,86
Fe_2O_3	-3,21	-2,05	-2,29	-2,12	-2,35	-1,77	-1,60	0,84	-0,89	-0,91	1,30
CaO	4,15	3,65	8,40	9,30	13,90	12,30	9,50	8,98	13,70	13,79	10,64
MgO	2,20	2,97	2,87	2,34	0,03	0,27	0,04	11,19	7,65	8,09	3,39
Na_2O	-0,76	-0,69	-0,22	-1,43	-1,70	-1,58	-1,28	-1,73	-1,75	-5,22	-5,20
K_2O	-0,51	-0,40	-0,68	-0,67	-0,67	-0,65	-0,59	-0,11		-0,01	-0,05
TiO_2	-0,25	-0,10	-0,13	-0,09	0,03	0,12	0,16	0,69	0,45	-0,03	0,20
MnO	-0,04	-0,02	-0,03	-0,02	-0,03	-0,02	-0,01	0,18	0,14	0,00	0,06
P_2O_5	-0,02	0,00	-0,02	0,00	0,00	0,02	0,01	0,02	0,01	0,00	0,01
Co	1,95	5,95	5,05	3,15	-5,15	-2,95	-3,85	24,50	10,50		0,00
Cr	220,0	270,0	290,0	240,0	80,0	90,0	70,0	575,0	395,0	1444,0	228,0
Ni	108,0	131,0	135,0	104,0	29,0	33,0	20,0	195,0	125,0	412,0	37,0
Th	-0,21	-0,17	-0,20	-0,17	-0,13	-0,10	-0,06	-0,30	-0,32		-0,30
Ta	-0,10	-0,10	-0,10	0,00	0,00	0,00	0,00	-0,02			0,00
Nb	-1,15	-0,65	-0,75	-0,65	-0,15	0,15	0,35	-0,35	-0,45		1,00
Hf	-0,45	-0,15	-0,25	-0,15	0,05	0,15	0,35	0,90	0,60		0,70
Y	-7,30	-3,30	-4,30	-3,40	-1,50	0,10	1,60	15,55	11,35	2,50	5,20
Zr	-15,00	-4,00	-6,00	-4,00	2,00	8,00	11,00	20,50	14,50	-0,80	11,20
La	-0,65	-0,55	-0,85	-0,75	-0,35	0,05	0,25	-0,29	-0,42	-0,10	0,10
Ce	-1,65	-1,05	-1,65	-1,25	-0,35	0,55	1,25	0,55	0,07	-1,10	0,20
Pr	-0,29	-0,13	-0,20	-0,15	-0,03	0,09	0,19	0,36	0,26	-0,08	0,12
Nd	-1,25	-0,45	-1,05	-0,65	-0,05	0,45	1,05	3,17	2,48	-0,50	0,90
Sm	-0,48	-0,17	-0,23	-0,14	0,18	0,20	0,41	1,55	1,27	0,10	0,60
Eu	-0,17	-0,01	-0,07	-0,07	0,08	0,05	0,14	1,80	3,06	-0,05	0,11
Gd	-0,63	-0,19	-0,34	-0,27	-0,02	0,18	0,40	2,25	1,78	0,15	0,62
Tb	-0,15	-0,07	-0,10	-0,08	-0,02	0,00	0,05	0,47	0,35	0,06	0,15
Dy	-1,09	-0,47	-0,64	-0,46	-0,15	0,03	0,32	2,85	2,03	0,29	0,82
Ho	-0,28	-0,11	-0,16	-0,10	-0,05	0,01	0,05	0,54	0,39	0,09	0,20
Er	-0,85	-0,44	-0,58	-0,43	-0,16	-0,06	0,14	1,49	1,03	0,30	0,57
Tm	-0,14	-0,08	-0,09	-0,06	-0,06	-0,01	-0,01	0,20	0,13	0,08	0,10
Yb	-0,96	-0,49	-0,60	-0,54	-0,31	-0,16	-0,03	1,12	0,73	0,37	0,59
Lu	-0,14	-0,07	-0,10	-0,07	-0,06	-0,01	0,02	0,15	0,09	0,03	0,09

ues of MO-8 and ME-29 samples for the original rock in Van-Özalp field and average values of OD-1 and OD-2 samples and OMD-1 sample for Otrhys were used in the table.

According to the results of Isocon method, it was seen that SiO_2, Na_2O, K_2O major oxides presenting negative (-) coefficient values were depleted from original rocks in all rodingite samples. However; CaO and MgO major oxides presenting (+) coefficient values were enriched as a result of rodingitization. The assessment of samples which presents both (+) and (-) coefficient values in table 2 could be made by looking at the proportional difference between (+) and (-) coefficients. For example, Co as the transient element

has weighted positive coefficient values in rodingite samples with respect to the original rock. This situation indicates that Co element was enriched in rodingites. It can be stated that values most approaching to zero on the Table of Isocon analysis were relatively least affected from metasomatism. This especially comes out in values of trace and REEs of rodingites investigated. The ionic potential of five rodingite samples is approximately 7. However, it was observed that, Ta element, with its 0 (zero) ionic potential value, is the most immobile element during metasomatic processes among all elements. Zero integer is the immobility indicator in isocon analyses in which the mathematical proportionality was used. It is quite difficult although this value is expected to reach. Trace and REEs of rodingitized dykes in ophiolites in Van-Özalp field were enriched or depleted at various grades (though minimum) according to the results of isocon analysis. It is seen that this situation was mainly neutralized in terms of proportionality between the (+) and (-) coefficients in analysis results. Furthermore; coefficient values whether these are (+) or (-), are in less value ranges compared to Otrhys rodingites. Especially; Van-Özalp field rodingites of Ree, in samples MO-2 and MO-3, the depletion is observed in all Ree though less. However, all other Rees are enriched. Despite that, significant enrichments are generally observed in Ree contents of Otrhys rodingites with positive coefficient values. This is one of the most important differences between Otrhys rodingites and Van-Özalp rodingites. So; the metasomatic source which produced Otrhys rodingites must have been enriched by Rees more than the metasomatic source producing Van-Özalp rodingites. It is known that the alkalinity of fluids due to the intensity and result of equilibrium reactions have developed in metasomatic processes. The enrichment by Rees is normally expected as a result of reaction of alkaline fluids at high grades with peridotites forming the host rocks of dykes. This situation might have caused Ree enrichment in rodingite rocks at last stages of rodingitization. Nevertheless; it is stated that peridotites of Otrhys ophiolite have been depleted by Lrees (Bizimis et al., 2000; Barth et al., 2003; Tsiokuras et al., 2009). Then, it can be considered that peridotitic pyroxenes have very little Lree addition to the metasomatic source.

RESULTS

Within the light of analytical data of mafic rocks which was investigated in this study, the equilibrium reactions of Ca metasomatism despite the enrichment in CaO values in these rocks were encountered by the depletion in SiO_2 values. As a result of reaction of Ca-Mg silicates with calcic plagioclases, the grossularite (hydrogrossularite) and chlorite which are the characteristic minerals of rodingites are formed as the secondary products. Therefore; a distinct increase in MgO values in rodingites was encountered. However; there was not observed a significant change in Al_2O_3 and Fe_2O_{3t} values. Whereas; transients metals such as; Cr, Ni, Co are enriched in rodingites.

Geochemical analysis values of diabase dyke samples taken from Özalp ophiolites and dolerites and rodingites samples belonging to Otrhys ophiolite were correlated. This correlation indicated that, differences in rock chemistry found at the source area where Ca metasomatism had occurred could cause significant changes over the element mobility during rodingitization process.

Th, Ta, Nb, Hf, Ti and REEs are used as reliable indicators in petrogenetic interpretations of ophiolitic mafic rocks. It was determined that these elements were not relatively affected from Ca metasomatism at rodingitization grades which could both petrographically and geochemically be distinguished in mafic rocks of Özalp region. In addition to other trace elements except for Ta element, there is a relative mobility in Otrhys dolerites due to rodingitization in REEs as well. There was not observed a distinct mobility

in contents of trace and REEs mentioned in rodingitized dykes of the study area. Despite that, the overall element enrichment in rodingitized dykes of Otrhys was encountered. However, it is considered that the metasomatic source which produced Otrhys rodingites might have been enriched by fluids that had interacted with more enriched rocks in terms of element contents due to local geological factors in the region. Besides; these changes also depend on the regional geology, tectonical setting of the environment, the factors such as temperature, oxygene fugacity and chemical composition of fluids that might have developed and on the rodingite development that had occurred at various stages.

ACKNOWLEDGEMENTS

This study was performed within the framework of project numbered as 108Y209 supported by TUBITAK. The authors are grateful to Ed. Prof. Ergun Gökten and to all reviewers who contributed to this article.

Manuscript received March 24, 2011

REFERENCES

Austrheim, H. and Prestvik, T., 2008, Rodingitization and hydration of the oceanic lithosphere as developed in the Leka ophiolite, north-central Norway. Lithos, 104, 177–198.

Bach, W. and Klein, F., 2009, The petrology of seafloor rodingites: insights from geochemical reaction path modelling. Lithos, 112, 103–117.

Barazangi, M., Sandvol, E. and Seber, D., 2006, Structure and tectonic evolution of the Anatolian plateau in eastern Turkey, in Dilek, Y. and Pavlides, S., eds., Post collisional tectonics and magmatism in the Mediterranean region and Asia: GSA Spesial Paper, 409, 463-474.

Barth, M.G., Mason, P.R.D., Davies, G.R., Dijkstra, A.H. and Drury, M.R., 2003, Geochemistry of the Othris ophiolite, Greece: evidence for refertilization?, Journal of Petrology, 44, 1759–1785.

Bassaget, J.P., Michel, R. and Richard, F., 1967, Les rodingites et les ophisherites du massif ultrabasique de la province de Muğla (Taurus occidental, Turquie). Comparaison avee les analyses ehimiques re”eentes de rodingites des Alpes. Trav, Lab. Geol. Grenoble, 43, 23-39.

Bozkurt, E., 2001, Neotectonics of Turkey – a synthesis. Geodinamica Acta, 14, 3–30.

Bizimis, M., Salters, V.J.M. and Bonatti, E., 2000, Trace and REE content of clinopyroxenes from supra-subduction zone peridotites, Implications for melting and enrichment processes in island arcs, Chemical Geology, 165, 67–85.

Cawood A.P., Kröner A., Collins J.W., Kusy M.T., Mooney D.W. and Windley F.B., 2009, Accretionary orogens through Earth history, Geological Society, London, Special Publications 2009; v. 318; 1-36.

Cann, J.R., 1970, Rb, Sr, Y, Zr and Nb in some ocean floor basaltic rocks, Earth and Planetary Science Letters, 10, 7–11.

Coish, R.A., 1977, Ocean floor metamorphism in the Betts Cove Ophiolite, Newfoundland, Contributions to Mineralogy and Petrology, 60, 277–302.

Coleman, R.G., 1967, Low-temperature reaction zones and alpine ultramafic rocks of California, Oregon, and Washington, U.S. Geological Survey Bulletin, 1247, 1–49.

————,1977, Ophiolites, Springer-Verlag, Berlin (1977), 229.

Çakır, Ü., 2009, Structural and geochronological relationships of metamorphic soles of eastern Mediterrranean ophiolites to surrounding units: Indicators of intra-oceanic subduction and emplacement, International Geology Review, Vol. 51, pp.189-215.

Çoğulu, E. and Vuagnat, M., 1965, Sur l'existence de rogingites dans les serpentinites des environs de Mihaliççik, (Vilayet d'Eskişehir, Turquie), Bull, suisse Mineral, P6tr, 45, 17-20.

Dilek, Y., Furnes, H. and Shallo, M., 2008, Geochemistry of the Jurassic Mirdita Ophiolite (Albania) and the MORB to SSZ evolution of a marginal basin oceanic crust, Lithos100, 174–209.

———— and ————, 2009, Structure and geochemistry of Tethyan ophiolites and their petrogenesis in subduction rollback systems, Lithos, 113 (2009), 1–20.

Dubinska E, 1995, Rodingites of the eastern part of Jordanów-Gogoów serpentinite massif, Lower Silesia, Poland, Canadian Mineralogist, 1995, 33: .3585-3608.

————, 1997, Rodingites and amphibolites from the serpentinites surrounding Göry Sowie block (Lower Silesia, Poland): record of supra-subduction zone magmatism and serpentinization, Neues Jahrbuch für Mineralogie Abhandlungen, 171, 239–279.

Elitok, Ö. and Dolmaz, M.N., 2008, Mantle flow-induced crustal thinning in the area between the easternmost part of the Anatolian plate and the Arabian Foreland (E. Turkey) deduced from the geological and geophysical data, Gondwana Research, 13, 3, 302-318.

Elthon, D., 1979, High magnesia liquids as the parental magma for ocean floor basalts: Nature, v. 278, 514-518.

Frost, R.B. and Beard, A.S., 2007, On silica activity and serpentinization, Journal of Petrology, 48, 1351–1368.

Floyd, P.A. and Winchester, J.A., 1975, Magma type and tectonic setting discrimination using inactive elements, Earth and Planetary Science, Letters, 27, 211–18.

Göncüoğlu, M.C., Dirik, K. and Kozlu, H., 1997, Pre-Alpine and Alpine Terranes in Turkey: explanatory notes to the terrane map of Turkey, Annales Geologique de Pays Hellenique, 37, 515–536.

Grant, J. A., 1986, The Isocon diagram a simple solution to Gresens' equation for metasomatic alteration, Economic Geology, 81, 1976–1982.

Hopf, S., 1993, Behaviour of rare earth elements in geothermal systems of New Zealand, Journal of Geochemical Exploration, 47, 333–357.

Humphris S.E. 1984, The mobility of the rare earth elements in the crust. In: Henderson P. (ed.), Rare earth element geochemistry, Elsevier, Amsterdam, 315-341.

————————, and Thompson G., 1978, Hydrothermal alteration of oceanic basalts by sea water, Geochim., Cosmochrn.Acte, 42, 107-125.

Keskin, M., 2005, Domal uplift and volcanism in a collision zone without a mantle plume: Evidence from Eastern Anatolia, URL: http://www.mantleplumes.org/Anatolia.html

Koçyiğit, A., Yılmaz, A., Adamia, S. and Kuloshvili, S., 2001, Neotectonics of East Anatolian Plateau (Turkey) and Lesser Caucasus: implication for transition from thrusting to strike-slip faulting, Geodinamica Acta, 14 (2001), 177–195.

Koutsovitis P., Magganas A. and Pomonis P., 2008, Rodingites within scattered ophiolitic occurrences from the northern and eastern Othrys area, Greece, RMS DPI 2008-1-52-1 http://www.minsoc.ru/2008-1-52-1.

Li, X.P., Rahn, M. and Bucher, K., 2008, Eclogite facies metarodingites - phase relations in the system, SiO_2–Al_2O_3–Fe_2O_3–FeO–MgO–CaO–CO_2–H_2O: an example from the Zermatt–Saas ophiolite, Journal of Metamorphic Geology, 26, 347–364.

Michard A., 1989, Rare earth element systematics in hydrothermal fluids. Geochim., Cosmochim., Acta, 53, 745-750.

Normand, C. and Williams-Jones, A.E., 2007, Physicochemical conditions and timing of rodingite formation: evidence from rodingite hosted fluid inclusions in the JM Asbestos mine, Asbestos. Québec. Geochemical Transactions, 8, 11p.

Okay, I.A. and Tüysüz, O., 1999, Tethyan sutures of northern Turkey. Geological Society, London, Special Publication, v. 156; 475-515.

Palandri, J.L. and Reed, M.H., 2004, Geochemical models of metasomatism in ultramafic systems: Serpentinization, rodingitization and seafloor carbonate chimney precipitation, Geochimica et Cosmochimica Acta 68, 1115-1133.

Pearce, J.A., 1975, Basalt geochemistry used to investigate past tectonic environments on Cyprus, Tectonophysics, 25, 41-67.

————,1982, Trace element characteristics from destructive plate boundaries. In: R.S. Thorpe (Ed.), Andesites: Orogenic andesites and related rocks. John Wiley, Chichester, 525-548.

————, 1983, The role of sub-continental lithosphere in magma genesis at destructive plate margins, In: C.J. Hawkesworth, and M.J. Norry (eds), Continental Basalts and Mantle Xenoliths, pp. 230-249.

———— and Cann, J.R., 1973, Tectonic setting of basic volcanic rocks determined using trace element analyses: Earth and Planetary Science Letters, v. 19, 290–300.

Pearce, J.A. and Norry, M.J., 1979, Petrogenetic implications of Ti, Zr, Y and Nb variations in volcanic rocks, Contributions to Mineralogy and Petrology, 69, 33–47.

————, Alabaster, T., Shelton, A.W. and Searle, M.P., 1981, The Oman ophiolite as a Cretaceous arc-basin complex: evidence and implications, Phil. Trans. R. Soc., Lond. A 300, 299-317.

———— and Stern, R.J., 2006, Back-Arc Spreading Systems: Geological, Biological, Chemical, and Physical Interactions Geophysical Monograph Series, 166, Published in 2006 by the American Geophysical Union,10.1029 /166GM06.

Pişkin Ö., 1975, Çelikhan Çevresi Ultrabazikleri içindeki Rodenjitler ve Kimyasal Analizleri, Türkiye Jeoloji Bülteni, 17-21.

Puga, E., Nieto, J.M., Diaz de Federico, A., Bodinier, J.L. and Morten, L., 1999, Petrology and metamorphic evolution of ultramafic rocks and dolerite dykes of the Betic ophiolitic association (Mulhacen Complex, SE Spain): evidence of Neo-Alpine subduction following an ocean-floor metasomatic process, Lithos 49, pp.23-56.

Putnis A., and Austrheim H., 2010, Fluid-induced processes: metasomatism ano metamorphism, Geofluids 10, 254-269.

Robertson, A.H.F. and Dixon, J.E., 1984, Introduction: aspects of the geological evolution of the Eastern Mediterranean. In: Dixon, J.E., Robertson, A.H.F. (Eds.), The Geological Evolution of the Eastern Mediterranean. Geological Society, London, Special Publication, 17, 1–74.

Saunders, R.S., Roth, L.E., Downs, G.S. and Schubert, G., 1980, Early volcanic–tectonic province: Coprates region of Mars, In: Reports of Planetary Geology Program, NASA Tech. Memo., 81,776, 74–75.

Shervais, J.W., 2001, Birth, death, and resurrection: The life cycle of supra subduction zone ophiolites: Geochemistry, Geophysics, Geosystems, v. 2, paper number 2000GC000080.

Spear, F.S., 1981, An experimental study of hornblende stability and compositional variability in amphibolite, American Journal of Science, 281, 697–734.

Staudigel, H.T., Plank, W., White, W. and H.U. Schmincke, 1996, Geochemical fluxes during seafloor alteration of the basaltic upper oceanic crust: DSDP Sites in Subduction Top to Bottom. G.E. Bebout, D.W. Scholl, S.H. Kirby, and J.P. Platt, eds, American Geophysical Union Monograph Series 96, Washington, DC 417–418 (Overview). 19–38.

Sun, S.S. and McDonough, W.F., 1989, Chemical and isotopic systematics of oceanic basalts: implications for mantle composition and processes. In: Saunders, A.D., Norry, M.J. (Eds.), Magmatism in Ocean Basins, Geological Society of London Special Publications, vol. 42, 313–345.

Şenel, M., 2002, 1/500.000 Türkiye Jeoloji Haritası Van Paftası, Maden Tetkik Arama Genel Müdürlüğü, Ankara, Turkey.

Şengör, A.M.C. and Yılmaz, Y., 1981, Tethyan Evolution of Turkey: a plate tectonic approach: Tectonophysics, 75, 181-241.

————, Özeren, S., Zor, E. and Genç, T., 2003, Doğu Anadolu Litosfer Mekaniğine Yeni Bir Yaklaşım, İTÜ Avrasya Yerbilimleri Enstitüsü, Kuvaterner Çalıştayı IV, 101-110.

————, Özeren, M.S., Keskin, M., Sakınç, M., Özbakır, A.D. and Kayan, İ., 2008, Eastern Turkish high plateau as a small Turkic-type orogen: Implications for post-collisional crust-forming processes in Turkic-type orogens, Earth-Science Reviews, 90, 1–48.

Tsikouras, B., Karipi, S., Rigopoulos, I., Perraki, M., Pomonis, P. and Hatzipanagiotou, K., 2009, Geochemical processes and petrogenetic evolution of rodingite dykes in the ophiolite complex of Othrys (Central Greece): Lithos, 113, 540–554.

Tüysüz, N. and Erler, A., 1993, Geochemistry and Evolution of Listwaenites in the Kağızman Region (Kars, NE-Turkey): Chem., Erde 53, 319p.

Uçurum, A., Koptagel, O. and Lechler, P.J., 2006, Main-Component Geochemistry and Platinum-Group-Element Potential of Turkish Chromite Deposits, with Emphasis on the Muğla Area: International Geology Review, v. 48, 241–254.

Ustaömer, T. and Robertson, A.H.F., 1997, Tectonic-sedimentary evolution of the north Tethyan margin in the Central Pontides of northern Turkey. In: Robinson, A.G. (Ed.), Regional and Petroleum geology of the Black Sea and Surrounding Region. Memoir-American Association of Petroleum Geologists, vol. 68, 255–290.

Yilmaz, Y., 1993, New evidence and model on the evolution of the Southeast Anatolia Orogen, Geologial Society of America Bulleting 105, 251– 271.

Winchester J.A. and Floyd, P.A., 1976, Geochemical magma type discrimination; application to altered and metamorphosed basic igneous rocks. Earth and Planetary, Science Letters, 28, 459-469.

———— and ————,1977, Geochemical discrimination of different magma series and their differentiation products using inactive elements: Chemical Geology, v. 20, 325-343.

Wood, D.A., 1980, The application of a Th-Hf-Ta diagram to problems of tectonomagnetic classification and to establish the nature of crustal contamination of basaltic lavas of the British Tertiary volcanic provence. Earth and Planetary Science Letters, 50, 11-30.

Mineral Res. Expl. Bull., 144, 23-50, 2012

ORGANIC GEOCHEMICAL AND PETROGRAPHİCAL CHARACTERISTICS OF KARLIOVA HALIFAN (BINGOL) COALS

Orhan KAVAK* and Selami TOPRAK**

ABSTRACT.- In this study, petrographic and organic geochemical characteristics of the Tertiary Karlıova-Halifan coals (Bingöl) were investigated. Determination of coal quality was based on chemical (moisture, volatile matter, fixed carbon, ash) and elemental analyses (C, H, O, S, N). The values of the huminite reflectances in organic matter-rich coal levels change between 0.368 and 0.573 %, which correspond to low maturity levels. These parameters are in good aggrement with their fluorescence colors, calorific value (average original-2266, dry-3177 Kcal/kg, upper calorific value) and average T_{max} (417 ^{o}C) values. The organic material in studied coals show low grade transformation due to low lithostatic pressure. Therefore, the petrographic characteristics and quality values of Karlıova Halifan coals suggest classification as sub-bituminous coal – Lignite. Rock Eval analysis results point to an immature to early mature hydrocarbon generation for hydrocarbon derivatives formed by type II/III and III kerogen with average T_{max} values of 417 ^{o}C. The coals mainly constitute huminites, with small amounts of inertinite and liptinite type macerals. The Karlıova Halifan coals have high contents of ash and sulphur , clay and calcites as minerals, and gelinites as individual macerals.

Key words: Halifan, Bingöl Karlıova, Organic Geochemistry, Organic Petrography, Tertiary, Coal.

INTRODUCTION

Coal, as one of the most important energy sources, takes an important place in human life. Coal is mostly used in thermic power plants to produce electricity, thermal energy, coke for steel production, natural gas, and also used in various branches of industry such as production of chemical materials.

Besides to be an energy source, substantial amount of coal is used in petrochemical products. Because of these, finding new sources near the present reserves and hydrocarbon generation potential of coal have atracted the researchers' interests. Particularly some studies showing that the organic material included in terrestrial sediments have potential in producing oil and natural gas due to increasing heat by deep burial, formed basement for detailed studies (Hubbard, 1950). After pyrolysis analysis showed that some coals gas generation potential the studies have been concentrated in these fields (Durand and Paratte, 1983; Espitale et al., 1985; Kalkreuth et al., 1998). The studies show that the coals of Jurassic-Tertiary age interval tent to have high petroleum generation index (Wilkins and George, 2002). Increasing oil prices and demands, even in our country, has brought up the efficient utilization of coals and research as on hydrocarbon generation potential of coals recently.

The study area is located in around Halifan (Derinçay) Village of Karlıova Town of Bingöl City (Figure 1). Besides the known coal area, there is another locality near Hacatur, 30 km to the South of Kiği Town in Bingöl, containing three lignite seams within Eocene flysch. These seams are very thin, 0.30 m thick at most, and carry no economic value at all, therefore, only the coals in Halifan (Derinçay) regions were found to be valuable to study. The coal region is 5 km away from Bingöl Karlıova road, 45 km away from Bingöl City and

* Dicle Üniversitesi Mühendislik Fakültesi, Maden Mühendisliği Bölümü 21280 Diyarbakır
** Maden Tetkik ve Arama Genel Müdürlüğü, Maden Analizleri ve Teknoloji Dairesi 06800 Ankara

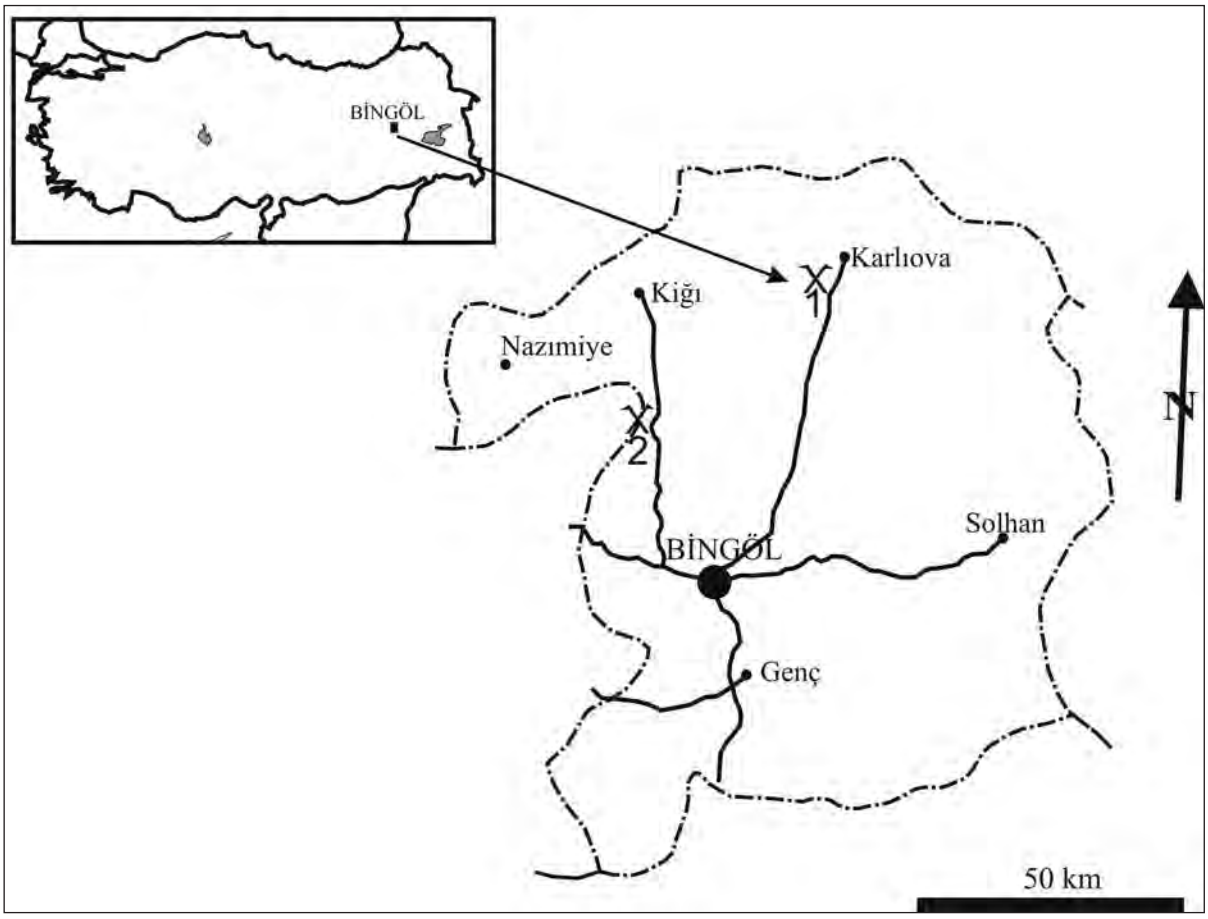

Figure 1- Location map of the studied area.

comprise of folds from North to South. Göynük Creek limits the coal extention. Karliova Halifan (Derinçay) coals have many industrial utilisations.

The first study in the region started in 1965 by MTA with geologic mapings. 5722 m of driling and nine outcropping work were conducted between 1968 - 1974 years. Geologic studies continued in the years between 1978 - 1981 . After these works, investments were conducted by TKI, later 2 - 3 thousand tons of coal was produced with open pit operation. In order to determine the utilisation of the reserve in a power plant, an operation Project was requested from the METU Mining Engineering Research Center by TKI (ODTÜ, 1984). The coal reserve of the region was calculated as 13.909.105 ton for open pit, 74.935.652 ton for under ground mining, with considering the density as 1.5 ton/m^3. 10 % of operation loss for open pit, and 25 % for under ground operation, were encountered and the coal reserves were calculated respectively as 9.989.149 ton for open pit 46.555.995 ton for under ground mining. The analysis results of the main characteristics of the coal were figured out on table 1.

According to a study performed by METU Mining Engineering Research Center in 1984, it was reported that 26.124.200 tons of coal could be produced with conducting 276.107.939 m^3 of overburden removal, and taking a calorific value

of 1458 Kcal/kg as the lower calorific value into consideration, it was suggested that the reserve meets 24 years fuel demand of a 100 mw power plant. The purpose of this study is to exhibit geochmical, petrographical and quality properties of the coals and their relations with each other. Hydrocarbon generation potential of source rocks was also investigated in the study.

GENERAL GEOLOGY OF THE STUDIED AREA

Geologic history of the East Anatolia is subdived into four main sections. Palaeozoic Early Mesozoic aged metamorphics of these comprise the oldest units (granite, gneiss, mica, schist, calcschist, marble and so on). Early Mesozoic-Late Cretaceous aged ophiolithic melanges are the products of the Northern Branch of Neotethys (Şengör, 1980). While Late Cretaceous, Middle Miocene marine sediments are represented by flysch, reefal, limestone and limestones. Middle Miocene recent formations are the products of the Neotectonic era and contain the structures of this period (Şaroğlu et al., 1987). Coal formation has developed in Neotectonic period in the studied area. As a result of continent-continent collision at the end of Middle Miocene time, the topography of the region started to be undulated by the effect of N-S directed compressive tectonies which caused to form individual basins separated by uplifted ridges. The coalification has predominantly developed in shallow lake facies within an intermontane basin, as a result of the locality changes of the coastal facies. Very fast erosion took place, soon after Pliocene period, related to the thickening of the continental crust which caused the erosion of the big amount of the Neogene series. This erosional period has been accompanied by a volcanic activity in the region which is continued in the Middle Pleistocene time and volcanic material spreaded out almost over the whole region and covered the Neogene units (Gümüşsu, 1984). In Pliocene period, the swampy area was submerged under water and cyclic depositions took places with epeirogenic events. A thickness of 40 m of basalt flow was encountered over the Pliocene aged coal deposits. Volcanism continued also towards to the end of Pliocene period. Andesite, basalt and tuffs cover the Pliocene units unconformably.

Pliocene age series in the area are mostly NE-SW directed. The region has been experienced by effective faultings at the end of Pliocene, NE extending Göynük Fault brought juxtapose the Mesozoic age crystallized limestone and the Pliocene series. The fault forms a boundary of two different reliefs. While the metamorphic series form the higher places of the region, the Pliocene series cover the low lands. Along with Göynük Creek at North, the basement basalts exhibit contacts with the coaly series by faulting. The fault with 100 m dip-slip displacement caused the coal horizon to be at much deeper places at the east of the line between Kurik and

Table 1- Analysis results of the coals.

Analysis	Available site, suitable for open pit operation	Underground operation sites
Moisture %	48,5	43
Ash %	24,2	24,6
Volatile Matter %	16	18,3
Fixed Carbon %	12,3	15,2
Total Sulphur %	0,4	0,6
Low Calorific Value (Kcal/kg)	1318	1663

Azizan Villages (Gümüşsu, 1984).

The geologic units in the Bingol Karliova coal region are illustrated in figure 2, the basement of the coal containing Pliocene series is composed of a dense volcanic activity which has 50 - 100

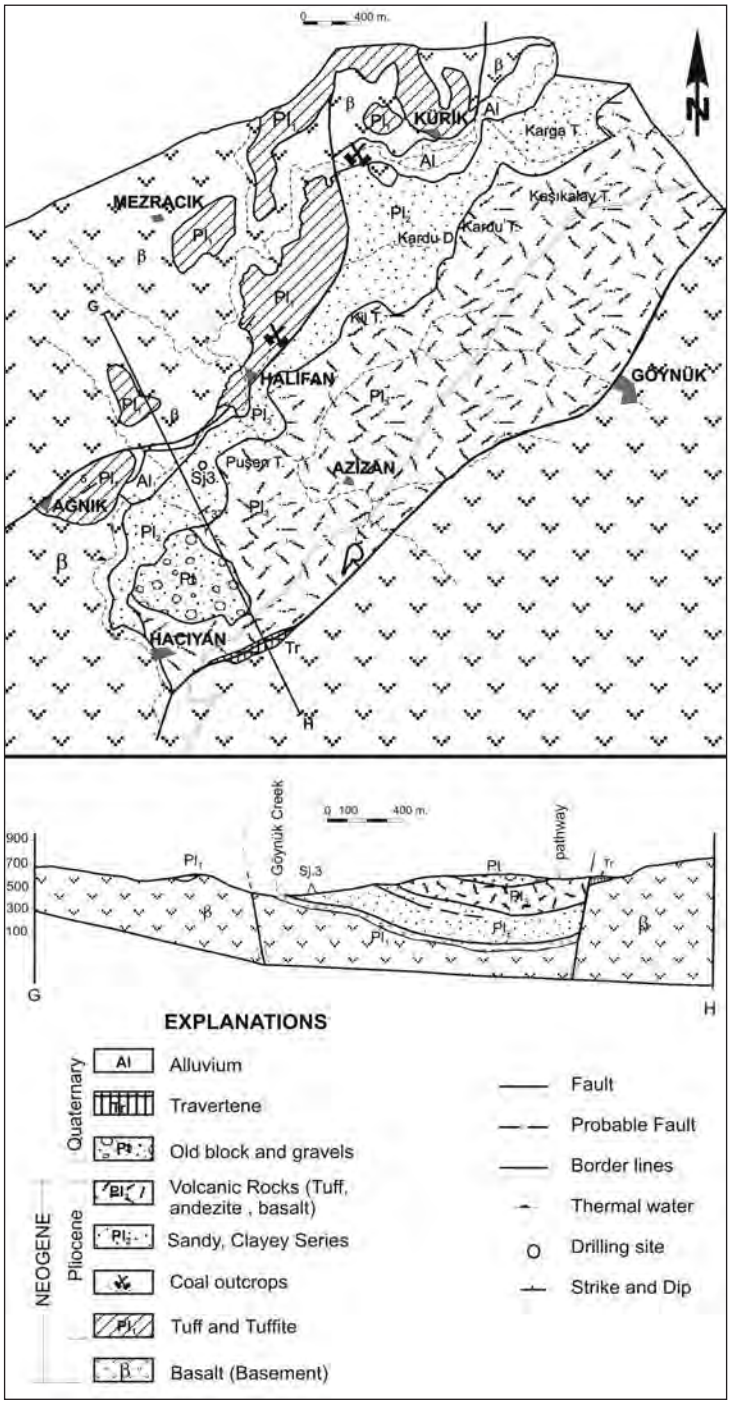

Figure 2- Geological map and geologic section, the coal seams and drilling sections of the studied coals (Gökmen et al., 1993).

m thick basalt, andesite and trachyte flows occurred at the end of Miocene period. Pliocene series overlying unconformably the basement rock, starts with agglomerates and braccias. It continues upward with a succession of silt, sand, gravel, tuff and tuffite levels. The coal deposited right straight on these units. The coal thickness varies between 4 - 13 m and has an average thickness of 8.5 m. Two coal containing levels are present in the basin. Two poor quality coal levels composing of 0.30-0.75 m thick coaly clay and 0.90 m thick clayey coal take place in the alternation of clay, tuffite, sand and gravel 30-35 m above the lower coal seam. Young volcanic products such as aglomerate, tuff, andesite and basalts cover the coal containing series. The dip angle of the coaly Pliocene layers are about 2-5 ^{0}C, and almost horizontal (Dagyaran, 1976). The angles eastwardly tend to increase . Halifan Fault, extending along Berce Creek, divides the coaly area into two sectors (Figure 2 and 3).

Figure 3- Field views (a,c,d) and drilling sites (b) of the studied coals.

MATERIAL AND METHODS

20 channel coal samples with 5 - 10 cm intervals have been collected. Inorganic composition of the samples was analyzed at Ankara TPAO Research Laboratory with XRD instrument. For chemical and elementary analysis, the coal samples were ground along ASTM standarts.(Figure 4) Firstly, they were ground to < 100 mesh size, then, homogenized and analyzed in MTA General Directorate's MAT Department Laboratories. Chemical analysis (total moisture, ash, volatiles , fixed carbon and calorific value) were conducted with IKA

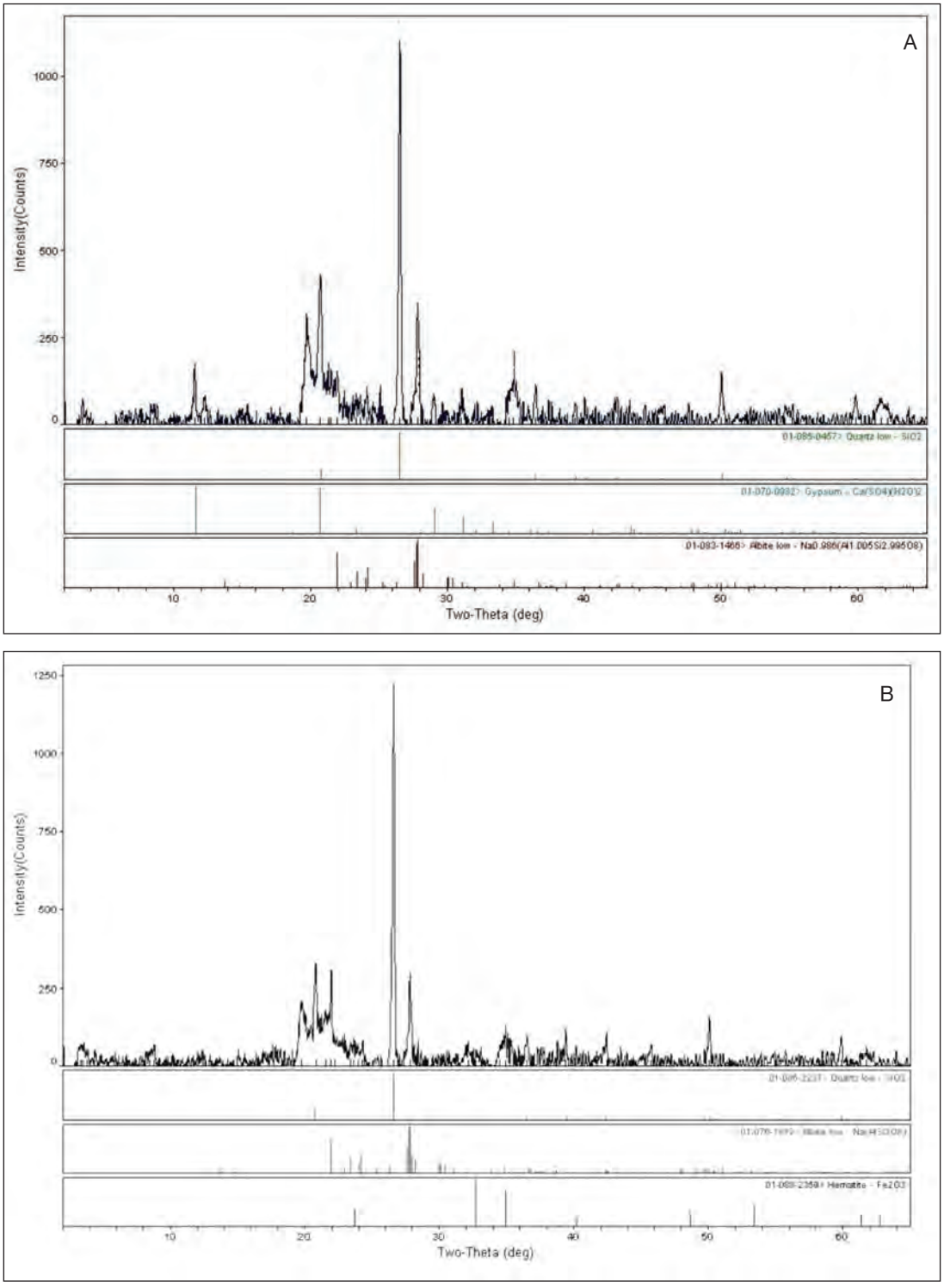

Figure 4- X-ray graphics of the samples . A(the sample contains of quartz, gypsum, albite and the rel evant peak signs are shown at below) B(the sample contains of quartz, albite and very low amount of hematite, and the relevant peak signs are shown at below)

4000 adiabatic calorimeter and in TUBİTAK MAM Laboratories. Elementary analysis, as total sulphur, carbon, hydrogen and nitrogen, were carried out in the same laboratory with LECO analyser. Evaluations were performed on each 7 samples, for the analysis. For coal petrographic analysis, 14 samples were prepared according to ICCP standart (1998 and 2001) technics. In order to determine maceral and mineral contents, white, reflected and fluorescence lights were used. A Leitz MPV-SP microscope was used to determine petrographic and mineralogic properties as well as reflectance measurements of the samples. Reflectance values of the samples were performed with using 32x and 50x oil objectives, at 546 m wavelengths. For each modal analysis, 500 point and for reflectance measurements 100 point measurements were taken as basis. The refractive index (n) of the oil, used for reflectance measurement is 1.518 and the reflectance value of the used standart, saphire, is 0.548 %. MPV Geor software programme was used for the reflectance measurements.

Standart palynologic methods (Durand and Nicaise, 1980; Tissot and Welte, 1984) were used to prepare kerogen slides of 5 samples, taken from the studied area. Kerogen spore alteration color indexes as well as organic content of the samples were determined with polarized microscope in the TPAO Research Center Laboratories (in Ankara). Hydrocarbon source rock properties of 14 samples were determined with TOC-Rock Eval pyrolysis analysis (Espitalié et al., 1985; Peters, 1986). For biomarker analysis, 5 samples differentiated with aid of Rock Eval, TOC results, were taken to dissolve in 40 hours within Dicloromethane in ASE 300 (Accelerated solvent Extraction). After dissolving, the leached materials were separated from asphalts with column chromatography and the dense material were analyzed with Agilent 6850 whole leachate GC, but gas chromatography mass spectrometer analysis were carried out in TUBİTAK MAM Laboratories with agilent 7890A/5975C GC-MS instrument.

FINDINGS AND DISCUSSIONS

Chemical and elementary analysis evaluations

Elementary analysis of coals include C, H, N+O and S. Elemantary analysis of the samples showed the C ratio to be (23 - 25 %), H to be 2.1 - 2.3 %, N+O 10.9 – 13 %, S 0.6 - 0.7 %. Air dried samples tend to have C ratio as 35.2 - 36.4 %; H content to be as 3.1 - 3.3 %; N+O, as 15.1 - 16.1 %; S, as 1.09 - 1.12 % (Table 2). Ash content of 7 coal samples were determined, the

Table 2- Elementary analysis of Karlıova Halifan coals.

Sample	Original Sample				Dry Sample			
	C (%)	H (%)	(N+O) (%)	S (%)	C (%)	H (%)	(N+O) (%)	S (%)
BNOK-1	23,1	2,16	12,80	0,62	36,30	3,31	15,40	1,09
BNOK-2	24,4	2,12	10,85	0,64	36,42	3,15	15,63	1,11
BNOK-3	23,5	2,15	11,26	0,64	35,55	3,17	16,11	1,11
BNOK-4	24,7	2,32	12,30	0,61	35,72	3,14	15,56	1,07
BNOK-5	25,1	2,17	12,20	0,60	35,69	3,12	15,27	1,09
BNOK-6	24,1	2,20	12,97	0,65	36,01	3,32	15,12	1,12
BNOK-7	25,1	2,15	12,04	0,63	35,16	3,18	15,45	1,08

dominant ingredient was found to be SiO_2 with 32.4 - 44,5 % Al_2O_3+TiO_2 content is between 15.0 - 18.1 %, Fe_2O_3 between 7.8 - 8.8 %, CaO between 13 - 20 %, MgO between 4.5 - 5.8 %, SO_3 between 10.6 - 16.4 % and Na_2O+K_2O between 1.4 - 1.5 % (Table 3). High calcium rate stands for plant remnant's bacterial decay, high collinite and pyrite content of coals are thought to be derived from bacterial reduction of sulfates. Pyrite content of the coals and associated clays are considerably high and observed as framboidal at most (Figure 5a, b). Minerals within macerals are observed with various shapes, thicknesses and as filling voids as well as veins (Figure 5c, d).

Table 4 and 5 exhibit the coal's moisture, ash, volatile matter, petrographic composition and calorific value as well as huminite reflection (R_{max}) values. Carbon values of the coals, in original sample, vary between 23 – 25 %, 35 – 36 % as air dried basis; the hydrogen content of the original samples between 2.1 - 2.3 %, 3.1 - 3.3 % as air dried basis; sulphur content of the original samples between 0.6-0.65 %, 1.07-1.12 as air dried basis; in addition, nitrogene + oxygene values of the original samples vary between 10.9 – 13 and 16.7 % as air dried basis. The ash content of the coals are ratherly high and show variations between 16 - 56 for original samples, 26 - 76 % for air dried sam-

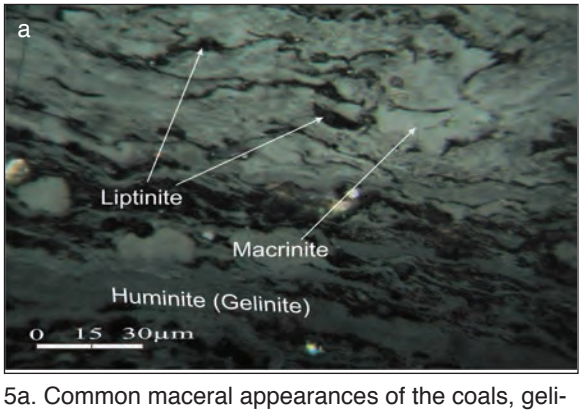

5a. Common maceral appearances of the coals, gelinite, liptinites and white shapeless macrinites.s

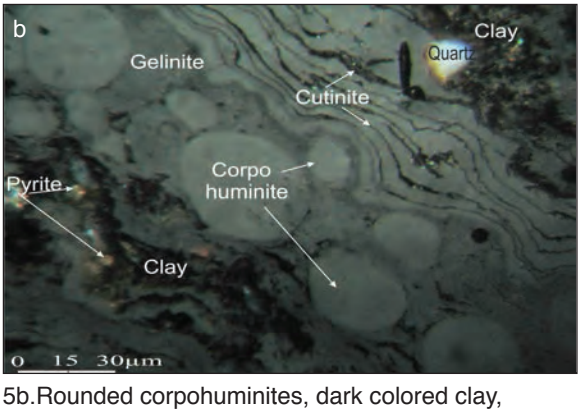

5b.Rounded corpohuminites, dark colored clay, quartz, cutinites and pyrites observed in the coals.

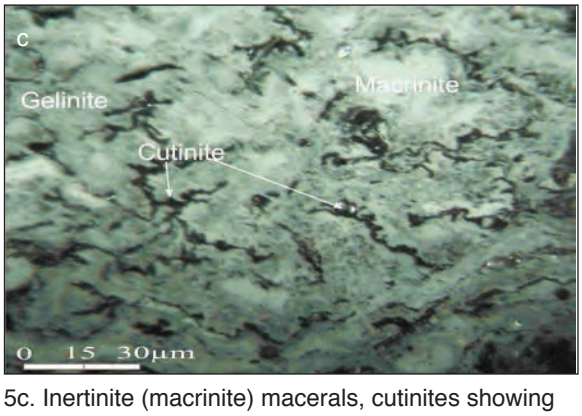

5c. Inertinite (macrinite) macerals, cutinites showing lineations and predominant textureless gelinites, observed in th

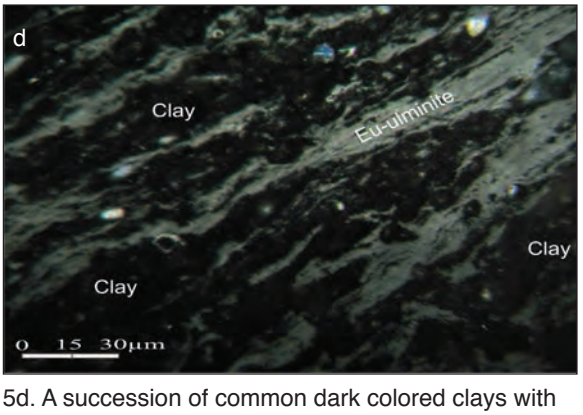

5d. A succession of common dark colored clays with eu-ulminites which possess textures.e coals.

Figure 5- Petrographic images of the Bingol Halifan Coals.

Table 3- Ash components of Karlıova Halifan coal samples.

Sample	SiO_2 (%)	Al_2O_3 +TiO_2 (%)	Fe_2O_3 (%)	CaO (%)	MgO (%)	SO_3 (%)	Na_2O+K_2O (%)
BNOK-1	44,5	17,1	8,77	12,69	4,85	10,66	1,40
BNOK-2	32,4	17,1	8,20	20,05	4,50	16,33	1,42
BNOK-3	42,4	15,7	7,84	14,30	5,80	12,50	1,51
BNOK-4	33,5	18,1	8,10	18,09	4,50	16,36	1,35
BNOK-5	43,5	16,1	8,70	14,79	4,87	10,60	1,48
BNOK-6	35,4	15,0	8,22	20,10	4,60	16,24	1,40
BNOK-7	41,3	15,1	8,20	13,62	4,80	15,44	1,50

Table 4- Proximate analysis of Karlıova Halifan coal samples.

In Original Samples						
Sample	**Moisture %**	**Volatile Matter %**	**Ash %**	**Total Sulphur %**	**High Calorific Value (Kcal/kg)**	**Low Calorific Value (Kcal/kg)**
BNOK-1	28,3	31,2	18,4	0,77	3237	2938
BNOK-2	20	34	25	0,67	2968	2717
BNOK-3	14,8	31,9	32	0,76	3265	3037
BNOK-4	26,2	10,4	56	0,36	828	645
BNOK-5	49,2	12,8	33,5	0,15	774	457
BNOK-6	34,7	20,1	32,9	0,34	1954	1673
BNOK-7	38,1	26,3	16,1	0,59	2834	2614
In Dry Samples						
Sample		**Volatile Matter %**	**Ash %**	**Total Sulphur %**	**High Calorific Value (Kcal/kg)**	**Low Calorific Value (Kcal/kg)**
BNOK-1		45,5	25,7	1,07	4510	4318
BNOK-2		42,5	31,3	0,83	3703	3533
BNOK-3		37,4	37,5	0,9	3825	3659
BNOK-4		14,1	75,9	0,48	1121	1069
BNOK-5		25,2	65,9	0,3	1520	1432
BNOK-6		30,8	50,5	0,53	2989	2856
BNOK-7		42,5	26	0,96	4571	4380

ples, which comply with petrographic composition as well. This data reveals the coal formation, mostly in brackish water conditions, high organic material decaying and abundant inorganic material composition as a result of these (Teichmuller et al., 1998). The coals showing 0.2 - 0.8 % original and 0.3 - 1.07 % air dried sulphur content and high amount of ash con-

Table 5- Maceral analysis and Rmax (as %) values of Karlıova Halifan coal samples.

No	Sample	Rmax (%)	Huminite								Liptinite						Inertinite					Pyrite				INOR (Cl+Qz +Ca)
			HTEL			DHUM		HCOL		TOT HUM	Sp	Alg	Rs	Cut	Ldt	TOT LIP	Fus	Ma	Fg	Idet	TOT INER	Fr	Eu	Fil	TOT PYR	
			Tex	Tul	Eul	Att	Dn	Gel	Cor																	
1	BNOK-1	0,378	6	5	4	2	6	28	1	52	3	1	0	1	0	5	1	3	0	0	4	3	1	1	5	34
2	BNOK-2	0,462	2	3	4	2	4	32	1	48	2	0	0	1	0	3	1	3	0	0	4	3	1	0	4	41
3	BNOK-3	0,456	3	4	5	2	7	28	1	50	2	2	0	1	0	5	1	3	0	0	4	2	1	1	4	37
4	BNOK-4	0,532	3	4	4	0	5	26	1	43	2	2	0	0	0	4	2	3	0	0	5	2	0	0	2	46
5	BNOK-5	0,517	1	2	3	0	3	24	0	33	2	0	0	0	0	2	0	3	0	0	3	2	0	0	2	60
6	BNOK-6	0,468	3	5	6	3	7	23	2	49	3	2	0	1	0	6	1	3	0	0	4	3	1	1	5	36
7	BNOK-7	0,573	2	4	7	3	8	29	2	55	3	2	0	1	0	6	2	6	0	0	8	2	1	0	3	28
8	BNOK-8	0,368	7	4	4	3	7	23	2	50	2	1	0	1	0	4	2	4	0	0	6	4	1	1	6	40
9	BNOK-9	0,478	3	2	2	5	4	29	1	46	3	2	0	1	0	6	1	3	0	0	4	4	1	0	5	44
10	BNOK-10	0,446	4	3	4	2	6	30	2	51	2	1	0	0	0	3	1	4	0	0	5	3	0	1	5	41
11	BNOK-11	0,541	3	2	2	4	5	26	1	43	4	1	0	0	0	5	2	3	0	0	5	3	0	0	4	47
12	BNOK-12	0,509	4	2	2	3	4	29	2	46	1	1	0	0	0	2	2	1	0	0	3	3	0	0	2	49
13	BNOK-13	0,491	5	3	3	4	4	33	1	53	1	3	0	0	0	4	1	4	0	0	5	4	1	1	2	38
14	BNOK-14	0,548	4	2	3	2	5	24	1	41	1	2	0	0	0	3	1	5	0	0	6	3	1	0	4	50

HTEL- Telohuminite; DHUM- Detrohuminite; HCOL- Gelohuminite; TOT- total; HUM- huminite; LIP- Liptinite; INER- Inertinite; PYR- Pyrite; Cl- Clay; Qz- Quartz; Ca- Calcite; INOR- Inorganic Material; Tex- Textinite; Tul- Texto-ulminite; Eul- Eu-ulminite; Att- Attrinite; Dn- Densinite; Gel- Gelinite; Cor- Corpohuminite; Sp- sporinite; Alg- Alginite; Rs- Resinite; Cut- Cutinite; Ldt- Liptodetrinite; Fus- Fusinite; Ma- Macrinite; Fg- Funginite; Idet.- Inertodetrinite; Fr.- Framboidal; Eu- Euhedral crystalline; Fil.- Crack or void filling pyrite.

tent, the coals imply to be deposited in a highly elevated continental area. Inorganic content of the coals were also analyzed and clay-mica minerals, quartz as well as plagioclase minerals were found abundantly (Figure 4a, b). The volatile matter content of the coals with 10 – 34 % as original and 14 - 46 % as air dried, and the elementary analysis of the coals seem to comply with the coal rank (Figure 4).

Higher calorific values of the coals exhibit 774 - 3265 (averagely 2266) Kcal/kg of the original samples, as in air dried basis 1121 - 4571 (averagely 3177) Kcal-kg. The chemical analysis and reflectance (R_{max}) measurements indicate the coals as subbituminous-lignite coalification ranks (ASTM 1983 and 1992) (Table 5). As ash content of the coals increases, calorific value decreases, while fixed carbon and volatile matter content increases, in the some way and rate. Fixed carbon values are in dried basis and match with organic carbon determined with Rock Eval method. As hydrogen content increases, carbon ratio increases as well, but oxygene decreases. There is a negative relation between volatile matter and ash contents which are the parameters to determine coal quality.

High sulfur content of the coals may be resulted from lake water or brackish water conditions or high pH as well as low Eh conditions and sulphate ion abundances within the lake waters, or be derived from primary organic material as well as associated rocks (Stach et al, 1982)

Petrographic evaluations

The studied coal succession is dominantly dull, in addition, they are observed as with dull banded succession of lithotypes. The bands were not defined in detail because of high inorganic material contents of the coals. The coal petrographical determinations were carried out according to Stach et al., (1982) and ICCP methods (1998 and 2001), the maceral groups lignite, huminite and inertinite were determined and exhibited on ternary diagrammes (Figure 6a). Petrographic composition of the samples re-

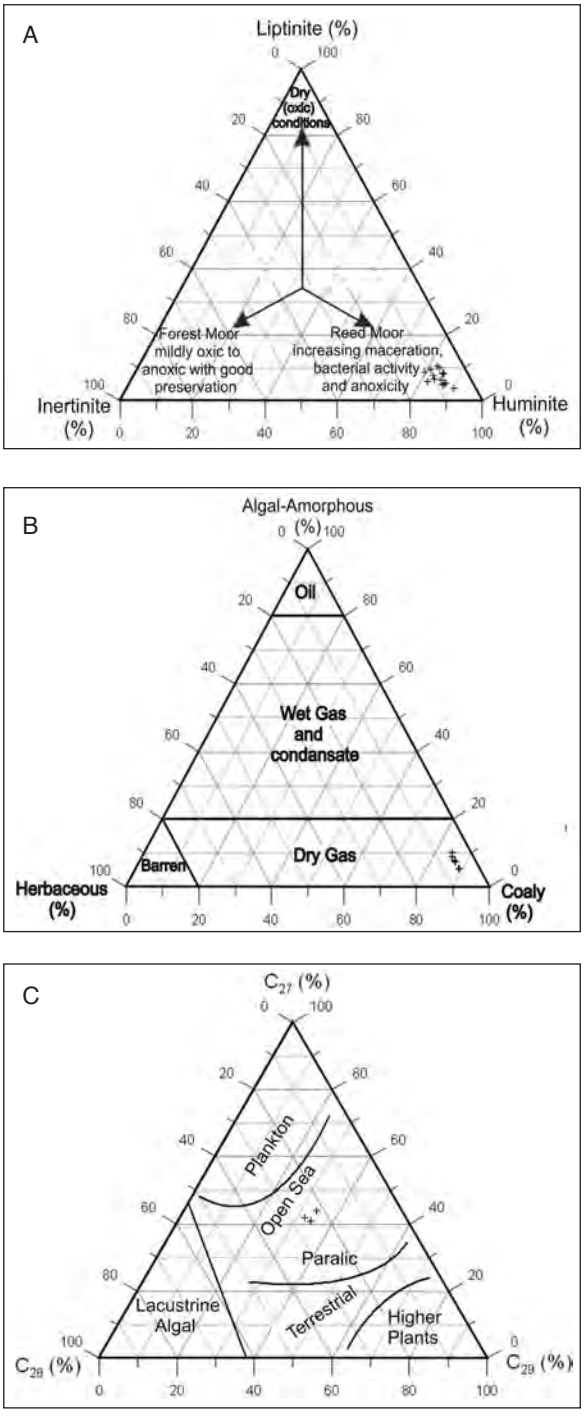

Figure 6- A, B, C. Triangular diagrammes of organic material types, of Karlıova Halifan coal samples.

vealed that a heterogeneous input of materials were common during peatification period. To the analyses of 14 coal samples, the coals tend to contain of huminite macerals dominantly (33 - 55 %) and the predominant maceral is gelinite. Gelinite is a submaceral of huminite maceral group, showing gelification but no cellular structures at all. Gelinite content of coals varies between 23 - 33 % and their characteristic features are exhibited on microphotos (as on Figure 5a, b, c). In Halifan coals, eu-ulminite (Figure 5d) which shows cellular sructure traces and corpohuminite macerals (Figure 5b) may clearly be observed. Corpohuminites exhibit distinctive large surrounded shapes. Inertinite and liptinites are comperatively lesser in the coals (Table 5). Some of the liptinites show lineations of cutinites as if they are wood tissue lines (Figure 5b) some own various lineations and shapes which they are sporinites and cutinites (Figure 5a, c). Liptinite contents vary between 2 - 6 %, liptinite and huminite macerals sow much more resistance, there fore they are rather more abundant and indicate woddy moor type depositranal environments (Flores, 2002). Macrinite and fusinites are the most common (3 – 8 %) inertinite maceral group (Figure 5 a and b) .The result shows that high inertinite containing coals carry ratherly higher gas generation potentials. Maceral group raties and huminite reflection values of the coals, which vary between 0.368 - 0.573 %, are shown on table 5.

High gelinite content imply tissue deterioration of the organic materials, pH value increases up to neutral levels during formation. Fusinite and inertinite macerals indicate increase of oxidation and decrease of water levels within swamps (Figure 5a, c) (Flores, 2002; Stach et al., 1982). The coals contain high amount of spores and clay minerals also which indicate abundant bacterial activities as well as decayings, in reed moor environment and underwater conditions. Mineral matter ratio changes between 31 - 62 % and mostly formed with carbonates, clays and silicate minerals which probably formed as a result of biologic activities in the region (Figure 5b, c). Petrographic compositions of Turkish coals, as pointed out by Toprak (2009), show similarities and give impressions to have limnic formations. This claim was supported also with other clues. As seen in the studied coals, high calcium rate indicates alkaline depositional environment, bacterias the imply formations of humic gells, nitrogene and hydrogen rich coal products (Teichmuller et al., 1998). These properties were also observed in the Amyneto Basin Pliocene aged lignites as in the same way (lordanidis and Georgakopoulos, 2003). TPI (Tissue Preservation Index) and VI (Vegetation Index) values were used to determine the paleodepositional environments, in the study. GWI (Ground water Index), GI (Gelification Index) values are used by Georgakopoulos and Valceva (2000) and TPI-VI by Diessel (1986) to determine paleoenviroments for coal depositions. Low TPI values developed either depending on the vegetation type (high angiosperm / gymnosperm ratio), or on low tissue preservation conditions (Kolcon and Sachsenhofer, 1999; Bechtel et al., 2005). TPI values for Karlıova Halifan coals vary between 0.15 – 0.35 %. The GI value indicates under ground water level and/or pH level. For gelification, regular water flow, bacterial activity and low asidic conditions are essentials (Kolcon and Sachsenhofer, 1999). For Karliova Halifan samples, GI values change between 2.3 - 6.2; GWI value between 2.9 – 11 %; VI value between 0.57 - 1.6 % TPI's value being lower than 0.5 % GI value higher than 1, GWI value heigher 1 and VI value less than 2, in addition to higher pyrite content, as well as common gastropod shells, indicate the coals to be deposited in a lake environment. Coal formation took place within high under ground water table, average subsidence rate and autochotonous to hypoautochotonous way of depositon. Here, high alkaline conditions and fresh water effects are mainly observed. Low TPI value indicates high bacterial activity and high pH value, in addition, common presence of gastropods are good supporting evidences for alkaline environmental conditions such as seen in

Amyneto Basin (Greece) (Iordanidis and Georgakopoulos, 2003). Relatively higher reflectance values of the coals than the other Turkish coals which possess the same quality are probably due to the little distance of the coals to very important tectonic lines (NAF and EAF). According to the XRD analysis results, plagioclase ratio change between 5 - 15 %, quartz between 7 - 15 %, gypsum 3 - 8 % and clay+ mica 70 - 85 % (Table 6 and figure 4). Most of the inorganics are clay-mica minerals, quartz and plagioclase and are thought to be of continental origin (Stach et al., 1986; Toprak, 1996).

GEOCHEMICAL EVALUATIONS

As geochemical evaluations, Total Organic Carbon (TOC), organic material type and for maturation, Rock-Eval Pyrolysis analysis was carried out. GC, GC-MS and GC-IRMS analysis were conducted to determine biomarker data of the samples. Organic material abundance, organic type, diagenetic development and source rock potential of the organics were produced with Rock–Eval pyrolysis data. This tecnique is mainly performed on carbonate shale like rocks, which are thought to have source rock potentials, since Rock- Eval device works well on coaly samples and has well additions to petrographical investigations, the usage of it became very common for coal researches, as well (Teichmuller and Durand, 1983; Durand and Parette, 1983; Fowler et al., 1991; Korkmaz and Gulbay, 2007; Erik, et al., 2008; Kavak, et al, 2010; Kavak and Toprak, 2011).

Table 6- XRD analysis results and mineral distribution of Karlıova Halifan coals.

Sample	Plagioclase (%)	Calcite (%)	Quartz (%)	Gypsum (%)	Hematite (%)	Clay+Mica (%)
BNOK-1	10	-	7	3	-	80
BNOK-2	10	-	15	-	trace	75
BNOK-3	5	-	15	-	trace	80
BNOK-4	7	-	15	8	-	70
BNOK-5	5	-	10	-	-	85
BNOK-6	15	-	10	-	trace	75
BNOK-7	5	-	10	-	-	85

Organic material quantity (Total Organic Carbon)

Total Organic Carbon (TOC %) analysis was applied on 14 samples and the values vary between 4 - 41.2 % (Table 7). These results show that Karliova Halifan coals are rich in organic material contents (TOC >0.1) and indicate that the coals may be thought as source rocks. Irregular TOC values of the coals may be resulted from biologic productivity, physico-chemical conditions, grain size, sedimentation velocity and the rock type which all have effects on organic material productions in an environment. As water column over the sediments is rich in organics, the organic material content, as well, gets enriched which is called as biologic productivity. As grain size decreases in sediments, organic material contents get increased (Hunt, 1967) in addition with sedimentation velocity increase, organic material quantity gets increased as well (Heath et al., 1977). Organic material quantity is also dependent on rock types; clay and mudstones are rich in organics, but sandstones are poor and carbonates stand between these two (Kavak, 2011). Determined low content of organic materials of the studied samples

Table 7- Total organic carbon (TOC %) and Rock-Eval pyroliysis results of Karliova Halifan coal samples.

Sample	TOC	S1	S2	S3	S2/S3	Tmax	HI	OI	PI	PY
BNOK-1	38,6	0,7	44,0	35,1	1,25	409	114	91	0,015	44,72
BNOK-2	41,1	1,5	42,2	64,2	0,65	410	103	156	0,034	43,66
BNOK-3	38,6	4,4	58,7	32,1	1,82	405	152	83	0,07	63,08
BNOK-4	4,1	0,03	0,8	3,1	0,25	431	19	74	0,03	0,8
BNOK-5	12,8	0,5	19,4	23	0,84	432	152	180	0,026	19,91
BNOK-6	23,5	0,96	41,2	20,1	2,05	418	175	85	0,022	42,17
BNOK-7	32,4	0,8	42	41,5	1,01	419	130	128	0,017	42,7
BNOK-8	38,8	0,7	44,1	35,1	1,25	405	112	93	0,015	44,77
BNOK-9	41,2	1,4	42,1	64,2	0,65	415	107	152	0,032	43,52
BNOK-10	38,3	4,3	58,6	32,1	1,82	401	150	87	0,068	62,95
BNOK-11	4,01	0,1	0,8	3,1	0,25	435	16	71	0,02	0,93
BNOK-12	12,9	0,6	19,3	22,9	0,85	425	151	179	0,029	19,92
BNOK-13	23,4	0,9	41,2	20,1	2,05	422	178	82	0,021	42,12
BNOK-14	32,5	0,8	42	41,6	1,01	415	133	130	0,018	42,73

TOC: Total organic carbon (%), S_1: mg HC\g rock, S_2: Hydrocarbons formed as a result of disintegrations Kerogens (mg HC/ g TOC); S_3: CO_2 value (mg CO_2\g TOC), T_{max}: Maximum thermal value as S_2 gets to maximum level along Pyrolysis analysis; HI: Hydrogen Index (mg HC/ g TOC), OI: Oxygen Index (mg CO_2\g TOC), PI: Production İndex (mg HC\g TOC), S_2\S_3: Hydrocarbon type index, PY: Potential efficiency (mg HC\g TOC).

may also be originated from the mentioned reasons (Burwood et al., 1992)

ORGANIC MATERIAL TYPE

In order a rock to carry the properties of a source rock, it should absolutely contain enough organic material. Besides organic petrographic analysis, Hydrogen Index (HI), Oxygen Index (OI) and Tmax analysis' results are used to determine organic types of the materials with evaluating HI-OI and HI-Tmax diagrammes of the samples. According to HI and OI data, organic material points out three types of kerogones which may carry petroleum generation potentials; TYPE I: This group has the highest liquid hydrocarbon generation potential. Its oxygen ratio is low, hydrogen ratio is high. TYPE II: Hydrogen quantity of them are less than those of the type 1 but oxyen amount is much higher. It represents algae, spore, pollen, cuticule and woody organic material content. TYPE III: Hydrogen content is very low and oxygen content is ratherly very high. They may generate very little amount of gasses (Tissot and Welte, 1984; Hanson et al., 2000).

Hydrogen index values of Karlıova Halifan coals vary between 16 - 178 mg HC/g TOC and oxygen index values between 71 - 180 mg CO_2/g TOC. Production İndex (PI): Sı / (S_1+S_2) value especially should be higher than 0.05 %, then, interpretation becomes important. Karlıova Halifan samples exhibit an average of 0.034 % value (Figure 8).Some high oxygene index values (>150 mg CO_2/g TOC) have probably developed due to mineral matrice and mineral decomposition during pyrolysis. If mineral matter content of

the studied samples is especially rich in clay and carbonates, the results of pyrolysis process may, then, be affected (Peters, 1986; Langford and Blanc-Valleron, 1990).

While there is a negative relation between HI and liptinite content, a positive relation developes with HI, when huminite ratio is added to liptinite content (Figure 7). Carbon values with addition of total organic carbon and elementary analysis tend to exhibit a strong positive relation. Besides this, there is a negative relation between mineral matter content and hydrogen index, TOC, Pc, Rc, values, the correlation coefficient (Pearson Coefficient) is very low, therefore, was not shown on the graphics.

According to the samples' values, put on Van Krevelen (Hydrogen Index-Oxygen Index) and HI-Tmax diagrammes, most of the samples tend

Table 8- Biomarker parameters derived from the m/z 217 and m/z 191 mass chromatograms.

			191			217			
Samples	^{13}C	Standart Deviation	H/(H+M)	Ts/Tm	$\frac{C_{31}\ 22S}{22S+22R}$	$\frac{C_{29}\ 20S}{20S+20R}$	C_{27} %	C_{28} %	C_{29} %
BNOK-1	-27,31	0,19	0,82	0,15	0,53	0,55	42	26	32
BNOK-6	-22,95	0,09	0,83	0,13	0,55	0,56	41	25	34
BNOK-7	-22,45	0,07	0,85	0,14	0,57	0,57	44	22	34

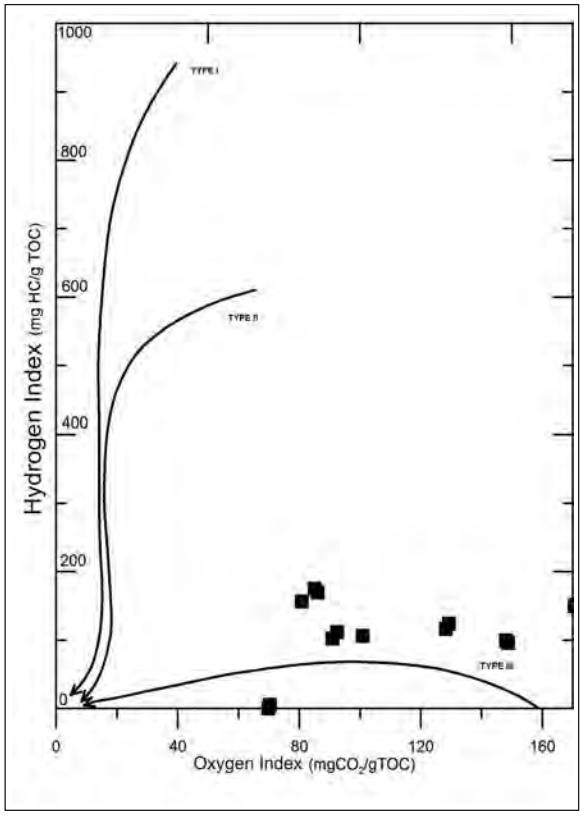

Figure 7- Hydrogen Index-Oxygen Index diagramme of the studied samples (Tissot and Welte, 1984).

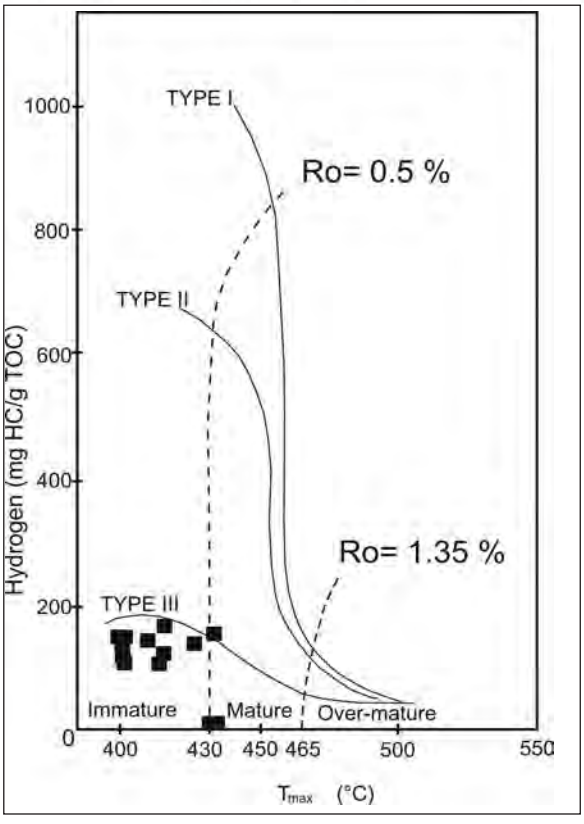

Figure 8- Classificiation of kerogene types by Hydrogen Index- T_{max} diagramme (Mukhopadyay et al., 1995).

to stay at the TYPE II-III (terrestrial and marine) and TYPE III areas (Figure 7 and 8). This definition is also supported with palynologic determinations from the Kerogen preparations, which indicates coaly-woody material dominance. Coaly organic matter of the samples seem to be of 84 - 89 %, woody 11 – 16 %, herbaceous 5 % and 10 % of algae amorphous organic matter (Figure 6). It is thought that amorphous organic materials probably formed during transportation of the terrestrial materials by alteration and disintegrations.

As a result of comparison, different analysis data exhibit important interrelations (Figure 8). Total organic carbon and high heat value show a strong positive bond. Total organic carbon and high calorific value exhibit a strong positive relation. As remnant carbon, which is a parameter of Rock Eval, increases, fixed carbon and carbon values increases, as well, but ash content decreases. Pyrolyzed carbon amount and fixed carbon, oxygene index-oxygene content have positive relation but S_3 ash and oxygene index-high calorific value as well as C and fixed carbon values.

Very low detection value of low carbon numbered n-alkanes, especially of n-C_6 and n-C_{17}, additionally not having of organic compounds above C_{32} in g as chromatogrammes, point out terrestrial as well as marine originated organic materials.İn biomarker analysis of the Halifan samples, high molecular abundat (C_{20}+) compounds on n-alkanes are predominant and predeminancy of odd numbered n-alkanes between C_{25}-C_{31} as well as C_{29} steranes against to C_{27} - C_{28}, and abundance of C_{29} ααα R isomers indicate organic matters derived from terrestrial materials.

Organic maturation

For hydrocarbon formation and the realization of the maturity of the organic matter, it is required that the thermal conditions should be raised to the thermal disintegration levels of the kerogens.

T_{max} (°C) value represents thermal maturity and it expresses maturation with the depth increase. T_{max} values of Karlıova Halifan coals vary between 401-435 °C and show 417 °C as average (Table 7). These values indicate organic matter rich parts of the coals to be immature and at premature zone. In kerogen preparantions light yellow and light brown organic material altertion colors, light yellow, colorless spores, low R_{max} values all support T_{max} data about maturation. Most of the samples scattered in the pre-mature and immature zones, on HI-T_{max} diagramme (Figure 8). PI values of these samples are < 0.1 and indicate low maturations. Huminite reflection (R_{max}) values of the samples vary between 0.368 - 0.573 %. Since high ash content effect the comparison of the samples, huminite reflection values of calorific values of the samples containing less than 15 % of ash were taken into considerations. Although both data individually indicates immature levels, there is a meaningful linear relation between huminite reflectance (R_{max}) and T_{max} values due to different petrographic compositions. 20 (S)/(20 s+20R), the ββ/(ββ+αα) sterane ratio and T_{max}, as well as reflection values inerease proportionally. Sterane ratios of the studied samples are less than 1 and correspond with immature phase. Ts / (Ts+Tm) ratio of the samples are between 0.11 - 1.15. Ts/Tm=1 value indicates the border between immature (Ts/Tm<1) and mature (Ts/Tm>1) organic maretials. 18 α (H) - 22, 29, 30- trisnorneonhopane (Ts)/(Tm) of Karlıova Halifan coals is between 0.13 - 0.15 (Table 7). Generally, C_{31} or C_{32} homohopanes are used to determine 25S / (22 S+22 R) ratios. This ratio increase, is between 0.53 - 0.57 for the studied samples. Diasterane /sterane ratios are ratherly low for immature sediments and are 2.9 - 4.2 for the samples (Arfaouni et al., 2007). Moretane / Hopane ratio is between 0.55 - 0.57 and generally decreasses with maturation increase (Kvenvolden and Simoneit, 1990).

Besides low bitumen/TOC ratio and dense peak scattering of sterane and triterpanes at chromatogrammes indicate the immature zone (Tissot and Welte, 1984). Another maturity parameter derived from C_{29} regular stranes is 5 α (H), 14ß (H), 17ß (H) C_{29} sterane and 5 α (H), 14 α (H), 17α (H) C_{29} sterane (αßß) / (αßß+ ααα) ratio.This ratio is always larger than 1. Ts/Tm ratio for the samples is 0.13 - 0.15.

Hydrocarbon generation potential

For this, analysis of the studied samples are used in source abundance diagramme (HI-TOC) (Jackson et al, 1985) (Figure 9). S1 values of the samples are considerably low, between 1.7 - 4 mg HC/g rock; S2 values between 38 - 63 mg HC/g rock (Table 6). Since S2 value of 4 mg HC/g rock is low, it indicates weak rock potential; but when higher than 4.0, a source rock is considered, in addition that S2 values define whether or not it is a good or better source rock (Table 8). To this data, the coals may be the source rocks and the other organic rich carbonate levels have no source rock potential at all. The most critical value is the presence of hydrogen rich organic material. To Hunt (1995), in order to generate hydrocarbons from coals and terrestrial materials, larger hydrogen index value from 200 mg HC/g TOC is essential. High hydrogene index value and HI-T_{max} diagramme scatter indicate the samples to contain of partial marine organic material influx and limited gas generation potential.

As in the studied samples, humic coals form from TYPE III kerogens and may generate gasses. Besides there is a capability of gas generation potential of Karlıova Halifan coals, their incomplete maturation has prevented it. Hydrocarbon generation index is also named as genetic potential or production index and show

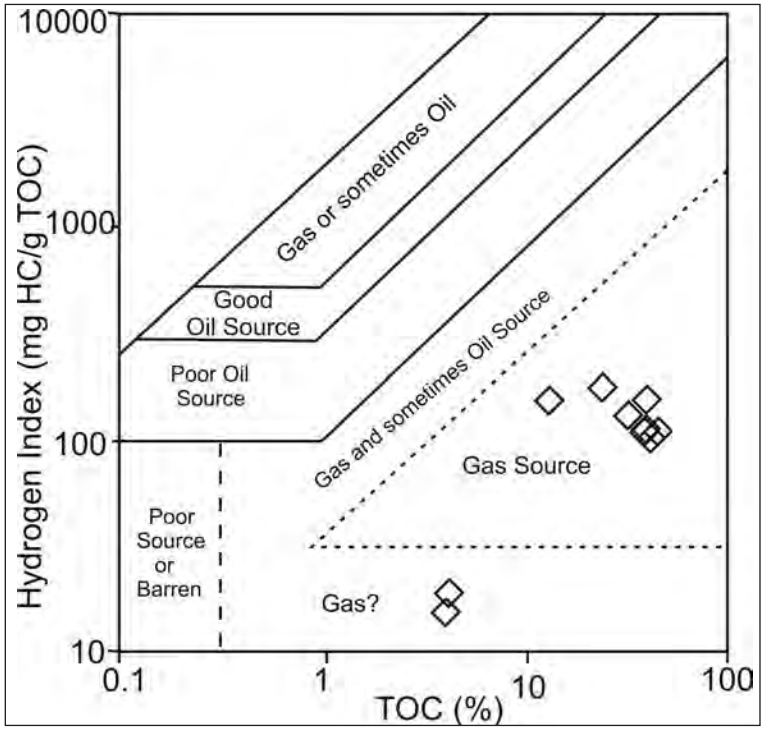

Figure 9- Hydrogen Index- T_{max} diagramme of Karlıova Halifan coal samples (developed from Jackson et al.,1985).

similar results in the same way of using (S1+S2), TOC values. Genetic potential values vary between 0.1 - 9.5 mg HC/g rock, but 6.18 mg HC/g as average. Due to finding lower values than 2 mg HC/g of the studied samples shows that they carry rare gas generation potentials (Welte, 1965; Tissot and Welte, 1984). Low values of S2/S3 from 2, PI value lower than 0.1 and T_{max} values indicate immature stages. Some samples scatter in the weak generation potential area of the HI-TOC diagramme and some samples indicate gas and little petroleum generation potential.

According to organic maturation data of the coals as well as organically rich levels, despite containing enough amounts, their maturation level is considerably low for generation. It was determined that there was a negative relation between diasterane/sterane ratio and positive relation between ßß/ (ßß/αα) ratio of T_{max} value, there is also a negative relation between R_{max} and C_{32}(22S / (22S + 22R)) ratios, in adition to these, their correlation coefficients are considerably low and were not given on the graphics.

Molecular Composition of the Coals

The leaching amount of the studied coals are low (between 14.7 and 92.4), the composition contain mostly resins and asphalthenes which are of low organic maturity. The distributions of steranes and triterpanes and their peak definitions were carried out on m/z 191 and m/z 217 chromatogrammes (Table 8, 9, 10, 11 and 12). n-alkane are distributed in C_{20}/C_{32} (Table 11) interval (Figure 10). In GC analysis low carbon numbered n-alkanes as n-C_{17}, n-C_{27}, n-C_{30} and n-C_3, as well as n-alkanes with CS_2 and benzene were determined. Typical saturated hydrocarbon GC-Mg data of the samples are shown on figure 11. Comperative abundance of long chained C_{27}-C_{31} alkanes to total n-alkanes indicate terrestrial plants (Moldowan et al., 1985), the short chained n-alkanes (<C_{20}) with their low ratio within the Karlıova Halifan samples mostly present abundantly in algaes and microorganisms. Predominantly medium and high molecular weighted n-alkanes (C_{21}-C_{25}) are common in the samples, indicating the presence of terrestrial and limnic organic material together. In m/z 217 mass chromatogrammes of the samples, C_{27}, C_{28}, C_{29} steranes and their 20S as well as 20R epimers (Table 8 and figure 11) were defined. Karlıova Halifan coal samples contain of C_{27} and C_{29} steranes with low amount of non-aromatic hydrocarbon compounds. C_{28} steranes and C_{28} diasteranes ratio of the samples are considerably low (C_{29}>C_{27}>C_{28}) (Figure 6). As it is indicated that algaes are the primary source of C_{27} steranes, C_{29} steranes are mostly derived from terrestrial plants. In addition, C_{20}, C_{21}, C_{23}, C_{24}, C_{26}, C_{28}, C_{29} tricyclic terpanes were also determined in the samples. The abundance of C_{24} tetracyclic terpane within the leachate is a 0.84 - 1.52; C_{28}/C_{29} sterane ratio between 1.30 - 1.45 in the coal samples. Especially, as in the coal samples, marine water influx to peat formation in terrestrial environments may be traced with C_{27} regular sterane abundance within C_{29} and C_{28} steranes. To Bray and Evans (1961), CPI (C_{24}-C_{34}) =1, CPI (C_{16}-C_{26}) = 2. At the m/z 191 mass fregmantogrammes, very low tricyclicterpane were traced in two samples. In Karlıova Halifan coal samples, C_{29} norhopane is much more abundant than C_{30} hopanes. Higher carbon numbered components from C_{32} homohopanes were recorded from three samples. Sterane / hopane ratio is between 0.82 - 0.85 and steranes are much more common. C_{29}/C_{30} hopane is used to differantiate carbonates from clastic lithologies (Waples and Machihara, 1991), and this ratio is between 0.53 - 0.57 for the samples (Table 8).

Depositional environment properties

The studied coals, complying with ASTM standarts, are thought to have formed in suitable terrestrial and limnic conditions which the plant parts get decayed at mostly high but oscillating

Table 9- Sterane peak determinations on m/z 217 mass chromatograms.

Component	Component Name
1	C27 13β(H),17α(H)-DIASTERANE (20S)
2	C27 13β(H),17α(H)-DIASTERANE (20R)
3	C27 13β(H),17α(H)-DIASTERANE (20S)
4	C27 13β(H),17α(H)-DIASTERANE (20R)
5	C28 13β(H),17α(H)-DIASTERANE (20S)
6	C28 13β(H),17α(H)-DIASTERANE (20R)
7	C28 13β(H),17β(H)-DIASTERANE (20S)
8	C27 5α(H),14α(H),17α(H)-STERANE (20S)+C28 13α(H),17β(H)-DIASTERANE (20S)
9	C27 5α(H),14β(H),17β(H)-STERANE (20R)+C29 13β(H),17α(H)-DIASTERANE (20S)
10	C27 5α(H),14β(H),17β(H)-STERANE (20S)+C28 13α(H),17β(H)-DIASTERANE (20R)
11	C27 5α(H),14α(H),17α(H)-STERANE (20R)
12	C29 13β(H),17α(H)-DIASTERANE (20R)
13	C29 13α(H),17β(H)-DIASTERANE (20S)
14	C28 5α(H),14α(H)-17α(H)-STERANE (20S)
15	C28 5α(H),14β(H)-17β(H)-STERANE (20R)+ C29 13α(H),17β(H)-DIASTERANE (20R)
16	C28 5α(H),14β(H)-17β(H)-STERANE (20S)
17	C28 5α(H),14α(H),17α(H)-STERANE (20R)
18	C29 5α(H),14β(H),17α(H)-STERANE (20R)
19	C29 5α(H),14β(H),17β(H)-STERANE (20R)
20	C29 5α(H),14β(H),17β(H)-STERANE (20S)
21	C29 5α(H),14α(H),17α(H)-STERANE (20R)
22	C29 5α(H),14α(H),17α(H)-STERANE (20S)
23	C30 5α(H),14β(H)-17β(H)-STERANE (20R)
24	C30 5α(H),14β(H)-17β(H)-STERANE (20S)
25	C30 5α(H),14α(H),17α(H)-STERANE (20R)

water levels. This event may be explained predominantly with abundance of huminite (gelinite) macerals. Abundance of gelinite macerals reveals terrestrial moor conditions, but fusinites moor oxidations or fires taken places (Toprak, 1996; Altunsoy and Özçelik, 1993). According to the reflection values (R_{max} %) and paleo-thermal values (Boggs, 1987), the environment was probably undergone, was of <100 °C or 100-125 °C thermal history.

Biomarker analysis of the coals is essential to reveal paleo-environmental properties. For instance, 17 α (H)-Homohopane ratio is an indicator of paleo climates (Waples and Machihara, 1991). As the ratio decrease, from C_{31} to C_{35} reflects clastic facies, high C_{31} hopane ratio indicates peat and coal presences. As evaluated in this manner, in the three samples, homohopanes are recorded and a gradual decrease of homohopane peak intensitive between C_{31}, and C_{35}, are typically observed for clastic lithol-

Table 10- Triterpane peak determinations on m/z 191 mass chromatograms.

Component	Component Name
1	C19 TRICYCLICTERPANE
2	C20 TRICYCLICTERPANE
3	C21 TRICYCLICTERPANE
4	C22 TRICYCLICTERPANE
5	C23 TRICYCLICTERPANE
6	C24 TRICYCLICTERPANE
7	C25 TRICYCLICTERPANE (22S+22R)
8	C24 TETRACYCLICHOPANE (SECO)
9	C26 TRICYCLICTERPANE 22 (S)
10	C26 TRICYCLICTERPANE 22 (R)
11	C28 TRICYCLICTERPANE
12	C29 TRICYCLICTERPANE
13	C27 18α(H)-22,29,30-TRISNORHOPANE (Ts)
14	C27 17α(H)-22,29,30-TRISNORHOPANE (Tm)
15	17α(H)-29,30-BISNORHOPANE
16	C30 TRICYCLICTERPANE
17	17α(H)-28,30-BISNORHOPANE
18	C29 17α(H),21β(H)-30-NORHOPANE
19	C29 Ts (18α(H)-30-NORHOPANE
20	C30 17α(H) DIAHOPANE
21	C29 17β(H),21α(H)-30 NORMORATENE
22	OLEANANE
23	C30 17α(H),21β(H)-HOPANE
24	C30 17β(H),21α(H)-MORETANE
25	C31 17α(H),21β(H)-30-HOMOHOPANE (22S)
26	C31 17α(H),21β(H)-30-HOMOHOPANE (22R)
27	GAMMACERANE
28	HOMOMORETANE
29	HOMOHOPANE
30	C32 17α(H),21β(H)-30,31-BISHOMOHOPANE (22R)
31	C33 17α(H),21β(H)-30,31,32-TRISHOMOHOPANE (22S)
32	C33 17α(H),21β(H)-30,31,32-TRISHOMOHOPANE (22R)
33	C34 17α(H),21β(H)-30,31,32,33-TETRAKISHOMOHOPANE (22S)
34	C34 17α(H),21β(H)-30,31,32,33-TETRAKISHOMOHOPANE (22R)
35	C35 17α(H),21β(H)-30,31,32,33,34-PENTAKISHOMOHOPANE (22S)
36	C35 17α(H),21β(H)-30,31,32,33,34-PENTAKISHOMOHOPANE (22R)

Table 11- Gas chromatography results of Karliova Halifan coal samples

Sample	Pr/Ph	n-Alkan Distribution	Explanation
BNOK-1	Not certain	n-C_{15}-n-C_{22} interval is distinctive	Biyomarkers are distinctive
BNOK-2	<1	n-C_{15}-n-C_{22} interval is distinctive	Biyomarkers are distinctive
BNOK-3	>1	n-C_{16}-n-C_{19} interval is distinctive	further Bio-degradation level second organic material
BNOK-6	Not certain	n-C_{15}-n-C_{32} interval is distinctive	Biyomarkers are distinctive
BNOK-7	>1	n-C_{15}-n-C_{22} interval is distinctive	Biyomarkers are distinctive

Table 12- Leach amount of the samples of Karliova Halifan Coals and their organic properties.

Sample	Asph %	Saturated %	Aromatic %	Polar %	Aromatic (g)	Saturated (g)	Total Leachate (ppm)	Total Leachate Amount (g)
BNOK-1	50	0.97	1.8	47.2	0.013	0.002	82.1	0.117
BNOK-2	51.7	0.44	1.9	45.9	0.003	0.001	92.4	0.110
BNOK-3	57.8	1.04	0.2	40.9	0.003	0.001	82.4	0.073
BNOK-4	-	-	-	-	0.0006	0.0001	14.7	0.010
BNOK-5	36.6	1.24	0.7	41.4	0.011	0.001	58.2	0.033
BNOK-6	48	0.59	0.3	51.1	0.013	0.002	71.5	0.117
BNOK-7	55.8	0.76	0.67	42.8	0.014	0.002	92.1	0.169

ogy (Waples and Machihara, 1991). In order to define carbonate and clastic lithology, C_{29}/C_{30} is used to characterize clastic deposition, C_{29} norhopane carbonate/ evaporite lithology (Connan, et al., 1986). Gammacerane ratio, which is an indicator of salinity, indicates layering in water column of deposition of the coals and the samples to be of Late Proterozoic age (waples and Machihara, 1991; Connan et al., 1993; Peters and Moldowan, 1993; Hunt 1995).

According to the C_{28}/C_{29} ratio, the obtained age data complies with geologic age (figure 11). Tricyclic terpanes are present in the whole samples. Comperative ratio of C_{24} tetracylic terpanes indicates terrestrial organic materrial content (Peters et. al., 2004). αß – moretane/ αß - hopane (moretane / hopane) ratio is between 0.5 - 0.6 and points out immature stage as well as salty depositional environment for organic material. Framboidal pyrites were recorded from the whole coal veins vastly and reflects anaerobic environmental conditions. Pr/Ph and diasterane/sterane ratios remark the variations in redox and depositional conditions (Peters and Moldowan, 1993; Bechtel et al., 2005). Low Pr/Pn (Ten Haven et al., 1987) value as between <0.5 and ≤ 2 as well as Pr/n C_{17} ratios to be $<$ 0.5 indicate anoxic and hypersaline environment. Low value or absence of C_{30} steranes point out limnic environment deposition, low values of C_{28} besides diasterane/sterane ratios also indicate limnic depositional environments (Peters and Moldowan, 1993). These data, previous geologic studies (Gumussu, 1984), common gastropod shells and petrographic findings, all claim that the coals have deposited in a limnic moor environment which was partially hypersaline, fault controlled and consisting of vast amount of volcanic as well as clastic materials (Table 11). Toprak (2009) also points out that similar coal occurences are very common in Turkey and

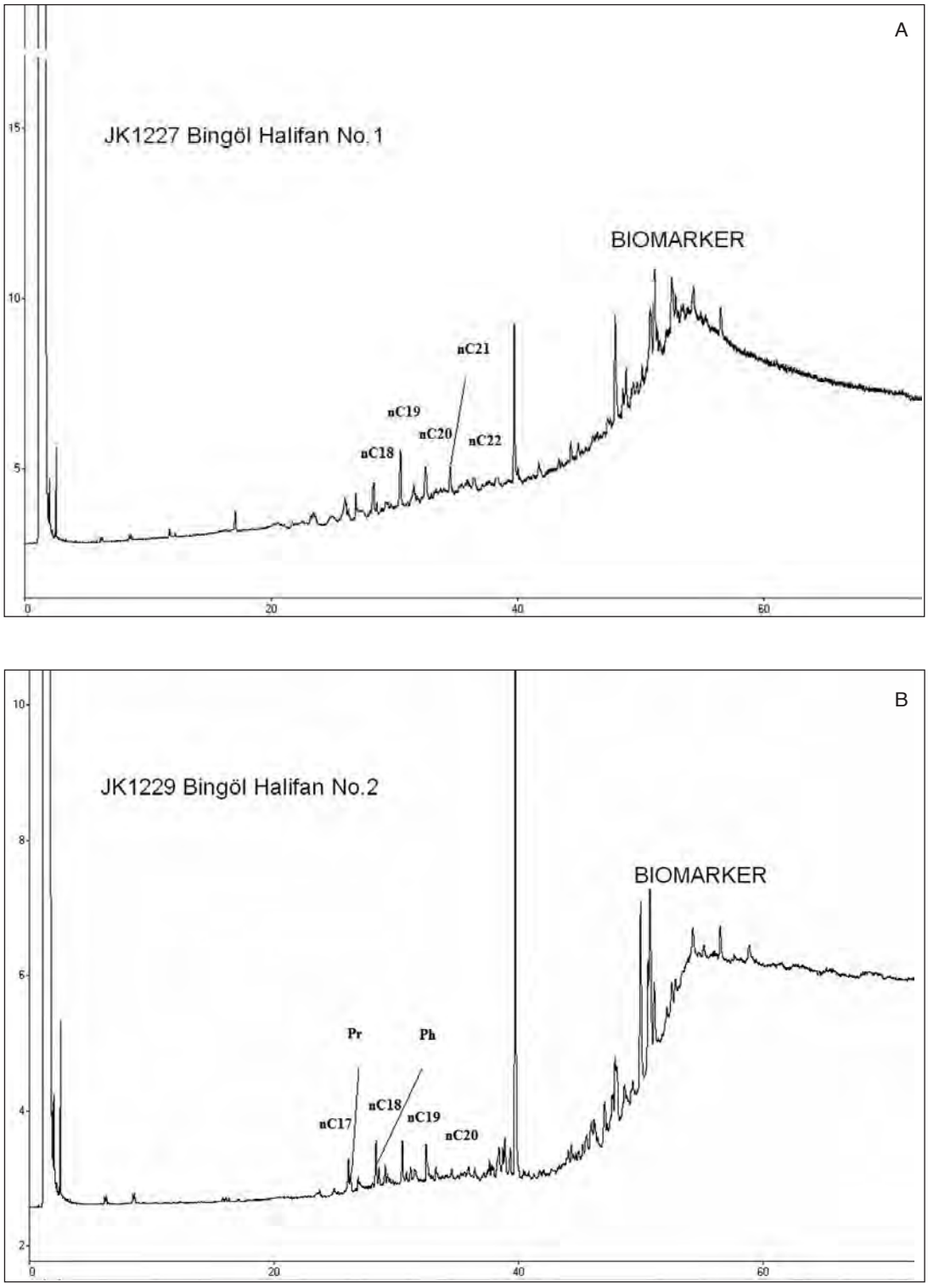

Figure 10- a,b. GC diagrammes (the mos important n-alkane series are shown on their peaks).

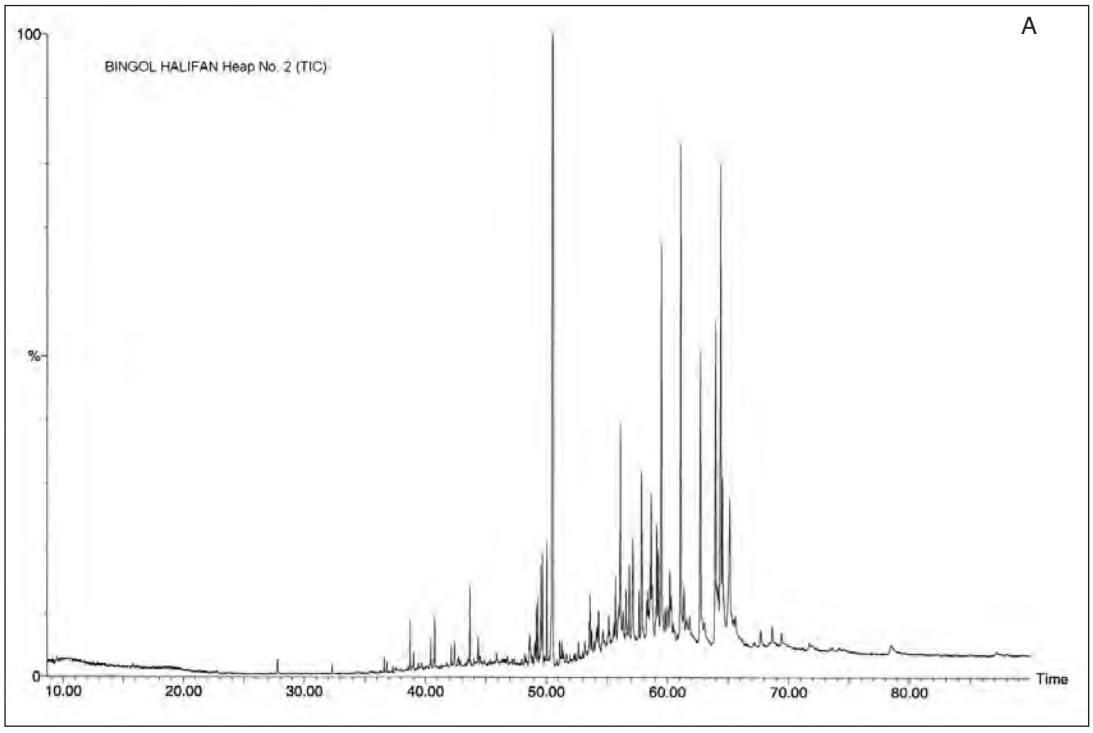

Figure 11a- GC-MS Total Ion Current (TIC) diagramme.

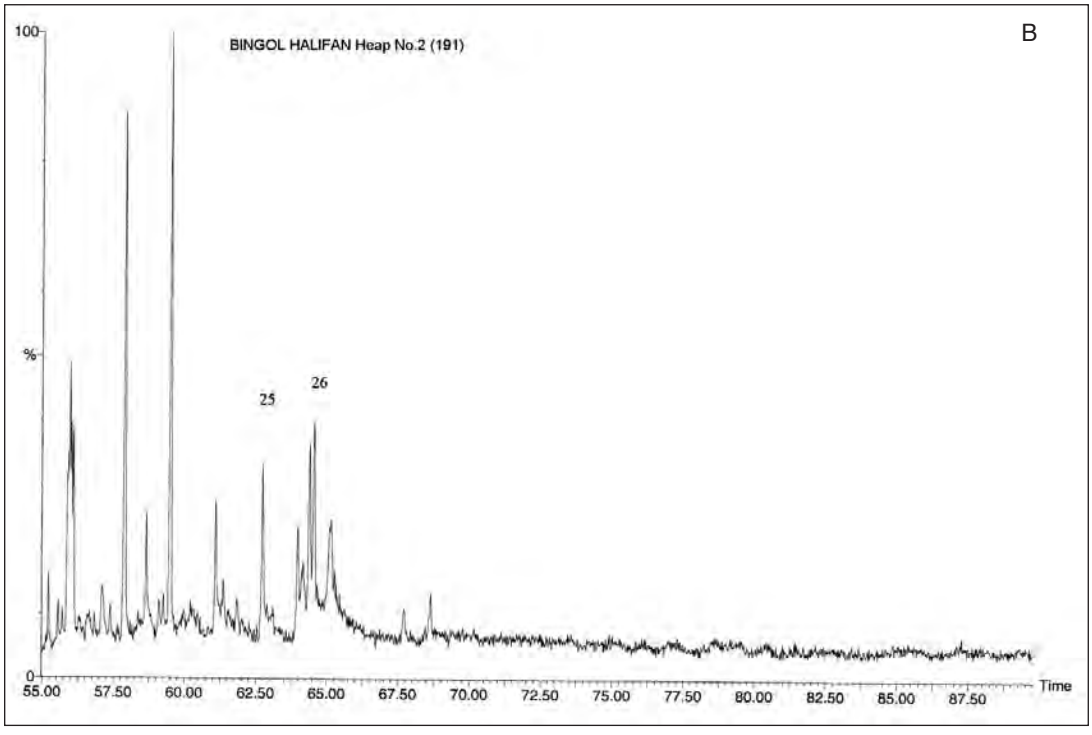

Figure 11b- GC-MS diagramme for 191

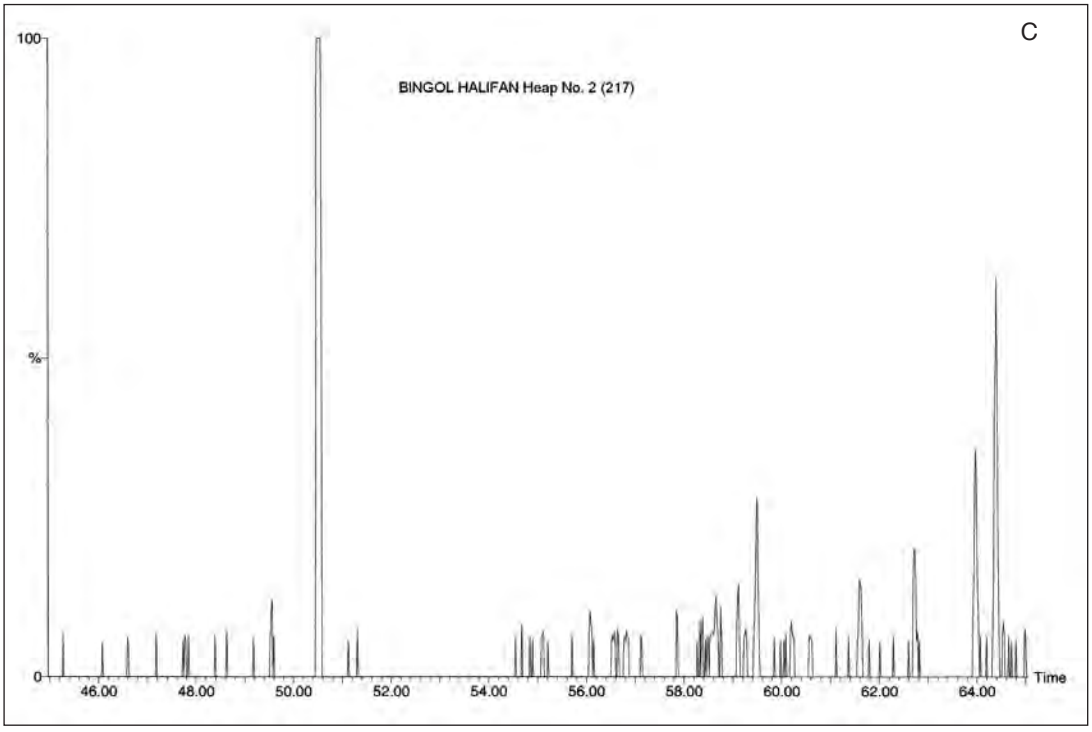

Figure 11c- GC-MS diagramme for 217

most of Tertiary coals were deposited in limnic environments.

CONSCLUSIONS AND RESULTS

In Karlıova Halifan Tertiary (Pliocene) coal basin, organic geochemical, petrographic analysis and coal quality evaluation studies were carried out on the organically rich and the coaly series. To petrographic evaluation results, Karlıova Halifan coals are rich in huminite group macerals but ratherly poor in liptinite and inertinites. Gelinite is the most abundant huminite maceral of the coals. Pyrite content of the coals is considerably high, mosty in the form of framboids.

Huminite reflection values change between 0.368 and 0.573 % and correpond to a diagenesis stage of maturity which is ratherly low. The reflection values of the coals imply that the coals have lignite and sub-bituminous coal ranks. Associated minerals of the coals are mostly clay-mica minerals, quartz and plagioclase minerals. T_{max} values vary between 401 and 435 °C (average T_{max} value is 417 °C).

These values indicate immature- premature organic stage. Alkane ratios, due to resin and asphalthene content, are considerably low and the maturity is low as well. On HI-T_{max} and hydrogen index-oxygen index diagrammes, TYPE II-III and TYPE III organic material seem to be much more abundant. The parameters obtained from organic geochemical analysis and coal petrography as well as coal quality values match with each other. Moretane/hopane and C_{32} homohopane isomerisation ratios comply with the other maturity parameters which correspond to an immature stage. As petrographic data, coal quality parameters also are compatible with Karlıova Halifan coalification rank and indicate alkaline as well as reduction environments. In general, there is a good correlation between op-

tical and geochemical data. The whole parameters indicate low lithostatic pressure effect and low maturity level. High ash content and low coalification rank of Karlıova- Halifan coals limit the utilization potential of them. According to the coal quality data, organic geochemistry and petrographical analysis results, the coals carry low maturity properties. Although they seem to exhibit some gas generation potentials, the low maturity level limits this potential.

Manuscript received september 9, 2011

ACKNOWLEDGEMENTS

This study was made possible along with DÜAPK-03-MF-85 and DÜBAP 10-MF-105 projects. The authors are thankful to Kıvılcım Önen, Veysel Yalçındağ, Muhyettin Sever, Ali Ekber Ulufer, Hüseyin Karakaş, Merve Fakıllı, Selçuk Gördük and Emine Cicioğlu Sütçü for their efforts and helps.

REFERENCES

Altunsoy, M. and Özçelik, O., 1993. Organik Fasiyesler, Jeoloji Mühendisliği Dergisi, 43, 34 - 39.

Arfaouni, A., Montacer, M., Kamoun, F. and Rig ane, A., 2007. Comperative study be tween Rock-Eval pyrolysis and biomarkers parameters: a case study of Ypresian source rocks in central-northern Tunisia: Marine and Petroleum Geology, 24, 566-578.

ASTM, 1983 and 1992. Annual book of ASTM Standarts. Gaseous Fuels; Coal and Coke (D-388-82, D-2798-79, D-3172-73, D-2799-72, D-3174-82, D-3175-82): 1916 Race Street, Philadelphia, PA 19103, 05.05, 520p.

Bechtel, A., Saschsenhofer, R. F., Zdravkov, A., Kostova, I. and Gratzer, R. 2005. Influence of floral assemblage, facies and diagenesis on petrography and organic geochemistry of the Eocene Bourgas coal and the Miocene Maritza East lignite (Bulgaria): Organic Geochemistry, 36, 1498–1522.

Boggs, S. 1987. Principles of Sedimentology and Stratigraphy. Merill Publishing Company: A Bell and Howell Company, 784p., Columbus Toronto London Melbourne.

Bray, E. E. and Evans, E. D. 1961. Distribution of n-paraffins as a clue for recognition of source beds: Geochimica et Cosmochimica Acta 22, pp. 2-15.

Burwood, R., Leplat, P., Mycke, B. and Paulet, J. 1992. Rifted margin source rock deposition: a carbon isotope and biomarker study of a West African Lower Cretaceous “Lacustrine” Section”: Organic Geochemistry 19, 41-52.

Connan, J. 1993. Molecular geochemistry in oil exploration (in: M. L. Bordenave, Editor): Applied Petroleum Geochemistry, Editions Technip, Paris, 175-204.

———, Bouroullec J. and Dessort, Albrecht, P. 1986. The microbial input in carbonate - anhydrite facies of a sabkha paleoenvironment from Guatemala: a molecular approach: Organic Geochemistry 10, 29-50.

Dağyaran. Y. 1976. Bingöl – Karlıova - Selekan Linyit Sahasına Ait Jeoloji Raporu Maden Tetkik ve Arama Genel Müdürlüğü Rapor No. 6134, Ankara (unpublished)

Diessel, K. 1986. The correlation between coal facies and depositional environments. Advances in the Study of the Sydney Basin: Proceedings of 20th Symposium, University of Newcastle, 19-22.

Durand, B. and Nicaise, G. 1980. Procedures for kerogen isolation. In: B. Durand, (Ed.), Kerogen- insoluble organic matter from sedimentary rocks): Paris, Editions Techniq, 35-53.

——— and Paratte, M. 1983. Oil potential of coals: a geochemical approach (in: Brooks, J. (Ed.), Petroleum Geochemistry and Exploration of Europe): Blackwell, Ox ford, 255-265. 51.

Erik. Y.N., Sancar, S. and Toprak, S. 2008. Hafik Kömürlerinin (Sivas) organik jeokimyasal ve organik petrografik özellikleri, TPJD Bülteni, Cilt 20, sayı 2, sayfa 9-33

Espitalié, J., Deroo, G., and Marquis, F. 1985. La pyrolyse Rock-Eval et ses applications (deuxiémepartie): Revue Institut Francais du Pétrole, v. 40, 755-784.

Flores, D. 2002. Organic facies and deposi-tional palaeoenvironment of lignites from Rio Maior Basin (Portugal): International Journal of Coal Geology, 48, 181-195.

Fowler, M. G., Gentzis, T., Goodarzi, F. and Fos-colos, A. E., 1991. The petroleum potential of some Tertiary lignites from northern Greece as determined using pyrolysis and organic petrological tech-niques: Organic Geochemistry. 17, 805-826.

Georgakopoulos, A. and Valceva, S. 2000. Petrographic characteristics of Neogene Lignites from the Ptolemais and Servia basins, Northern Greece: Energy Sources, 22, 587-602.

Gökmen, V. Memikoğlu, O., Dağlı, M., Öz, D. and Tuncalı, E., 1993. Türkiye Linyit Envanteri, Maden Tetkik ve Arama Genel Müdürlüğü, Ankara.

Gümüşsu M. 1984. Bingöl İli Karlıova İlçesi Çilliköy Kömür Sahası Jeolojisi Maden Tetkik Arama Genel Müdürlüğü Rapor No. 7686, Ankara (unpublished)

Hanson, A. D., Zhang, C., Moldowan, J. M., Liang, D. G. and Zhang, B. M., 2000. Molecular organic geochemistry of the Tarim Basin, Northwest China: American Association Petroleum Geology Bulletin 84, 1109-1128.

Heath, G.R. Moore, T.C. and Dauphin, J.P., 1977. Organic Carbon In Deep-Sea Sediments In: R.N.Andersen (Ed.), The Fate Of Fossil Fuel CO2 In The Oceans: Plenuem Press, New York.

Hubbard, B., 1950. Coal as a possible petroleum source rock: American Association Petro-leum Geology Bulletin 34 (12), 2347-2359.

Hunt, J.M. 1967. The Origin Of Petroleum In Carbonate Rocks, In G.V. Chilingar, H.J.Bissel And R.W. Farbridges eds, Car bonate Rocks, New York, Elsevier, 225-251.

———, 1995. Petroleum Geochemistry and Geology: W. H. Freeman and Company, New York, 743p.

International Committee for Coal and Organic Petrology (ICCP), 1998. The new vitrinite classification: Fuel 77, 349-358.

———, 2001. The new inertinite classification: Fuel 80, 459-471.

Iordanidis, A. and Georgakopoulos, A. 2003. Pliocene lignites from Apofysis mine, Amynteo basin, Northwestern Greece: Petrographical characteristics and depositional environment: International Journal of Coal Geology., 54, 57-68.

Jackson, K. S., Hawkins, P. J. and Bennett, A. J. R., 1985. Regional facies and geochemical evolution of Southern Denison Trough: APEA Journ., 20, 143-158.

Kalkreuth, W., Keuser, C., Fowler, M., Li, M., Mcintyre, D., Püttmann, W and Richardson, R., 1998. The petrology, organic geochemistry and palynology of Tertiary age Eureka Sound Group coals, Arctic Canada: Organic Geochemistry 29, 799-809.

Kavak, O., 2011. Organic Geochemical Comparison of Asphaltites of Şırnak Area with the Oils of the Raman and Dinçer Fields in Southeastern Turkey, Fuel, 90 (4), 1575-1583.

———, Connan, J., Erik, N.Y. and Yalçın, M.N., 2010. Organic Geochemical Characteristics of Şirnak Asphaltites in Southeast Anatolia, Turkey, Oil Shale, 27 (1), 58–83.

Kavak, O. and Toprak, S. 2011. "Gölbaşı Harmanlı (Adıyaman) Kömürlerinin Organik Jeokimyasal ve Petrografik Özellikleri", Jeoloji Muhendisliği Dergisi, Cilt 35, Sayı 1, Sayfa 43-78, Haziran, JMO, Ankara.

Kolcon, I. and Sachsenhofer, R. F. 1999. Petrography, palynology and depositional environments of the early Miocene Oberdof lignite seam, (Styrian Basin, Austria): International Journal of Coal Geology., 4, 275-308.

Korkmaz, S. and Kara G. R., 2007. Organic geochemical characteristics and depositional environments of the Jurassic coals in the Western Taurus of Southern Turkey: International Journal of Coal Geology., 70, 4, 292-304.

Kvenvolden, K. A. and Simoneit, B. R. T. 1990. Hydrothermal derived petroleum examples from Guaymas Basin, Gulf of California, and Escabana Trough, north-east Pacific Ocean: AAPG, 74, 223-237.

Langford, F. F. and Blanc-Valleron, M. M. 1990. Interpreting Rock-Eval pyrolysis data using graphs of pyrolizable hydro-carbons vs. total organic carbon:. American Association Petroleum Geology Bulletin 74, 799-804.

Moldowan, M., Seifert, W. K., and E. J., 1985. Gallegos, Relationship between petroleum composition and depositional environment of petroleum source rocks: American Association Petroleum Geology Bulletin. 69, 1255-1268.

Mukhopadhyay, P. K., Wade, J. A. and Kruge, M. A., 1995. Organic facies and maturation of Jurassic/Cretaceous rocks, and possible oil-source rock correlation based on pyrolysis of asphaltenes: Scotian Basin, Canada, Org. Geoch., 22 (1), 85-104.

Peters, K. E. 1986. Guidelines for evaluating petroleum source rock using programmed pyrolysis: American Association Petroleum Geology Bulletin., 70, 318-329

——— and Moldowan, J. M. 1993. The Biomarker Guide: Interpreting molecular fossils in petroleum and ancient sedi-ments: Prenctile-Hall, Englewood Cliffs, NJ.

————, Walters, C.C. and Moldowan, J.M., 2004. The Biomarker Guide Volume 2: Biomarkers and Isotopes in Petroleum Exploration and Earth History (second ed.): Cambridge, 475-1155.

ODTU,1984. Bingöl Karlıova Linyit Yatağı 100 MW Termik Santral İçin 1.115.000 Ton Yıl Üretim Kapasiteli Açık İşletme Projesi, Maden Mühendisliği Araştırma Merkezi.

Stach, E., Mackowsky, M.-Th., Teichmüller, M., Taylor, G. H., Chandra, D. and Teichmüller, R., 1982. Stach's textbook of coal petrology: Gebrüder Borntraeger, Berlin, 535p.

Şaroğlu. F. and Yılmaz. Y., 1987. Doğu Anadolu daki Neotektonik Dönemdeki Jeolojik Evrim ve Havza Modelleri Maden Tetkik Arama Dergisi Sayı 107. Ankara

Şengör. A. M. C., 1980. Türkiyenin Tektonik Esasları TJK Konferans Serisi 2-40 Ankara

Teichmuller, M. and Durand, B., 1983. Fluorescence microscopical rank studies on liptinites and vitrinites in peat and coals, and comparison with results of the Rock-Eval pyrolysis: International Journal of Coal Geology., 2,197- 230.

Teichmuller, M. and Littke, R. and Taylor, G. H., 1998. The origin of organic matter in sedimentary rocks (In Taylor, G. H., Teicmüller, M., Davis, A., Diessel, C. F. K., Littke, R., Robert, P., (eds)): Organic petrology, Gebrüder Borntraeger, Berlin, 704p

Ten Haven, H. L., de Leeuw, J. W., Rullkotter, J. and Sinninghe Damste, J. S. 1987. Restricted utility of the pristane/phytane ratio as a paleoenvironmental indicator: Nature 330, 641- 643.

Tissot, B. P. and Welte, D. H. 1984. Petroleum Formation and Occurrence: Springer-Verlag, Berlin, 699p.

Toprak, S. 1996. Alpagut-Dodurga (Osmancık Çorum) bölgesi çevresindeki kömürlerin oluşum ortamları ve özelliklerinin belirlenmesi, Hacettepe Üniversitesi Fen Bilimleri Enstitüsü, Doktora tezi çalışması, Ankara. (un published)

———, 2009. Petrographic properties of major coal seams in Turkey and their formation, International Journal of Coal Geology, V78, pp 263-275

Waples, D. W. and Machihara, T., 1991. Biomarkers for geologists-a practical guide to the application of steranes and triterpanes in petroleum geology: AAPG 9, p. 91.

Welte, D.H. 1965. Relation between Petroleum and Source Rock, American Association Petroleum Geology, Vol: 49, 2246-2267.

Wilkins, R. W. T. and George, S. C. 2002. Coal as a source rock for oil: a review: International Journal of Coal Geology., 50, 317–361.

Mineral Res. Expl. Bull., 144, 51-74, 2012

AN APPROACH TO PROVENANCE, TECTONIC AND REDOX CONDITIONS OF JURASSIC-CRETACEOUS AKKUYU FORMATION, CENTRAL TAURIDS, TURKEY

Ali SARI* and Derya KOCA**

ABSTRACT.- Late Jurassic-Early Cretaceous Akkuyu formation was deposited in a marine carbonate platform in Central Tarurids. The organic material of the unit is composed of Type III kerogen which is woody material transported from the land. Late Jurassic- Early Cretaceous is an important period which great anoxic events in deep sea bottom occurred due to the primary organic productivity in global sea surface. Use of several trace elements values (Ni, V, U, Cr, Co, Th) revealed that Late Jurassic-Early Cretaceous Akkuyu formation shows oxic, disoxic and anoxic paleoredox conditions. In this period the primary productivity was considerably high. Examination of specimen derived from Akkuyu formation revealed that there exist a very good positive relationship between the major oxides of Al_2O_3, SiO_2, Fe_2O_3, TiO_2, and K_2O. These combinations of major oxides indicate a detrital origin of source rock. Chemical weathering evaluations of Central Taurids in Jurassic-Cretaceous period indicated moderate and strong weathering of source rock. K_2O/Na_2O versus SiO_2; SiO_2/Al_2O_3 versus K_2O/Na_2O; Al_2O_3/SiO_2 versus Fe_2O_3 + MgO ve TiO_2 versus Fe_2O_3 + MgO diagrams indicated that Akkuyu formation was deposited along active and/or passive continental margin and derived from basalt and basalt+granite mixed rocks.

Key words: Late Jurassic-Early Cretaceous, Provenance, Central Taurids, Redox, Major oxide

INTRODUCTION

The study area is located 100 km NE of the city of Antalya (Figure 1). The late Jurassic-early Cretaceous Akkuyu formation was deposited in a marine carbonate platform in the Central Taurids. This carbonate platform was faulted and separated into several tectonic slices due to intense tectonic activity. In the late Jurassic-early Cretaceous period, as a result of global warming, ice sheets were melted, large-scale marine transgressions took place and anoxic events occurred at the sea bottom because of high primary organic productivity in the shelf areas depending on high oxygen, dissolved phosphate and nitrate abundance (Pedersen and Calvert, 1990; Caplan and Bustin, 1998).

The Akkuyu formation is within the Geyikdağı Unit of autochthon or parautochthon character and the basement of unit is comprised by gray colored, thin-medium bedded clayey limestones which change to clayey thin bedded limestones to the top. In addition, the unit is black colored, bituminous, foliated and contains shale interlayers (Figure 2).

There are some geological and petroleum geology studies conducted in the Central Taurids region and its vicinity (Blumenthal, 1951; Martin, 1969; Monod, 1977; Toker et al., 1993; Sonel et al., 1995; Albayrak, 1995; Sarı et al., 2008; Koca et al., 2010). In shelf areas, particularly dissolved phosphate, nitrate salts and big amount of oxygen content cause to organic productivity to be

* Ankara Üniversitesi, Mühendislik Fakültesi, Jeoloji Mühendisliği Bölümü, 06100 Tandoğan/Ankara ali.sari@eng.ankara.edu.tr

** Ankara Üniversitesi, Fen Bilimleri Enstitüsü, 06830 Gölbaşı/Ankara; (derya.koca@gmail.com)

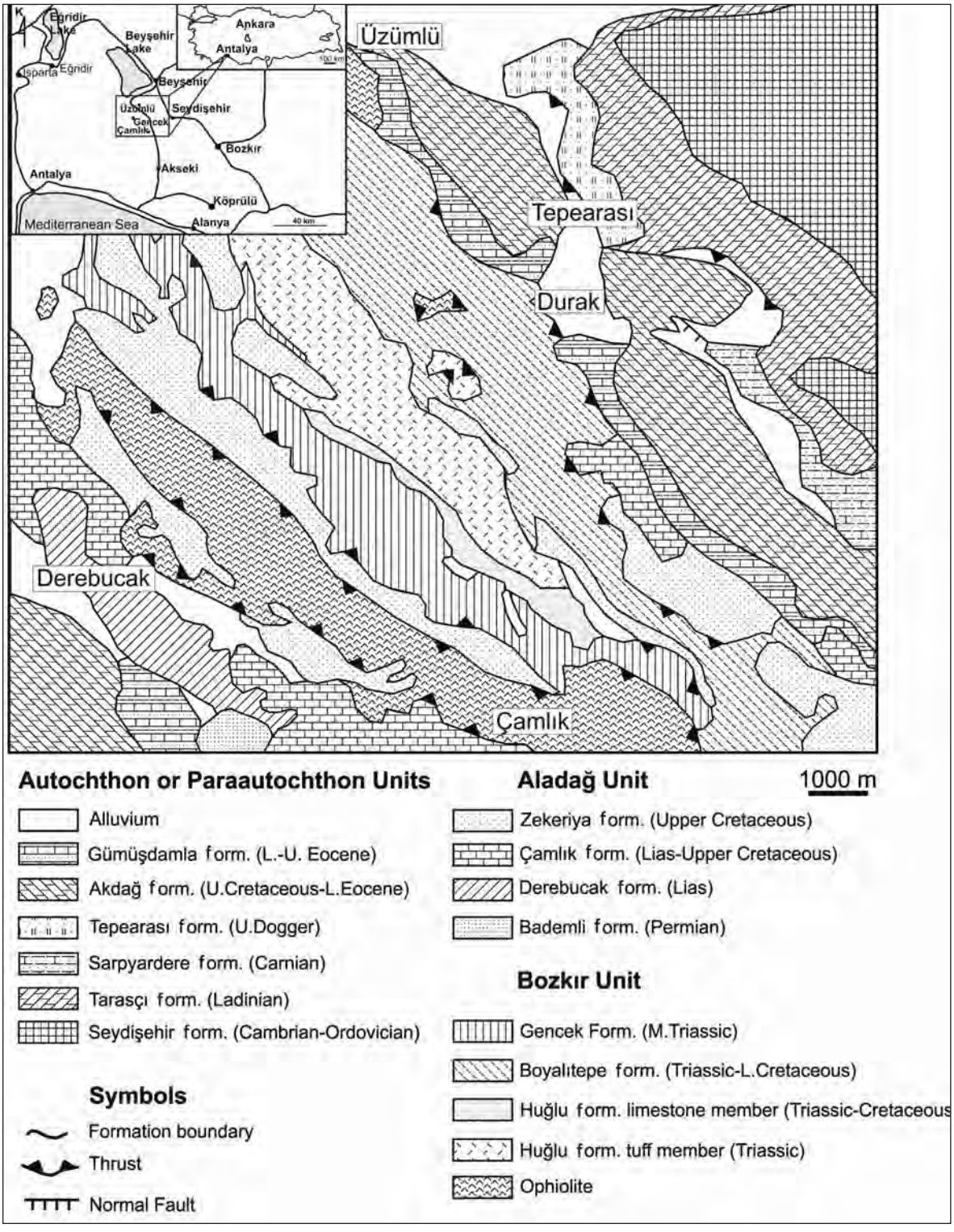

Figure 1- Geology map of the study area (Sarı et al., 1997)

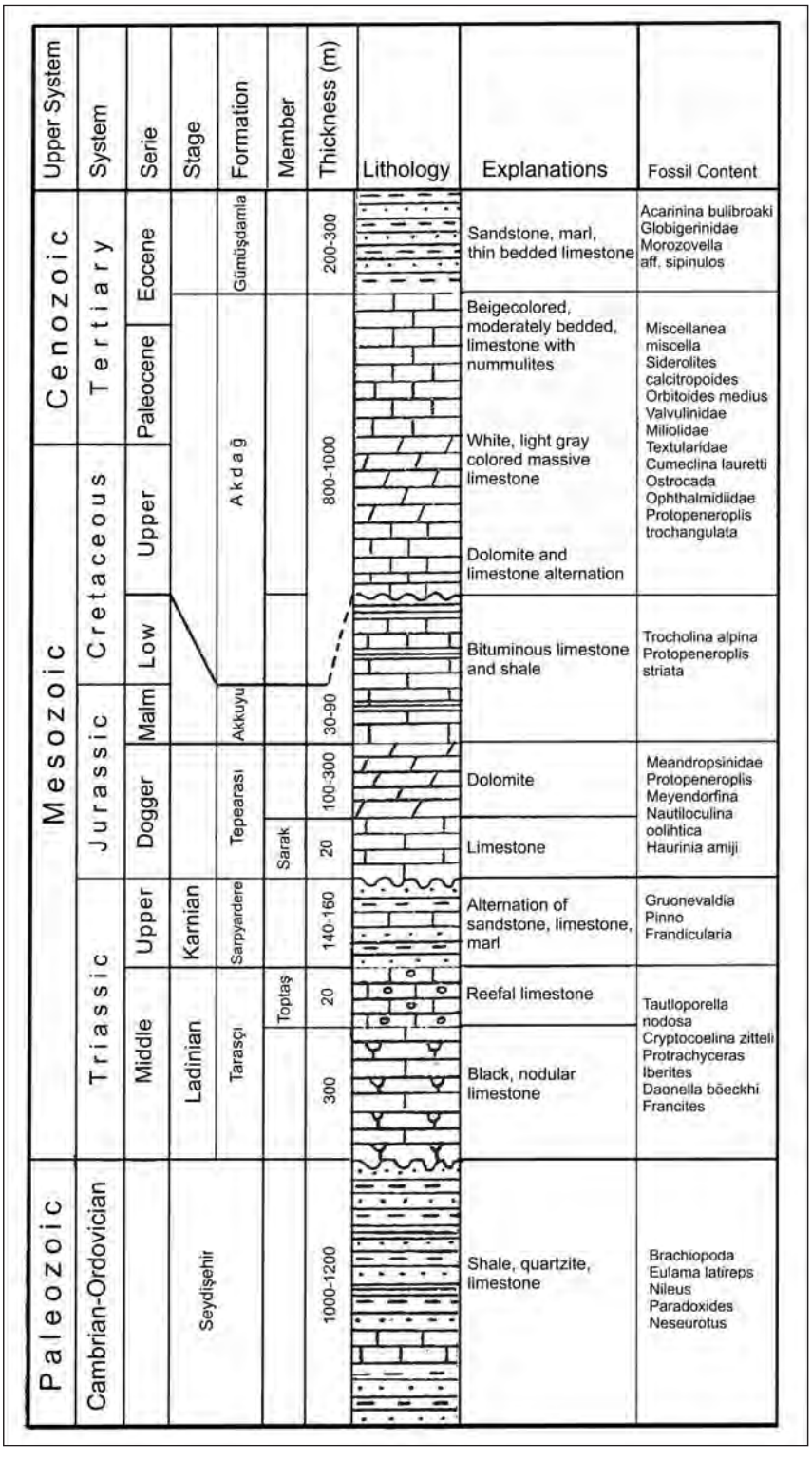

Figure 2- Stratigraphy column section of study area (Monod, 1977)

high. As a result of high organic productivity in the photic zone, upper water column cannot meet the oxygen demand of organisms in time and therefore, plant and animal planktons die in massive amounts and accumulate at the sea bottom. Because of oxygen deficiency and H_2S abundance and the organic accumulation at the bottom, bottom water changed its character to anoxic/euxinic in time which facilitated organic material enrichment like exampled in the Akkuyu formation of Central Taurides.

Organic material-rich rocks are not only important oil and gas sources but they also host economically essential elements and therefore comprise potential mineral deposits. There are a number of mineral deposits which are economically exploited from the organic material-rich rocks. For example, uranium is extracted from bituminous shales in Sweden (Andersson et al., 1985).

The main metal deposits in shale-like rocks were formed in Phanerozoic in Australia, North America and Africa. The most important and best known deposits in Africa are Zambia copper belts where a series of stratiform copper (Cu)–cobalt (Co) depositions occur in a 120 km^2 belt (Fleischer et al., 1976). The first mineralization contains at least $30x10^6$ metric tons of metallic copper (or 3% copper and 0.1-0.3% cobalt in 10^9 metric tons of deposit). Fleischer et al. (1976) described different types of Zambian copper-bearing shale deposits.

In some large, best known shale bed rocks such as Proterozoic aged Mt. Isa, Hilton, McArthur River and Lady Loretta in Australia, Pb-Zn-Ag were deposited (Gustavson and Williams, 1981). In North America best known shale-associated mineral deposits include Proterozoic White Pine Cu mineralization in Michigan and Sullivan Pb-Zn deposits in British Columbia. White Pine Cu mineralization occurs in Proterozoic Nonesuch shale which is thought to be lacustrine deposits in the Keweennawan Rift (Gustavson and Williams, 1981).

As the organic material content of rocks increases U, Ba, Sb, Cd, Mo, Rb, Se, As, Zn, Cu, Ni, Co, Cr and V element concentrations also increase. The reason for significant enrichment of these elements in organic material-rich rocks rather than country rocks is attributed to primary production of organic material in upper water, column sedimentation rate, redox conditions (Eh, pH) of depositional environment, H_2S enrichment by sulfate-reducing bacteria, organic material preservation and precipitation of sulfide components.

In this study, depositional conditions of organic material-rich rocks of Akkuyu formation are determined based on their organic material contents. The source and weathering levels of samples are also investigated.

MATERIAL AND METHOD

In this study, a number of 10 organic material-rich rock samples systematically collected from late Jurassic-late Cretaceous Akkuyu formation (Central Taurids) were subjected to various geochemical, petrographic and clay analyses. The organic carbon analysis (TOC %) was performed at TPAO laboratories using WR - 12 type carbon analysis device. Using the pyrolysis device (Oil Show Analyzer) S_1, S_2, S_3, T_{max}, oxygen index (OI) and hydrogen index (HI) values were determined. From HI and T_{max} values kerogen types were identified. Major oxide (Al_2O_3, SiO_2, MgO, CaO, K_2O and TiO_2) and trace element (U, Ba, Cu, Ni, Cr, As, V, Zn, Sb, Co, Mo and Cd) analyses of organic carbon-rich (C_{org}) samples of the Akkuyu formation were carried out at Engineering Faculty Geochemistry Laboratories of the Ankara University. Samples were first prepared for geochemical analysis at the Micro Analysis-ICP Laboratory. Samples were grinded on a Retsch brand automatic rock grinder and then crushed with a FRITSCH brand automatic crusher on a

carbide mill. 4 g sample was mixed with 0.9 g binding material (Wachs) and compressed under hydraulic press to have powder-pellets (with pellet diameter of 32 mm). The samples were analyzed at X-Lab 2000 model PED-XRF (Polarized Energy Dispersive XRF) device for major oxides and trace element contents. XRF analysis was conducted with Tq-7220 method. Whole rock clay analysis was carried out with Rigaku brand XRD device at MTA laboratories. The Pearson correlations were computed with the Statistica program.

Organic material type and element relations

Using the hydrogen index (HI: mgHC/g rock; S_2*100/TOC) and T_{max} (°C) values from pyrolysis analysis, with the exception of sample AK-8 (Type-II), the organic material type of analyzed samples was found as Type-III (Figure 3). Type II kerogens are composed of spore, pollen, terrestrial plant cuticles, lipids, resins and marine algae whilst Type-III kerogens are made up of terrestrial plants, trees and cellulose. Deposition of organic material-rich marine sediments depends on several factors which include anoxic/low oxygenated bottom water (Erbacher et al., 2001), high primary productivity facilitating organic carbon flux to the sea bottom (Pedersen and Calvert, 1990; Ibach, 1982), sedimentation rate (Pedersen and Calvert, 1990), fast burial preventing microbially-mediated organic material decomposition, upwelling (Suess et al., 1987), protective adsorption of organic materials on clay minerals (Hedges and Keil, 1995) and dilution by inorganic components (Demaison and Moore, 1980).

Under anoxic conditions accumulation and transfer ratios of certain trace elements could be high and noteworthy trace element exchange also takes place in seawater (Nijenhuis et al., 1999; Morford et al., 2001). In addition, under low oxygenated conditions, organic material-rich sediments are generally enriched in redox-sensitive and sulfide-forming metals which trap trace elements (Arnaboldi and Meyers, 2003; Brumsack, 2006). In this respect, the enrichment level of elements in organic material-rich rocks of the Akkuyu formation was investigated. Enrichments of some trace elements such as V, Co, Ni, Cu, Zn, Se, Cd, Mo, U are found to be greater than that of average shale.

Identification of Paleoredox conditions for Late Jurassic-Early Cretaceous Period

Under dioxic-anoxic and euxinic redox conditions, metals are mostly accumulated as metal sulfides. The greatest metal enrichment occurs under euxinic redox conditions which reflect complete sulfide phase (Warning and Brumsack, 2000; Arnaboldi and Meyers, 2003; Brumsack, 2006). Several trace elements such as Mo, Mn, Ni, V, U, Cr, Co have been used to evaluate paleoredox conditions (Hatch and Leventhal, 1992; Jones and Manning, 1994; Algeo and Maynard, 2004; Rimmer et al., 2004). Certain elements, which are sensitive to redox changes in marine environment and pore waters, are used for reconstruction of redox conditions in young and old sedimentary basins associated with organic material deposits and sulfide occurrences in oxygen-poor mediums (Brumsack, 2006; Tribovillard et al., 2006). Oxidation of sulfides produces a sulfate source for sulfate-reducing bacteria which facilitates anoxic conditions (Brüchert et al., 2003). It is believed that Ni and V are preferentially retained in tetrapyrrole structure which is preserved under anoxic conditions (Lewan and Maynard, 1982). Lewan (1984) suggested that V/Ni ratio in crude oil which is not altered by diagenesis reflects environmental conditions during the deposition and showed that V/(V+Ni) ratio for organics forming under euxinic conditions is greater than 0.5. According to Hatch and Leventhal (1992), V/(V+Ni) ratios are greater than 0.84 for euxinic conditions and in the range of 0.54 – 0.82 for anoxic conditions and between 0.46 and 0.60 for dioxic conditions. Vanadium which is incorporated into tetrapyrrole

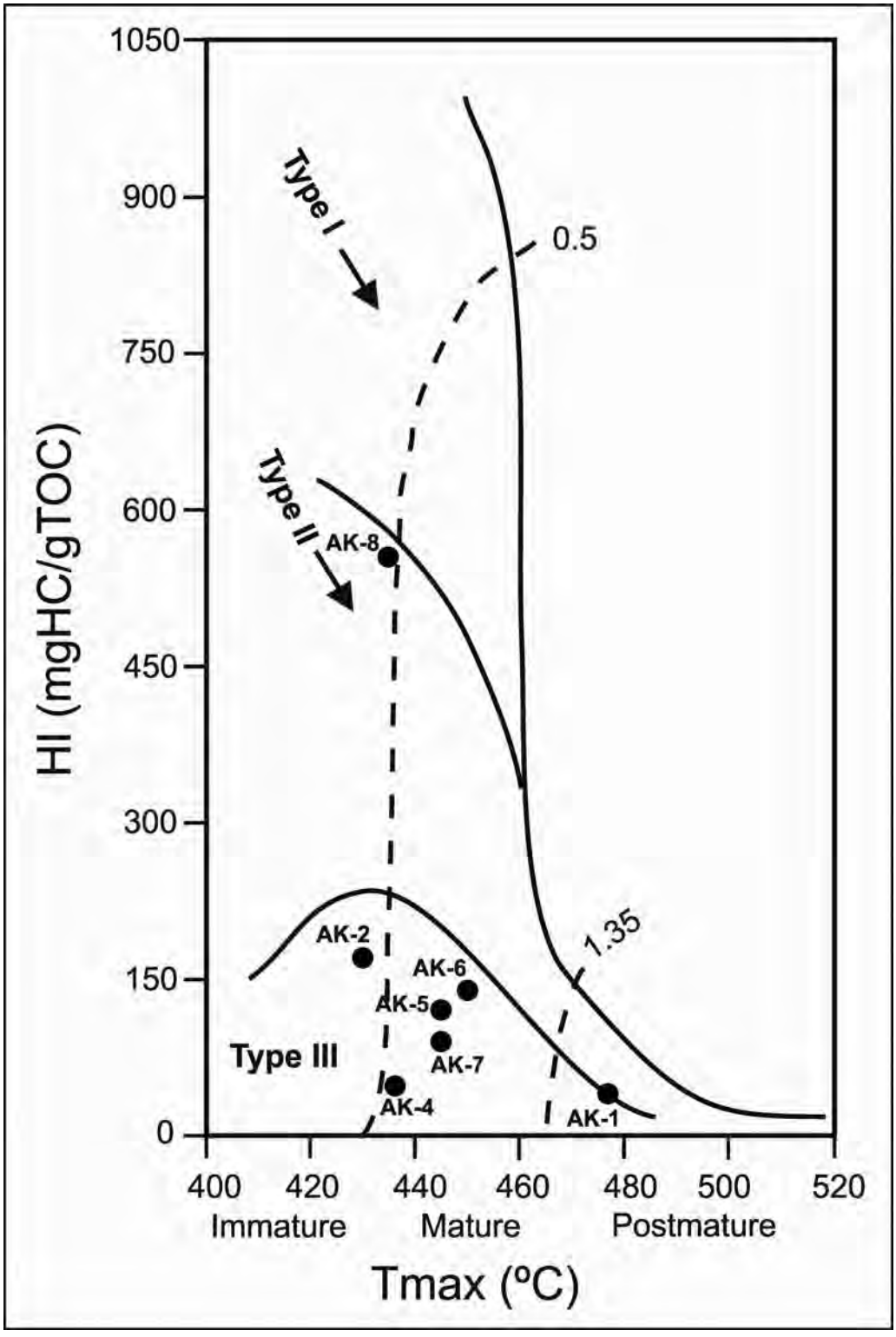

Figure 3- Kerojen Types of Akkuyu formation's samples according to HI-T_{max} graphic

structure under anoxic conditions may also be precipitated by adsorbing onto surface of clay minerals which most probably occurs after burial (Breit and Wanty, 1991). Cr is thought to be related only to detrital fraction (Dill, 1986) and it is not affected by redox conditions, and thus, high V/Cr ratios (> 4.25) are believed to reflect anoxic conditions (Jones and Manning, 1994). Jones and Manning (1994) used V/Cr ratio to evaluate the paleoenvironment characteristics. V/Cr ratio is suggested as an index for paleo-oxidation conditions (Dill et al., 1988). In reduced sediments Ni and V are retained by organic material (Lewan and Maynard, 1982). Cr and Co contents are thought to have a detrital origin (Ross and Bustin, 2006). Both Ni and Co are incorporated into pyrite structure. However, high Ni/Co ratios are believed to be related to anoxic conditions (Jones and Manning, 1994). Ni/Co value of samples of the Akkuyu formation reflects dioxic/anoxic; V/Cr ratio reflects oxic-dioxic and anoxic, V/V+Ni values reflect oxic and anoxic and U/Th ratio reflects dioxic and anoxic conditions (Figure 4; table 1).

As shown from figure 4, the basement of depositional environment of the Akkuyu formation was well oxygenated and organic productivity was abundant at surface conditions, but later, as a result of oxygen and nutrient deficiency in the upper water column, organisms (plankton and algae) were undergone a mass die off and H_2S-rich fluids issued at the bottom. In the middle levels dioxic conditions were prevailed due to insufficient H_2S whilst because of significant H_2S abundance to the upper levels anoxic conditions were dominant.

Paleoproductivity in the Late Jurassic-Early Cretaceous Period

Nutrient need of marine organisms, particularly planktonics, are met by phosphate and nitrate salts which are dissolved and transported by the rivers. Nitrogen (N) and phosphorus (P) exert a major control on biologic productivity in the marine environment (Holland, 1978). Changes in P concentration are attributed to variations in continental weathering (Algeo et al., 1995; Algeo and Scheckler, 1998), C/P variation in sedimentary organic material composition (Ruttenberg and Goñi, 1997) or variation in P flux under anoxic or very low oxygenated bottom water conditions (Ingall and Jahnke, 1997; Murphy et al., 2000). In general, Ba, P and Cd are used as geochemical indicators for paleoproductivity (van Capellen and Ingall, 1994; Filipelli et al., 1994). High P and Ba contents reflect strong primary organic productivity. The presence of P-bearing apatite which can concentrate Cd and rarely seen high Cd content can be attributed to reducing conditions prevailed at the bottom. Similarities of hydroxyapatite and frequently repeated Cd enrichment in phosphorite deposits are reported in various studies (Middleburg and Comans, 1991). In the studied samples, P and Cd concentrations are extremely enriched with respect to average shale while Ba shows slight enrichments (Figure 5). The similar Cd, P and Ba element enrichments are indicative of high productivity of environment.

The strong positive correlation between Cd/Al and P/Al pairs in the studies samples of

Table 1- Paleoredox proxies metals

	Oxic	Dysoxic	Anoxic	Euxinic
Ni/Co[1]	< 5	5 – 7	> 7	
V/Cr[2]	< 2	2 – 4.5	>4.5	
V/(V+Ni)[3]	< 0.46	0.46 – 0.60	0.54 – 0.82	> 0.84
U/Th[4]	< 0.75	0.75 – 1.25	> 1.25	

[1,2,4] Jones and Manning (1994)
[2] Dill et al. (1988)
[3] Hatch and Leventhal (1992)

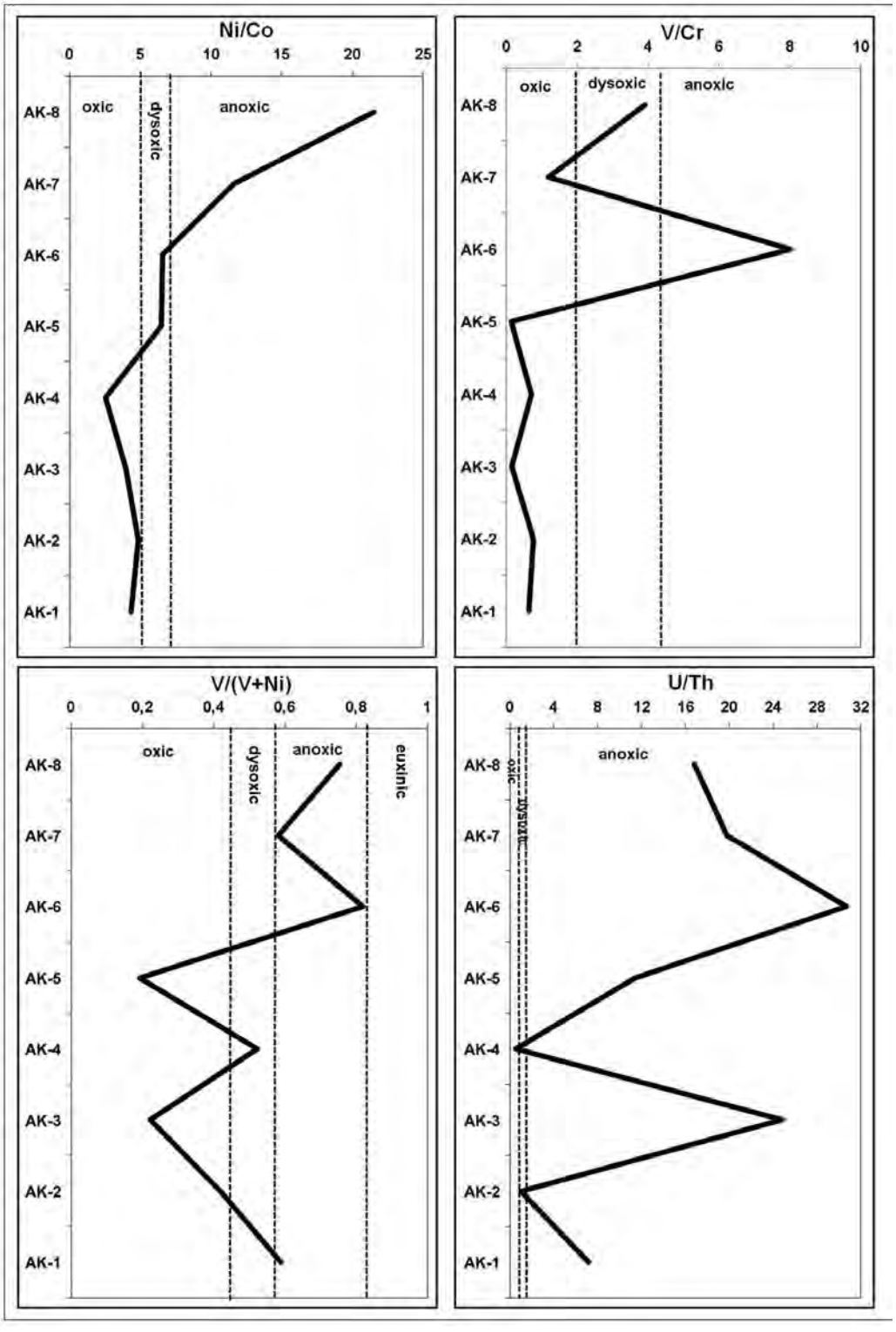

Figure 4- Paleoredox conditions of Akkuyu formation samples

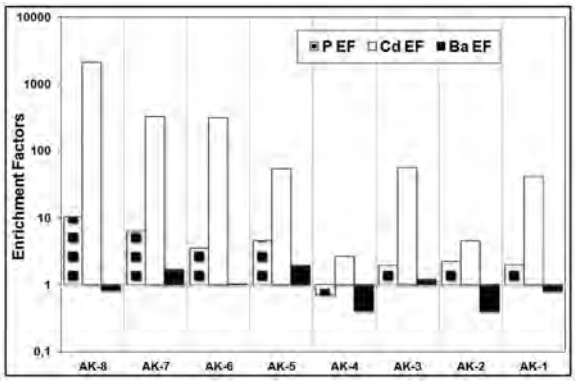

Figure 5- Cd, P and Ba enrichment factors

the Akkuyu formation (r=0.88; R^2=0.78) implies that primary paleoproductivity of the unit is high (Figure 6).

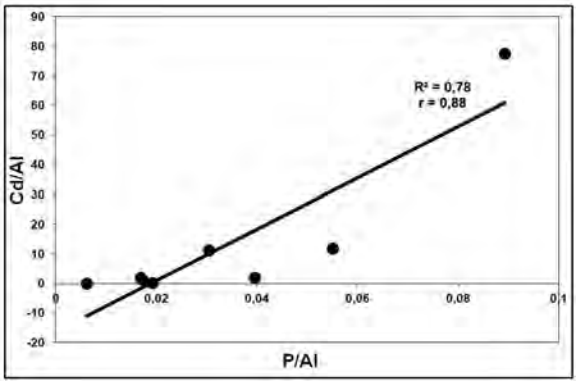

Figure 6- Relationship between Cd/Al and P/Al

Major Element Investigations in the Akkuyu formation

Major oxide compositions of samples are shown in table 2. CaO is the most abundant major oxide with a concentration range from 11.36 to 57.80%, excluding sample AK-4 (5.81%). In shales CaO content is 1-10% and rocks with high CaO content (25-75%) are generally categorized as marl. Ca in rocks is derived from Ca-rich plagioclases and particularly carbonates (e.g. calcite and dolomite). Calcium is also found in some clay minerals, gypsum and anhydrite. SiO_2 concentration in sample AK-4 is 48.83% and it ranges from 2.73 to 36.52% in other samples.

SiO_2 content in fine-grained rocks is controlled by silicate minerals but particularly quartz which is the main constituent of most shales and mudstones. Al_2O_3 concentration in sample AK-4 is 15.13% and it ranges from 0.76 to 9.99% in other samples. Al_2O_3 is particularly associated with the abundance of feldspar and clay minerals (Boggs, 2009). Since shale and marl are composed of the mixture of three major oxides – SiO_2 (detrital quartz and/or biogenic silica), Al_2O_3 (clay fraction) and CaO (carbonate content) – lithology of the samples can be investigated on the SiO_2-Al_2O_3-CaO triangular diagram (Table 2; figure 7). The diagram in figure 7 shows that samples tend to plot close to carbonate corner rather than detrital and clay fraction indicating that, with the exception of samples AK-4 and AK-2, all other samples are represented by the marl lithology.

Akkuyu samples have K_2O content of 0.26 – 2.85%, Mg content of 0.26 – 8.75% and Na_2O content of 0.09 –1.04% (Table 2). In average shale concentrations of both K_2O and MgO are less than 5%. K and Mg contents of shales and mudstones are greatly affected by clay minerals. In addition, Mg and K contents increase with in-

Table 2- Major oxides (%) and trace elements (ppm) values of study area samples

Sample	SiO_2	Al_2O_3	Fe_2O_3	MgO	CaO	Na_2O	K_2O	TiO_2	P_2O_5	MnO	V	Cr	Ni	Cd	U	Th	Co	Rb
AK-8	4,57	1,59	0,76	0,23	30,99	0,12	0,75	0,17	0,17	0,003	1011,66	259,31	328,09	65,5	15,1	0,9	15,26	12,62
AK-7	5,01	1,34	0,63	0,04	46,40	0,10	0,66	0,08	0,09	0,003	216,78	182,00	155,68	8,4	17,8	0,9	13,37	14,08
AK-6	7,13	1,47	0,53	0,49	49,32	0,09	0,50	0,08	0,05	0,002	570,25	71,16	125,42	8,8	18,4	0,6	19,03	15,36
AK-5	2,74	0,76	0,24	0,25	57,80	0,09	0,30	0,05	0,04	0,003	14,56	117,00	61,22	0,8	10,3	0,9	9,44	7,22
AK-4	48,83	15,13	5,88	3,01	5,81	0,23	2,85	0,77	0,11	0,048	147,88	207,31	135,72	0,8	7,6	14,5	52,93	131,95
AK-3	3,65	1,01	0,34	0,19	56,24	0,09	0,38	0,05	0,02	0,004	15,68	106,74	54,85	1,1	14,9	0,6	13,84	10,24
AK-2	36,52	9,99	6,43	8,75	11,36	1,04	1,56	0,52	0,23	0,137	136,68	177,21	189,62	0,9	7,5	7,5	38,93	66,02
AK-1	2,93	1,38	0,54	0,26	56,72	0,09	0,26	0,12	0,03	0,005	64,98	101,95	45,50	1,1	8,6	1,2	10,46	8,05

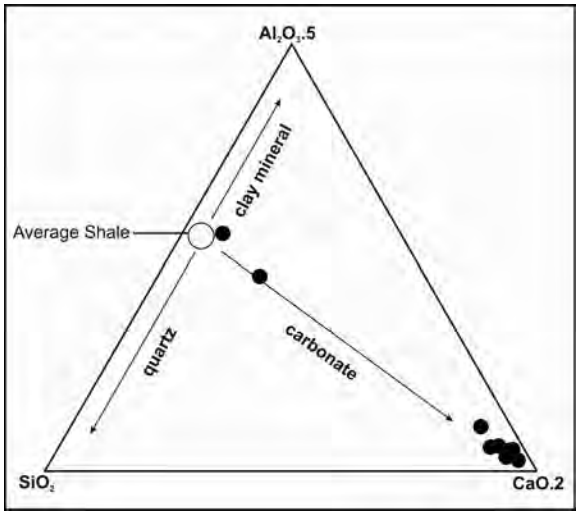

Figure 7- SiO_2-Al_2O_3-CaO ternary diagram (Brumsack, 1989)

creasing dolomite and K-feldspar abundances, respectively. Shales with >5% K_2O are quite rare. In other words, high K content of shales is closely related to presence of authigenic K-feldspar. The average Na_2O concentration in shales is about 1-3%. Na content is controlled by both smectite and Na-plagioclase. Fe_2O_3 content in the studied samples is in the range of 0.24 – 6.43%.

Iron is incorporated into iron-oxide minerals (hematite, limonite, and goethite), some micas (biotite, smectite and chlorite), clay minerals and carbonate minerals (siderite, ankerite). Furthermore, in some organic-carbon rich shales significant amount of iron exists in sulfide minerals (pyrite, marchesite).

Petrographic/microscopic methods and XRD determinations are effective tools for classification of rocks. In this respect, petrographic and XRD analyses of samples were carried out. Results of petrographic studies yield that samples are of micritic-sparitic packstone, mudstone and grain stone and show oil indication. Matrix is composed of micrite and less amount of sparite. Whole rock XRD determinations reveal that samples are composed of calcite, quartz, kaolinite, anorthite, illite and muscovite.

Si_2O/Al_2O_3 and Fe_2O_3/K_2O ratios are also used for classification of sedimentary rocks (Pettijohn et al., 1987; figure 8). Si_2O/Al_2O_3 ratio reflects clay and feldspar contents and quartz abundance (Potter, 1978). Based on Pettijohn et al. (1987) diagram, among the studies samples, samples AK-1, 3, 5 and 6 with CaO content above 47% are in the shale field while samples AK-2, 4, 7 and 8 with CaO content less than 47% are plotted in the wacke field. Among the methods used to classify detrital sedimentary rocks, the one based on Ca-enrichment shows the effectiveness of chemical processes in formation of rocks.

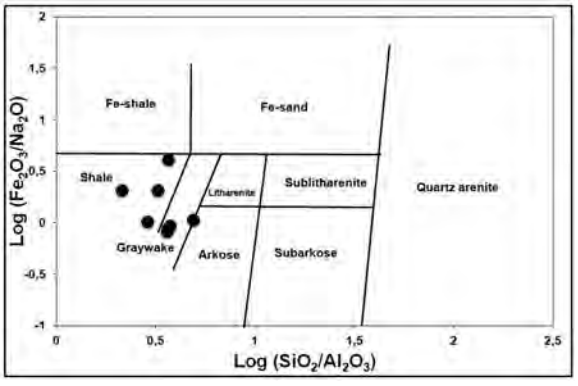

Figure 8- Fe_2O_3/K_2O versus Si_2O/Al_2O_3 diagram (Pettijohn et al., 1987)

Determination of source by major oxides

Al_2O_3 content of the samples is strongly and positively correlated with SiO_2, Fe_2O_3, TiO_2 and K_2O (Table 3, figure 9). This may indicate that SiO_2, Al_2O_3, Fe_2O_3, MgO and K_2O are derived from the same source and their source region is most probably detrital materials transported to the basin. However, as shown from table 3, there are strong negative correlations between CaO which represents for carbonate lithologies and SiO_2, Fe_2O_3, Al_2O_3, MgO and K_2O which repre-

Table 3- Correlations between major oxides

	C_{org}	SiO_2	Al_2O_3	Fe_2O_3	MgO	CaO	Na_2O	K_2O	TiO_2	P_2O_5	MnO	Cr_2O_3
C_{org}	1,00	-0,26	-0,29	-0,16	0,02	-0,12	0,13	-0,22	-0,21	0,54	0,01	0,49
SiO_2		1,00	**1,00**	**0,97**	**0,75**	**-0,92**	**0,62**	**0,96**	**0,98**	0,57	**0,76**	0,39
Al_2O_3			1,00	**0,95**	**0,70**	**-0,91**	0,57	**0,98**	**0,99**	0,54	**0,71**	0,42
Fe_2O_3				1,00	**0,89**	**-0,92**	**0,79**	**0,89**	**0,95**	**0,70**	**0,89**	0,41
MgO					1,00	**-0,74**	**0,98**	0,58	**0,69**	**0,77**	**1,00**	0,25
CaO						1,00	**-0,65**	**-0,92**	**-0,94**	**-0,82**	**-0,75**	**-0,68**
Na_2O							1,00	0,43	0,56	**0,79**	**0,98**	0,23
K_2O								1,00	**0,98**	0,53	0,59	0,53
TiO_2									1,00	0,59	**0,70**	0,49
P_2O_5										1,00	**0,77**	**0,73**
MnO											1,00	0,27
Cr_2O_3												1,00

sent for detrital materials. Strong positive correlations between Al_2O_3 vs. SiO_2-Fe_2O_3-TiO_2-K_2O also reflect association of these elements with clays.

SiO_2 is also strongly and positively correlated with MnO (r=0.76), MgO (r=0.75), Na_2O (r=0.62) and P_2O_5 (r=0.57) (Table 3, figure 9). Silica incorporating into sedimentary rocks is mostly of terrestrial origin. Detrital silicates maybe derived from both silica (e.g. quartz) and biochemical constituents (e.g. radiolarite, diatom and spicules). In marine environments, chert might be precipitated from silica in hydrothermal solutions. Strong and moderately strong correlations between SiO_2 and MnO-MgO-Na_2O-P_2O_5 in the studied samples indicate that these elements are of terrestrial origin and most probably transported to the basin as detrital constituents.

The presence of a negative correlation between Al_2O_3 and CaO (r= -0.91) implies that these two elements are derived from different sources (Table 3, figure 9). As known, Al_2O_3 is of terrestrial origin whilst CaO is derived from carbonates. The abundances of terrestrial elements Al_2O_3, SiO_2, Fe_2O_3, MgO, MnO, K_2O and TiO_2 are very low but CaO contents are generally high. The fact that Late Jurassic Akkuyu formation is mostly comprised by micrites which are accompanied by oil shales might indicate that the unit was deposited in a restricted carbonate platform in the central Taurids.

Al_2O_3 vs. TiO_2 plots for most clastic rocks are commonly used to determine source rock composition. In the Al_2O_3-TiO_2 diagram (Amajor, 1987) basaltic and granitic source rocks were discriminated (Figure 10).

Al_2O_3 vs. TiO_2 diagram shows that source material of most samples is in basalt composition while composition of samples AK-2 and AK-4 is in the range of granite to basalt. Although in the Al_2O_3-TiO_2 diagram samples are clustered at the beginning of basalt curve, in K_2O-Rb graphic (Figure 17) two samples (AK-2 and 4) are represented by acidic+intermediate composition and other 6 samples are plotted in the basic composition field indicating that samples are mostly of basaltic composition. The Al_2O_3/TiO_2 ratio is 3-8% for mafic magmatic rocks, 8-21% for rocks of mixed composition and 21-70% for felsic rocks. The Al_2O_3/TiO_2 ratio which includes rocks with intermediate composition also reflects Ti-bearing mafic phases derived from felsic and basic rocks (Table 4).

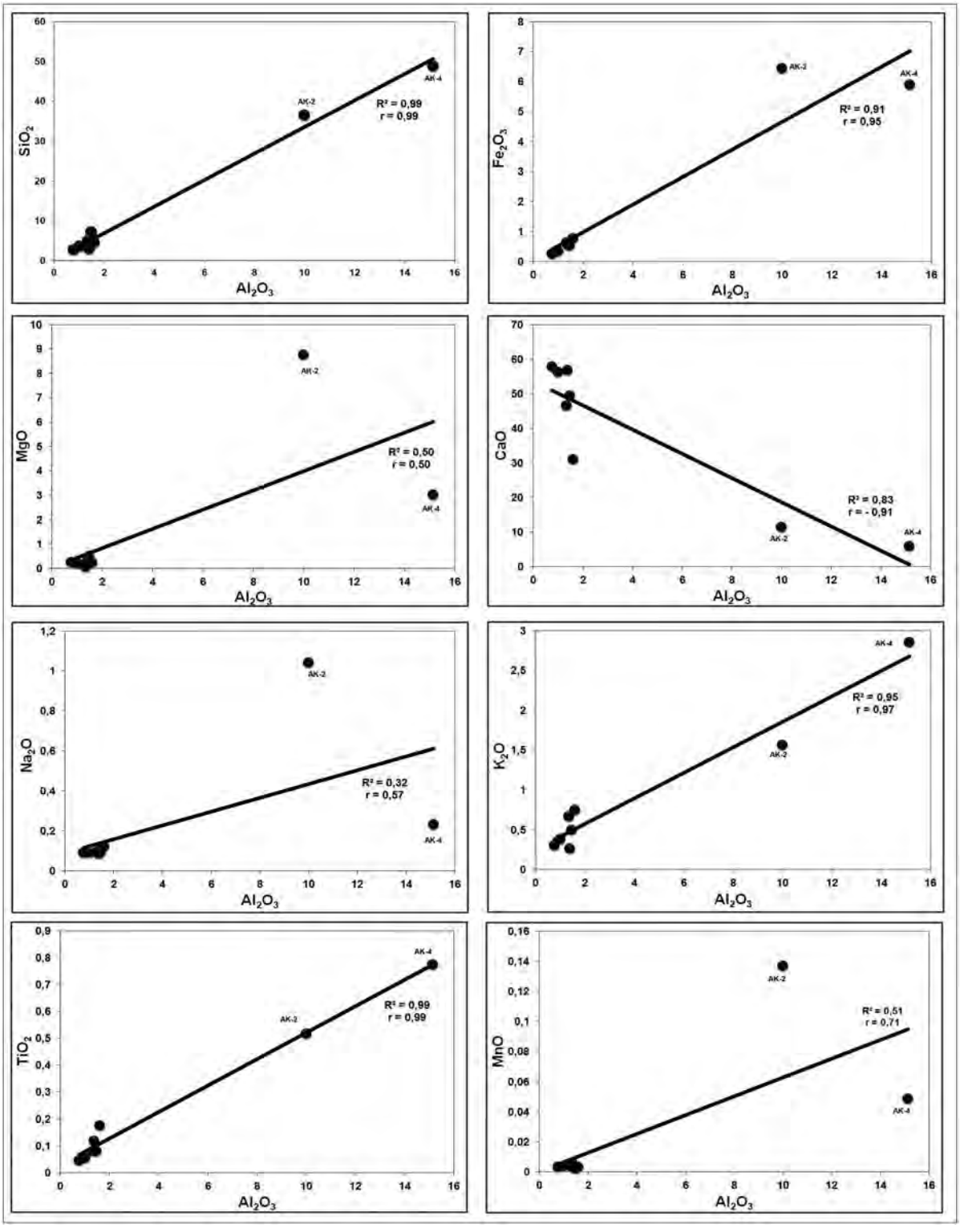

Figure 9- Relationship between Major oxides and Al_2O_3

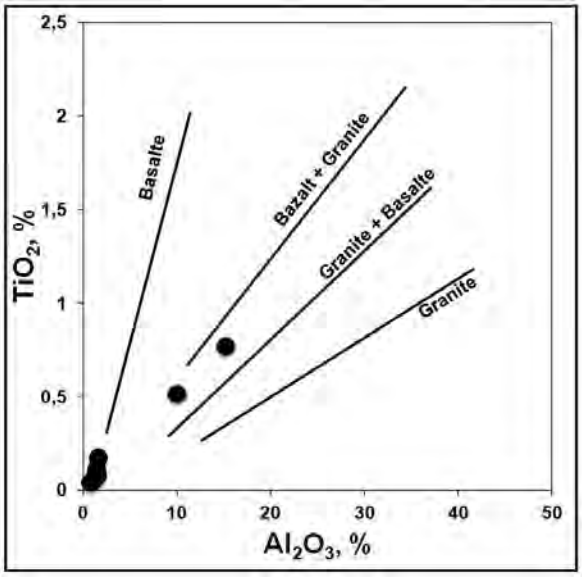

Figure 10- TiO_2 versus Al_2O_3 diagram

Table 4- Al_2O_3/TiO_2 ratio of Akkuyu formation samples

Sample	Al_2O_3/TiO_2
AK-8	9,15
AK-7	16,71
AK-6	18,28
AK-5	16,86
AK-4	19,57
AK-3	18,66
AK-2	19,35
AK-1	11,75
Mafic Magmatic	3 – 8
Intermediate	8 – 21
Felsic	21 – 70

Strong correlation between Cr and Ni and high concentrations of these elements were used by several authors to determine source of the sedimentary rock changing from mafic to ultramafic (Hiscott 1984; Garver et al., 1994, 1996). Cr and Ni concentrations in shales reflect Cr and Ni incorporation into clay particles during the course of weathering of chromite other Cr- and Ti-bearing minerals in the ultramafic rocks (Garver et al., 1996). In the studied samples Cr-Ni pair shows strong and positive correlations (r=0.82; figure 11). High Cr content in samples is most probably derived from variations in source composition and detrital materials of intermediate/basic composition (Floyd and Leveridge, 1987).

Investigation of chemical weathering during the Jurassic-Cretaceous period

Weathering is described as a complex interaction of physical, chemical and biotic processes which alter and disintegrate the rocks at the surface or close to the surface (Selby, 1993). Chemical weathering indices are

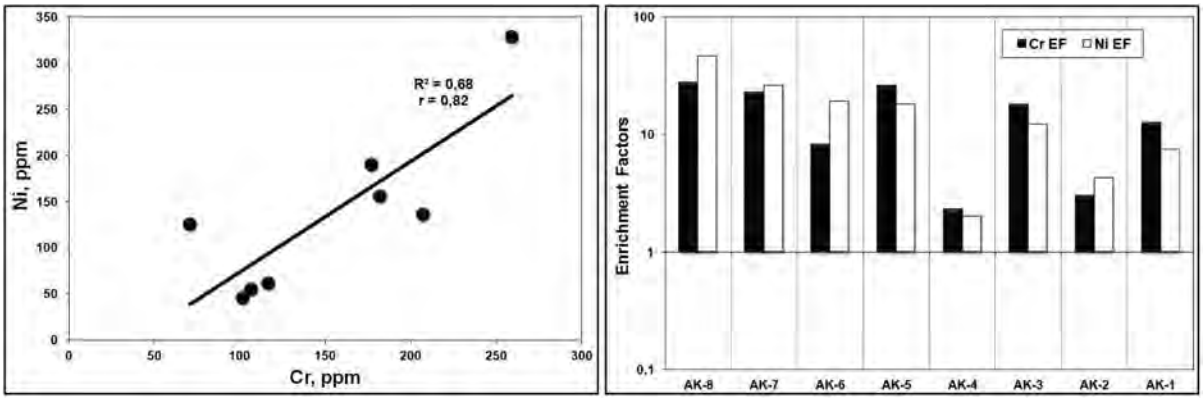

Figure 11- Correlation and element enrichments of Cr and Ni

commonly used in recent and old weathering profile studies (Kirschbaum et al., 2005; Goldberg and Humayun, 2010). Weathering index and chemical alteration index are used to measure the degree of weathering of the terrestrial land from which sediment grains are derived. The degree of compositional maturity of shales can be estimated from the weathering index graphic (Kronberg and Nesbitt, 1981).

In the erosion index graphic the constructed plotting $(Na_2O+K_2O)/(Al_2O_3+Na_2O+K_2O)$ vs. $(SiO_2+Na_2O+K_2O)/(SiO_2+Al_2O_3+Na_2O+K_2O)$, Akkuyu samples are generally within the illite, Ca-feldspar and Na-feldspar fields (Figure 12). This indicates that feldspars are altered to clay minerals and K_2O deriving from altered feldspars is captured by Na_2O in illite, smectite and montmorillonite (Kronberg and Nesbitt, 1981).

Using weathering indexes of CIW (Harnois, 1988), CIA (Nesbitt and Young, 1984, 1989), PIA (Fedo et al., 1995) and V (Vogt, 1927), weathering of source rock can be investigated. Data computed based on these indices for the Akkuyu formation are given in table 5. Examination of weathering and alteration ranges reveals that CIW values of Akkuyu samples are indicative of strong chemical weathering while CIA values yield moderately chemical alteration and PIA values indicate a strong alteration (Table 5; figure 13).

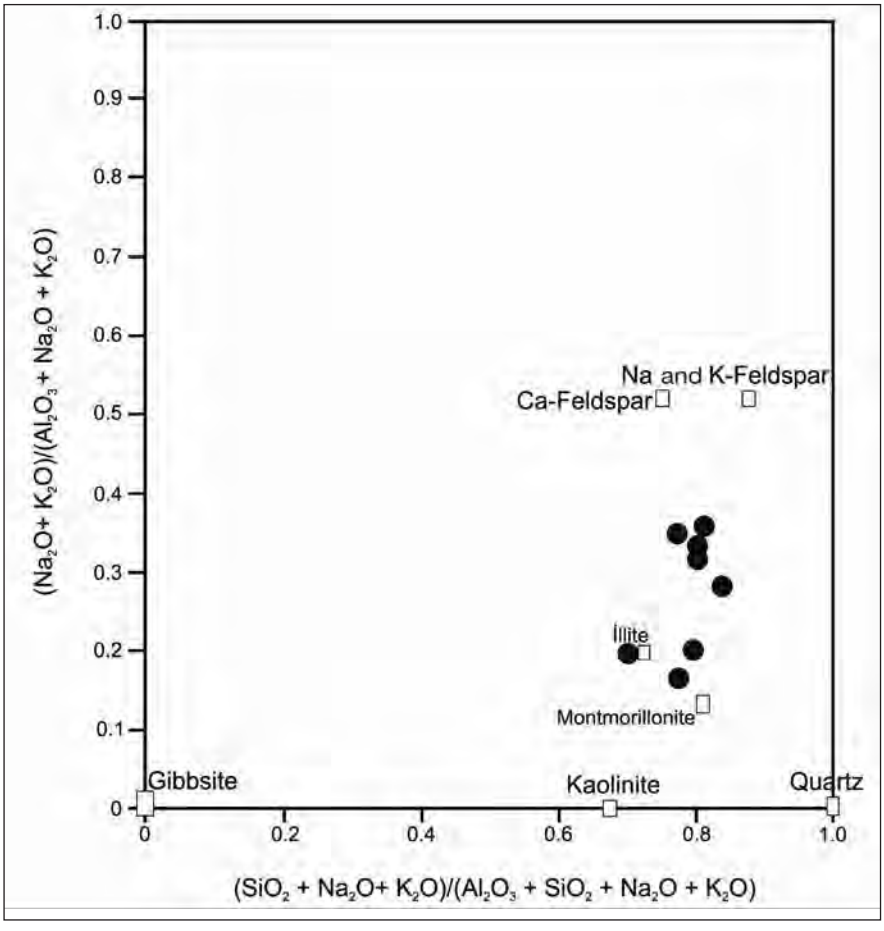

Figure 12- Graphic of Weathering Index (Kronberg and Nesbitt, 1981)

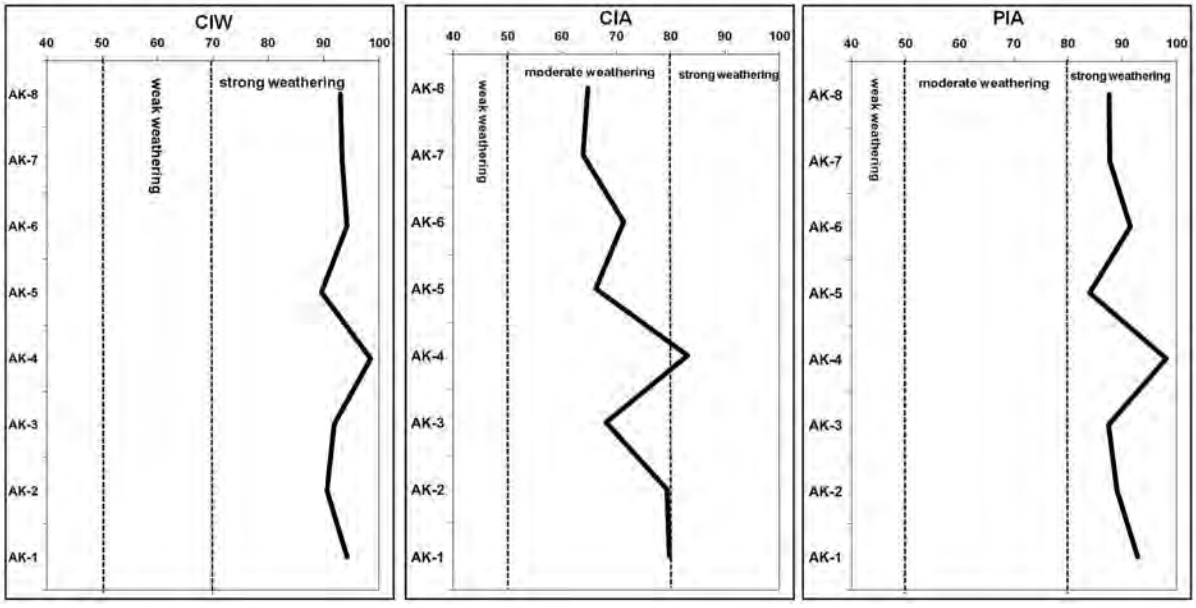

Figure 13- Weathering index of Akkuyu formation samples

Vogt Residual Index (V)

Vogt (1927) suggested a method for evaluating residual sediment maturation which is known as Vogt Residual Index. Roaldset (1972) used this index to determine weathering status of clays in Quaternary deposits in the Numedal region, Norway. Roaldset (1972) used "V" index to compare whole rock chemistry of moren and marine clay deposits and concluded that moren clays are more weathered than marine clays. Vogt Residual Index values indicate that Akkuyu samples are represented by weathering indexes ranging from weak to strong (Figure 14).

Table 5- Averages of CIW, CIA ve PIA weathering index of studied samples

Sample	CIW	CIA	PIA
AK-8	93,00	64,82	87,61
AK-7	93,39	63,86	87,70
AK-6	94,22	71,42	91,51
AK-5	89,65	66,27	84,01
AK-4	98,50	83,09	98,16
AK-3	91,87	68,11	87,52
AK-2	90,57	79,34	89,02
AK-1	94,18	79,82	92,90

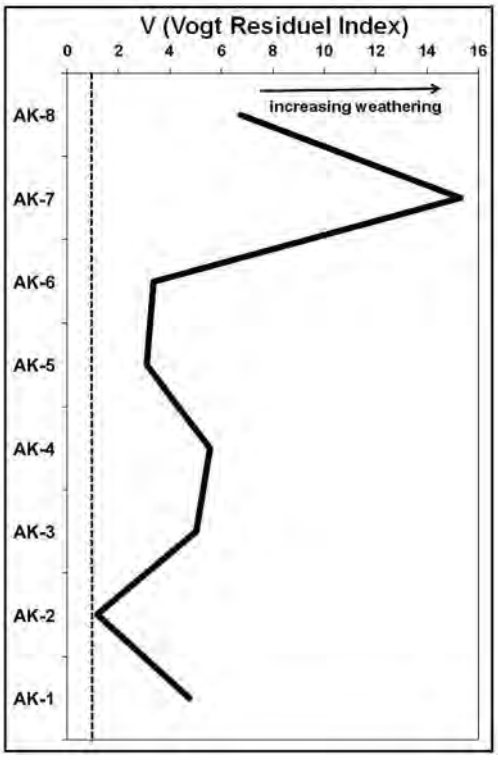

Figure 14- Vogt Residuel Index Results of Akkuyu formation samples

Hot and humid climates accelerate alteration of less stable minerals and rock fragments whereas cold and very dry climate regimes facilitate preservation of more stable components. In addition, low relief and slightly inclined topography raises chemical weathering due to slow erosion of landscape by the particles. In the contrary, high relief and steep slopes result in rapid erosion then significant weathering. Sethie et al. (1998) stated that Na, Mg, Ca, U and Rb are easily affected by weathering and diagenesis while rare earth elements (REE) are highly resistant to alteration and fragmentation during the weathering and diagenesis. Element concentrations in Akkuyu sediment samples seem to be affected by erosion, dissolution and sediment diagenesis. In the studied samples, concentrations of Al_2O_3, TiO_2 and SiO_2, which are indicator of terrestrial input, are genially found to be low. However, high carbonate (CaO) and organic material contents of samples and absence of any data to show lacustrine conditions and facies characteristics of the unit might indicate that the Akkuyu formation was deposited under sheltered reducing conditions.

Tectonic Conditions of Central Taurids Region During The Jurassic-Cretaceous Period

Bhatia (1983) and Roser and Korsch (1986) were used K_2O/Na_2O vs. SiO_2; SiO_2/Al_2O_3 vs. K_2O/Na_2O; Al_2O_3/SiO_2 vs. Fe_2O_3 + MgO and TiO_2 vs. Fe_2O_3 + MgO diagrams to have information on tectonic regime of the source region of detrital sediments. Studies samples of the Akkuyu formation are generally represented by similar distributions and plotted into fields of active and passive continental margins (Figures 15 and 16).

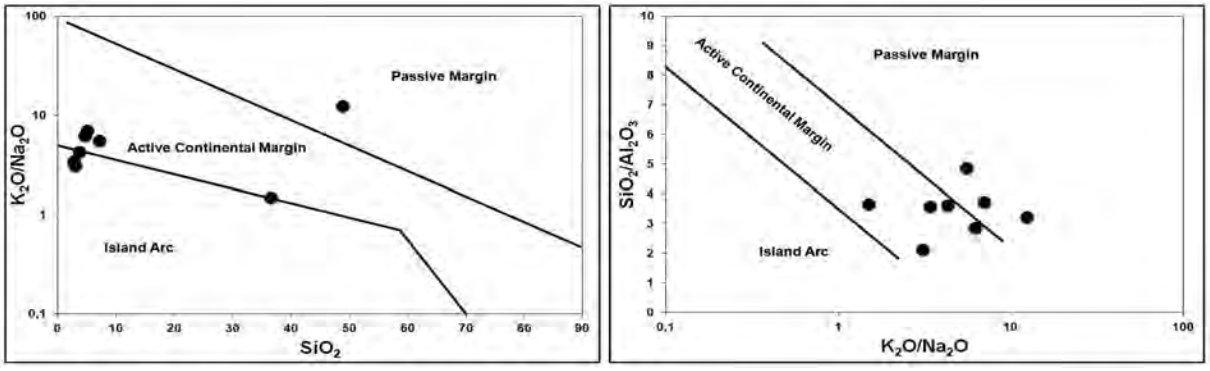

Figure 15- Major and trace elements diagrams for determining tectonic settings (Roser and Korsch, 1986)

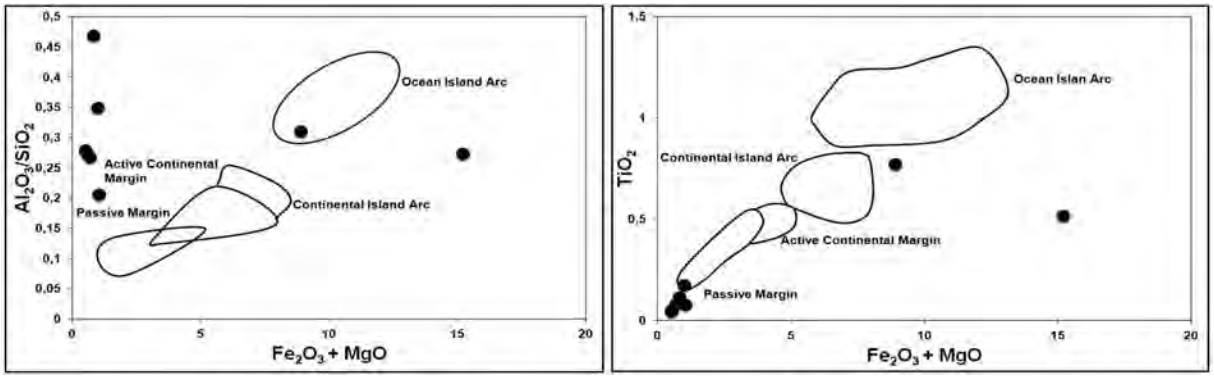

Figure 16- Discriminating tectonic settings diagram by major element compositions (Bhatia, 1983)

Geochemical compositions of sedimentary rocks yield information on tectonic regime of the source region and source rock type of detrital sediments. Considering that most elements are easily redistributed as a result of weathering and alteration, they must be carefully used in source determination. Therefore, trace element or trace element ratios combined with major oxide data are preferentially used for determination of source indicators (Mader and Neubauer, 2004; Gabo et al., 2009). Floyd and Leveridge (1987) used K_2O vs. Rb graphic to discriminate sediments which are derived from rocks of acidic to intermediate-basic composition. In K_2O vs. Rb graphic, rock samples under investigation, with the exception of two samples, mostly show basic rock compositions (Figure 17).

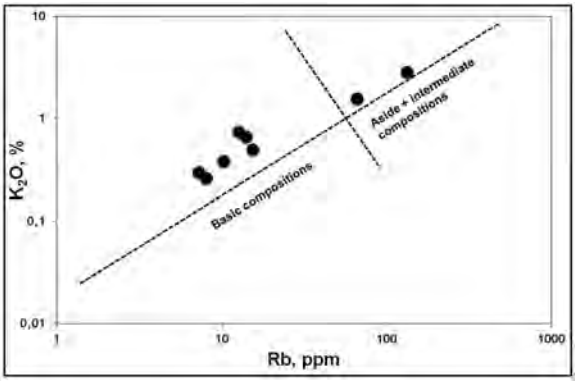

Figure 17- K_2O versus Rb diagram (Floyd and Leveridge, 1987)

Among the samples, K_2O and Rb compositions of sample AK-2 are 1.56% and 66.02 ppm and those of sample AK-4 are 2.85% and 131.95 ppm. K_2O and Rb contents of samples AK-1, 3, 5, 6, 7 and 8 are in the range of 0.26 to 0.75% and from 7.22 to 15.36 ppm, respectively. As shown from TiO_2 vs. Al_2O_3 diagram (Figure 10), most samples are plotted on the basalt axis whereas samples AK-2 and AK-4 are in the basalt+granite and granite+basalt fields supporting the results given above.

RESULTS AND DISCUSSION

• Facies characteristics and a dominant micrite lithology accompanied by bituminous levels imply that the Late Jurassic Akkuyu formation was deposited in a restricted carbonate platform in the central Taurids.

• Based on Hydrogen Index (HI) ve temperature (T_{max}, °C) relation, organic material type of organic material-rich, dark gray and black colored rocks of Akkuyu formation was determined to be Type-III kerogen.

• Redox conditions of Akkuyu formation rocks are found as dioxic-anoxic with respect to Ni/Co ratios, oxic-dioxic and anoxic with respect to V/Cr ratios, oxic and anoxic with respect to V/V+Ni ratios and dioxic and anoxic with respect to U/Th ratios.

• The positive correlation (r=0.84) between Cd/Al and P/Al indicates that primary paleoproductivity of the deposition basin is very high.

• According to SiO_2-Al_2O_3-CaO triangular diagram of,Akkuyu samples are composed of marl while Si_2O/Al_2O_3 ratio of Pettijohn et al. (1987) and Fe_2O_3/K_2O diagram suggest that samples are represented by shale-sand lithology.

• Results of petrographic studies imply that samples are composed of micritic-sparitic packstone, mudstone and grain stone and show oil indications. Matrix consists of micrite and less amount of sparite. Whole rock WRD determinations showed that samples are composed of calcite, quartz, kaolinite, anorthite, illite and muscovite minerals.

• In the studied samples Al_2O_3 is strongly and positively correlated with SiO_2, Fe_2O_3, TiO_2, and K_2O indicating that rocks might have siliciclastic associations and closely related to clay minerals.

• In order to have information on tectonic regime of the depositional environment of the Akkuyu formation, K_2O/Na_2O vs. SiO_2; SiO_2/Al_2O_3 vs. K_2O/Na_2O; Al_2O_3/ SiO_2 vs. Fe_2O_3 + MgO and TiO_2 vs. Fe_2O_3 + MgO diagrams were used. Samples were found to be associated with active and passive continental margins.

• Source rocks of the Akkuyu formation show wide range of composition from basalt and basalt+granite to granite+basalt.

Manuscript received March 23, 2011

REFERENCES

Albayrak, M., 1995. Akseki–Aydınkent (Antalya) arasının Jeolojisi ve Petrol Olanakları, Yüksek Lisans Tezi, Ankara Üniversitesi, Fen Bilimleri Enstitüsü.

Algeo, T.J., Berner, R.A., Maynard, J.B. and Scheckler, S.E., 1995. Late Devonian oceanic anoxic events and biotic crises: "rooted" in the evolution of vascular land plants? GSA Today, 5, 64–66.

——— and Scheckler, S.E., 1998. Terrestrial–marine teleconnections in the Devonian: links between the evolution of land plants, weathering processes, and marine anoxic events. Philosophical Transactions of Royal Society B: Biology Science, 353, 113–130.

——— and Maynard, J.B., 2004. Trace–Element Behavior and Redox Facies in Core Shales Of Upper Pennsylvanian Kansas-Type Cyclothems. Chemical Geology, 206, 289 – 318.

Amajor, L.C., 1987. Major and trace elements geochemistry of Albin and Turonian shales from the Southern Benue trough, Nigeria. Journal of African Earth Science, 6, 633 – 461.

Andersson, A., Dahlman, B., Gee, D.G., and Snäll, S., 1985. The Scandinavian Alum Shales. Sveriges Geologiska Undersoekning, Serie Ca: Avhandlingar och Uppsatser I A4, NR 56, 50 p.

Arnaboldi, M. and Meyers, P.A., 2003. Geochemical evidence for paleoclimatic variations during deposition of two Pliocene sapropels from the Vrica section, Calabria. Palaeogeography, Palaeoclimatology, Palaeoecology, 190, 257–271.

Bhatia, M.R., 1983. Plate tectonics and geochemical composition of sandstones. Journal of Geology 91, 611–627.

Blumenthal, M.M., 1951, Batı Toroslarda Alanya ard ülkesinde jeolojik araştırmalar. MTA dergisi, n.5, 194.

Boggs, Jr.S., 2009. Petrology of sedimentary rocks. Cambridge University Press, UK, 2nd edition, 600 p.

Breit, G.N. and Wanty, R.B., 1991. Vanadium accumulation in carbonaceous rocks: a review of geochemical controls during deposition and diagenesis. Chemical Geology, 91, 83-97.

Brüchert, V., R., Jorgensen, B.B., Neumann, K., Richmann, D., Schlösser, M. and Schulz, H., 2003. Regulation of bacterial sulfate reduction and hydrogen sulfide fluxes in the central Namibian coastal upwelling zone. Geochimica et Cosmochimica Acta, 67, 4505–4518.

Brumsack, H. J., 2006. The trace metal content of recent organic carbon-rich sediments: implications for Cretaceous black shale formation. Palaeogeography, Palaeoclimatology, Palaeoecology, 232, 344–361.

Caplan, M.L. and Bustin, R.M., 1998. Paleoceanographic controls on geochemical characteristics of organic rich Exshaw mudrocks: role of enhanced primary productivity. Organic Geochemistry, 30, 161–188.

Demaison, G.J. and Moore, G.T., 1980. Anoxic environments and oil source bed genesis. American Association of Petroleum Geologists Bulletin 64, 1179–1209.

Dill, H., 1986. Metallogenesis of Early Paleozoic Graptolite Shales from the Graefenthal Horst (Northern Bavaria-Federal Republic of Germany). Economic Geology, 81, 889–903.

———. Teschner, M. and Wehner, H., 1988. Petrography, inorganic and organic geochemistry of Lower Permian Carbonaceous Fan sequences (‘‘Brandschiefer Series’’)-Federal Republic of Germany: Contrints to their paleogeography and assessment of their source rock potential. Chemical Geology, 67, 307–325.

Erbacher, J., Huber, B.T., Norris, R.D. and Markey, M., 2001. Increased thermohaline stratification as a possible cause for an open ocean anoxic event in the Cretaceous period. Nature, 409, 325-326.

Fedo, C.M., Nesbitt, H.W. and Young, G.M., 1995. Unraveling the effects of potassium metasomatism in sedimentary rocks and paleosols, with implications for paleoweathering conditions and provenance. Geology, 23, 921– 924.

Filipelli, G.M., Delaney, M.L., Garrison, R.E., Omarzai, S.K. and Behl, R.J., 1994. Phosphorus accumulation rates in a Miocene low oxygen basins: the Monterey formation (Pismo Basin), California. Marine Geology, 116, 419-430.

Fleischer, V.D., Garlick, W.G., and Haldane, R., 1976. Geology of the Zambian Copperbelt; In: K.H. Wolf (ed). Handbook of Stata-Bound and Stratiform Ore Deposits, vol. 6. Elsevier, Amsterdam, 223–352.

Floyd, P.A. and Leveridge, B.E., 1987. Tectonic environment of the Devonian Gramscatho basin, south Cornwell: framework mode and geochemical evidence from turbidite sandstones. Journal of the Geological Society London, 144, 531–542.

Gabo, J.A.S., Dimalanta, C.B., Asio, M.G., Queaño, K.L., Yumul Jr., G.P. and Imai, A., 2009. Geology and geochemistry of the clastic sequences from Northwestern Panay (Philippines): Implications for provenance and geotectonic setting. Tectonophysics, 479, 111-119.

Garver, J.I., Royce, P.R. and Scott, T.J., 1994. The presence of ophiolites in tectonic highlands as determined by chromium and nickel anomalies in synorogenic shales: two examples from North America. Russian Geology and Geophysics, 35, 1-8.

Garver, J.I., Royce, P.R. and Smick, T.A., 1996. Chromium and nickel in shale of the Taconic Foreland: A case study for the provenence of fine-grained sediments with an ultramafic source. Journal of Sedimentary Research, 66, 100-106.

Goldberg, K. and Munir Humayun, M., 2010. The applicability of the Chemical Index of Alteration as a paleoclimatic indicator: An example from the Permian of the Paraná Basin, Brazil. Palaeogeography, Palaeoclimatology, Palaeoecology, 293, 175-183.

Gustavson, L.B., and Williams, N., 1981. Sediment-hosted stratiform deposits of copper, lead, and zinc; In: B.J. Skinner (ed). Seventy-Fifth Anniversary Volume, The Economic Geology Publishing Co., Yale, 139–178.

Harnois, L., 1988. The CIW index: a new Chemical Index of Weathering. Sedimentary Geology, 55, 319– 322.

Hatch, J.R. and Leventhal, J.S., 1992 Relationship between inferred redox potential of the depositional environment and geochemistry of the Upper Pennsylvanian (Missourian) Stark Shale Member of the Dennis Limestone, Wabaunsee County, Kansas, U.S.A. Chemical Geology, 99, 65–82.

Hedges, J.I. and Keil, R.G., 1995. Sedimentary organic matter preservation: an assessment and speculative synthesis. Marine Chemistry, 49, 81-115.

Hiscott, R.N., 1984. Ophiolitic source rocks for Taconic-age flysch: Trace element evidence. Geological Society of America Bulletin, 95, 1261-1267.

Holland, H., 1978. The Chemistry of the Atmosphere and the Oceans. Wiley Interscience, New York. 351 p.

Ibach, L.E.J., 1982. Relationship between sedimentation rate and total organic carbon content in ancient marine sediments. AAPG Bulletin, 66, 170-188.

Ingall, E.D. and Jahnke, R.A., 1997. Influence of water-column anoxia on the elemental fractionation of carbon and phosphorus during sediment diagenesis. Marine Geology, 139, 219–229.

Jones, B. and Manning, D.A.C., 1994. Comparison of geological indices used for the interpretation of palaeoredox conditions in ancient mudstones. Chemical Geology 111, 111-129.

Kirschbaum, A., Martinez, E., Pettinari, G. and Herrero, S., 2005. Weathering profiles in granites, Sierra Notre (Cordoba, Argentina). Journal of South American Earth Sciences, 19, 479–493.

Koca, D., Sarı, A., Koç, Ş., Yavuz, B. and Koralay, D.B., 2010. Denizel kaynak kayalarda ana ve iz element zenginleşmelerinde Türkiye'den bir örnek: Akkuyu Formasyonu (Orta Toroslar). Gazi Üniversitesi Mühendislik -Mimarlık Fakültesi Dergisi, 25, 243-256.

Kronberg, B. I. and Nesbitt, H. W., 1981. Quantification of weathering, soil geochemistry and soil fertility. Journal of Soil Science, 32, 453-459.

Lewan, M.D., 1984. Factors controlling the proportionality of vanadium and nickel in crude oils. Geochimica et Cosmochimica Acta, 48, 2231–2238.

Lewan, M.D. and Maynard, J.B., 1982. Factors controlling enrichment of vanadium and nickel in the bitumen of organic sedimentary rocks. Geochimica et Cosmochimica Acta, 46, 2547–2560.

Mader, D. and Neubauer, F., 2004. Provenance of Palaeozoic sandstones from the Carnic Alps (Austria): petrographic and geochemical indicators. International Journal of Earth Sciences, 93, 262–281.

Martin, C., 1969. Akseki kuzeyindeki bir kısım Torosların stratigrafik ve tektonik incelemesi. Maden Tetkik ve Arama Dergisi, 72, 157–175.

Middleburg, J.J. and Comans, R.N.J., 1991. Sorption of cadmium on hydroxyapatite. Chemical Geology, 90, 45-53.

Monod, O., 1977. Recherches géologiques dans les Taurus occidental au sud de Beyşehir (Turquie). Thèse de Doctorat, Université Paris – Sud (Orsay), 442 (unpublished).

Morford, J.L., Russell, A.D. and Emerson, S. 2001. Trace metal evidence for changes in redox environment associated with the transition from terrigenous clay to diatomaceous sediment, Saanich Inlet, BC. Marine Geology, 174, 355–369.

Murphy, A.E., Sageman, B.B., Hollander, D.J., Lyons, T.L. and Brett, C.E., 2000. Black shale deposition and faunal overturn in the Devonian Appalachian Basin: clastic starvation, seasonal watercolumn mixing, and efficient biolimiting nutrient recycling. Paleoceanography, 15, 280–291.

Nesbitt, H.W. and Young, G.M., 1984. Prediction of some weathering trends of plutonic and volcanic rocks based on thermodynamic and kinetic considerations. Geochimica et Cosmochimica Acta, 48, 1523–1534.

——— and ———, 1989. formation and diagenesis of weathering profiles. Journal of Geology, 97, 129–147.

Nijenhuis, I.A., Bosch, H.-J., Sinninghe Damsté, J.S., Brumsack, H.-J. and De Lange, G.J., 1999. Organic matter and trace element rich sapropels and black shales: a geochemical comparison. Earth and Planetary Science Letters, 169, 277–290.

Pedersen, T.F. and Calvert, S.E., 1990. Anoxia vs. productivity: what controls the formation of organic-carbon-rich sediments and sedimentary rocks? American Association of Petroleum Geologists Bulletin, 74, 454–466.

Pettijohn, F.J., Potter, P.R. and Siever, R., 1987. Sand and sandstones. Springer, New York, 2nd edition. 553p.

Potter, P.E., 1978. Petrology and chemistry of modern big river sands. Journal of Geology, 86, 423–449.

Rimmer, S.M., Thompson, J.A., Goodnight, S.A. and Robl, T.L., 2004. Multiple controls on the preservation of organic matter in Devonian–Mississippian marine black shales: geochemical and petrographic evidence. Palaeogeography, Palaeoclimatology, Palaeoecology, 215, 125–154.

Roaldset, E., 1972. Mineralogy and geochemistry of Quaternary clays in the Numedal Area, southern Norway. Norsk Geolisk Tidsskrift, 52, 335– 369.

Roser, B.P. and Korsch, R.J., 1986. Determination of tectonic setting of sandstone mudstone suites using SiO_2 content and K_2O/Na_2O ratio. Journal of Geology, 94, 635–650.

Ross, D.J.K. and Bustin, R.M., 2006. Sediment geochemistry of the Lower Jurassic Gordondale Member, northeastern British Columbia. Bulletin of Canadian Petroleum Geology, 54, 337–365.

Ruttenberg, K.C. and Goñi, M.N., 1997. Phosphorus distribution, C:N:P ratios, and ^{13}C in arctic, temperate, and tropical coastal sediments: tools for charac- terizing bulk sedimentary organic matter. Marine Geology, 139, 123– 145.

Sarı, A., Sonel, N. and Doğan A.O, 1997. Üzümlü-Çamlık arasında kalan bölgenin Stratigrafisi (Beyşehir Güneyi, Konya). Süleyman Demirel Üniversitesi Fen Bilimleri Enstitüsü Dergisi, 2, 17–38.

Sarı, A., Koca, D., Koc, S., Yavuz, B. and Koralay, D.B., 2008. Üst Jura denizel fasiyeslerinde iz element birikimlerinde organik madde içeriğinin rolü (Orta Toroslar ,Türkiye). Selçuk Üniversitesi Mühendislik-Mimarlık Fakültesi Dergisi, 23, 43-56.

Selby, M.J., 1993. Hillslope Materials and Processes. 2nd Edition Oxford University Press, Oxford, 480 p.

Sethie, P. S., Hannigan, R.E. and Leithold, E.L., 1998. Rare-earth element chemistry of Cenomanian–Turonian shales of the North American Greenhorn Sea, Utah. In: Schieber, J., W. Zimmerle, and P. Sethi (ed). Shales and Mudstones II:E. Schweizerbart'sche Verlagsbuchhandlung, Stuttgart, 296p.

Sonel, N., Sarı, A., Doğan, A.O. and Bozüyük, İ., 1995. Üzümlü (Beyşehir) civarının kaynak kaya fasiyesleri ve petrol oluşumunun organik jeokimyasal yöntemlerle incelenmesi. Türkiye Jeoloji Kurultayı Bülteni, 10, 34–40.

Suees, E., Kulm, L.D. and Killingley, J.S., 1987. Coastal upwelling and a history of organic-rich mudstone deposition off Peru. : In: J.Brooks and A.J. Fleet (ed). Marine Petroleum Source Rocks. Geological Society Special publication, 26, 181-197.

Toker, V., Sonel, N., Ayyıldız, T. and Albayrak, M., 1993. Akseki Kuzeyi–Üzümdere (Antalya) civarının stratigrafisi. Türkiye Jeoloji Kurultayı Bülteni, 36, 57–71.

Tribovillard, N., Algeo, T.J., Lyons, T. and Riboulleau, A., 2006. Trace metals as paleoredox and paleoproductivity proxies: An update. Chemical Geology, 232, 12-32.

van Cappellen, P. and Ingall, E.D., 1994. Benthic phosphorus regeneration, net primary production and ocean anoxia: a model of the coupled marine biogeochemical cycles of carbon and phosphorus. Paleoceanography, 9, 677-692.

Vogt, T., 1927. Sulitjelmafeltets geologi og petrografi. Norges Geologiske Undersokelse, 121, 1– 560 (in Norwegian, with English abstract).

Warning, B. and Brumsack, H.J. 2000. Trace metal signatures of Mediterranean sapropels. Palaeogeography, Palaeoclimatology, Palaeoecology, 158, 293–309.

Mineral Res. Expl. Bull., 144, 75-104, 2012

THE GEOLOGY, GEOCHEMISTRY AND GENETICAL FEATURES OF THE ORMANBAŞI HILL (SİNCİK, ADIYAMAN) COPPER MINERALIZATION

Nail YILDIRIM*, Semiha İLHAN**, Esra YILDIRIM*** and Cahit DÖNMEZ****

ABSTRACT.- The study area covers Ormanbaşı Hill of Adıyaman–Sincik County and its vicinity. Regional geological locations of Cu mineralizations that lie between the Southeastern Anatolian Foothill Belt and Taurus Orogenic Belt are conformable with thrust planes approximately extending in E-W directions. Cu mineralizations are observed in the form of lenses and layers within mudstone, diabase, spilite and claystone - shales of the Koçali complex. The primary genetic relations of these formations have completely been disappeared but have only been traced along thrust planes that are conformable with general tectonic lineaments. The ore structure is generally massive but is stockwork and disseminated in some zones. The ore bearing layer with pyrite towards deeper parts is observed, while the mineralization is observed in the form of iron ore cap (gossan) at surface. Ore paragenesis consists of pyrite, marcasite, chalcopyrite, sphalerite, bornite, chalcosine - covelline and native copper. All samples belonging to ore mineralizations plot on Cyprus type volcanogenic massive sulfide (VMS) area in Cu – Pb - Zn and Au - (Cu + Pb + Zn) - Ag ternary diagrams. All samples in Pb, Cu, Ag, Au and Zn spider diagrams which were normalized to primary mantle show a trend similar to VMS deposits. Besides, analyses carried out in massive pyrites indicated that these had Ni/Co ratio higher than 1% and less Ni content. Therefore; it was detected that hydrothermal processes had been affective in ore mineralizations. S^{32}/S^{34} ratios were obtained as 6.9 and 7.6 in sulfur isotope analyses performed by using pyrite and chalcopyrite samples. These values are both compatible with sulfur ratios in hydrothermal solutions related to volcanism and show a similar composition with that of Cyprus type VMS deposits on the world.

Keywords: Adıyaman, Sincik, Koçali complex, Cyprus type, VMS, Copper

INTRODUCTION

PURPOSE OF THE STUDY

The study area is located between the Southeastern Anatolian Fold Belt and Tauride Orogenic Belt and possesses a significant potential in terms of base and precious metals. Especially; the Adıyaman territory forms a rich sub region in terms of Cu mineralization. Numerous Cu anomalies were detected during prospective and geochemical studies which had been performed by MTA along the Southeast Anatolian Thrust Belt around the region (Cengiz, 1991). One of them is the Ormanbaşı Hill mineralization which is located at the southeast of Sincik, Adıyaman (Gültekin, 2004; Yıldırım 2011). The aim of this study is to define the mineralization model and contribute to the detection of similar mineralizations within the same belt zone by this method.

GEOGRAPHICAL LOCATION

The study area is located at Ormanbaşı Hill site within the boundary of Zeynelaslan settlement which is 20 km southeast of Sincik County of Adıyaman City and is 78 km away from Adıyaman city (Figure 1).

* Maden Tetkik ve Arama Orta Anadolu IV. Bölge Müdürlüğü, 44100 Malatya
** Çukurova Üniversitesi, Mühendislik ve Mimarlık Fakültesi, Jeoloji Mühendisliği Bölümü, 01330 Balcalı/Adana
*** Fırat Üniversitesi, Mühendislik Fakültesi, Jeoloji Mühendisliği Bölümü, 23100 Elazığ
**** Maden Tetkik ve Arama Genel Müdürlüğü Maden Etüt ve Arama Dairesi, 06520 Ankara

Figure 1- Location map of the study area

PREVIOUS STUDIES

Many geological investigations have been carried out in and around the study area with different purposes. General and structural geological studies were carried out by Kovenko (1943), Tolun (1955), Rigo de Righi and Cortesini (1964), Altınlı (1966), Ketin (1966), Pişkin (1972), Yazgan (1972), Özçelik (1985), Sungurlu (1973, 1974), Yalçın (1976), Perinçek (1978,1979), Perinçek and Kozlu (1984), Yazgan and Asutay (1987), Yılmaz et al. (1992), Yiğitbaş et al. (1992, 1993), Parlak et al. (2004, 2009), Parlak (2006), Beyarslan et al. (2009), Yıldırım (2010), Uzunçimen et al. (2011). These studies have great significance in revealing the regional geological model and understanding the mineralization in the region. As to the studies related with the topic, the article was summarized below in more detail.

Turgay (1968) stated that there had been two types of ore mineralization in the region in a copper prospection project carried out in Siltikuş Hill (Ormanbaşı Hill), Sincik Settlement, Kahta – Adıyaman. He defined the primary type mineralizations as diabase and exhalative sedimentary copper – pyrite deposits. However; the secondary type mineralization was defined as ore veins belonging to a hydrothermal facies of an acidic magma.

Şaşmaz et al. (1999) stated that ore mineralizations they had detected in Çüngüş Derdere Site, Diyarbakır indicated the general features of Cyprus type deposits located at the upper horizons of an ophiolitic deposit which was formed as a result of the sea-floor spreading.

Gültekin (2004) stated that Ormanbaşı Hill mineralizations had been traced along tectonic lineaments. He also defined that mainly the units belonging to Pütürge metamorphics, Koçali complex and Çüngüş formation cropped out in the region and limonitization were the common type of alteration in this area. The author also stated that the mineralizations over the area were suitable to epithermal type of mineralization because of the presence of minerals indicating

the low temperature conditions and structural – textural features.

Türkyılmaz (2004) defined that manganese mineralizations within the Koçali complex were in the form of irregular lenses and layers in pelagic radiolarites which belong to the Konak formation and that these mineralizations were exhalative hydrothermal in origin.

REGIONAL TECTONICS AND GEOLOGY OF THE STUDY AREA

The investigation area is located at the boundary of Southeast Anatolian Thrust Belt and Tauride Orogenic Belt (Ketin, 1966).

The Southeast Anatolian Orogenic Belt has developed as a result of geological events that had occurred during the closure of the southern branch of Neotethys which was bordered by Taurus at north and Arabian Platforms at south between Late Cretaceous – Miocene time period. The evolution of this belt especially consists of the movement of nappes relatively to the south, Arabian Plate between Late Cretaceous – Miocene (Yıldırım and Yılmaz 1991; Yılmaz, 1993; Yılmaz et al., 1993).

Southeast Anatolian Orogenic Belt consists of three different tectonic units which are E - W trending and separated from each other by north dipping main thrust planes (Yılmaz, 1990, 1993; Yılmaz et al., 1993). These tectonical units from north to south are the Nappe zone, Accretional Prism and the Arabian Platform (Figure 2).

The intensive tectonical activity that occurred at the end of Cretaceous and Miocene and caused the settlement of allochthonous units on the region has also given rise to the development of marine deposition at the same period and to the closure of the basins. Allochthonous units have taken their recent positions at the end of Upper Miocene as gravity sliding and overthrust sheets.

Units cropping out in and around the study area were investigated in two parts as allochthonous and autochthonous (lower and upper series) considering their locations in the region and mutual relations with neighboring units.

Late Cretaceous Koçali complex has tectonically been settled on Karadut complex (lower allochthonous series) at bottom and on the Kastel formation forming the uppermost horizons of the

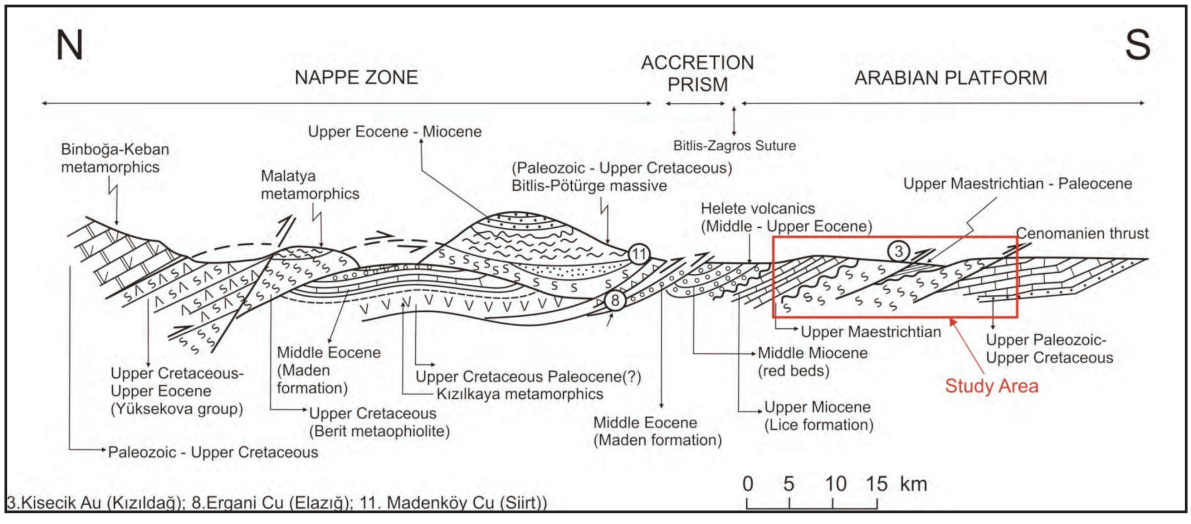

Figure 2- Structural model of SE Anatolian Orogenic Belt (modified from Yılmaz, 1993)

Arabian Plate. These are uncomformably overlain by Upper Maestrichtian – Paleocene transgressive deposits (Terbüzek formation, Besni formation and Germav formation) of the Arabian Platform belonging to the Autochthonous Series. The region has been transgressed at the beginning of Eocene and Lower Eocene – Lower Miocene transgressive deposits (Gercüş formation, Midyat formation, Gaziantep formation and Fırat formation) have uncomformably overlain units at bottom. Lice formation which is formed by the alternation of shale – marl – sandstone unconformably overlies this unit (Figures 3, 4 and 5).

The Çüngüş Formation belonging to the Upper Allochthonous Series, Maden complex, Kömürhan ophiolite (Yüksekova ophiolite) and Pütürge metamorphic tectonically settled over Autochthonous units in Middle – Upper Miocene. Since these tectono-stratigraphical units were tectonically associated with each other, their primary relations in them were completely disappeared (Figures 3, 4 and 5).

Since ore mineralizations in the study area has been observed in Koçali complex, this deposit has been mentioned below in more detail.

KOÇALİ COMPLEX

Sungurlu (1973) is the first investigator who nomenclatured and mapped the Koçali complex in three different formations as Tarasa, Konak and Kale formation. Tarasa formation is composed of volcanites (basalt, diabase, spilite), Konak formation is composed of the al-

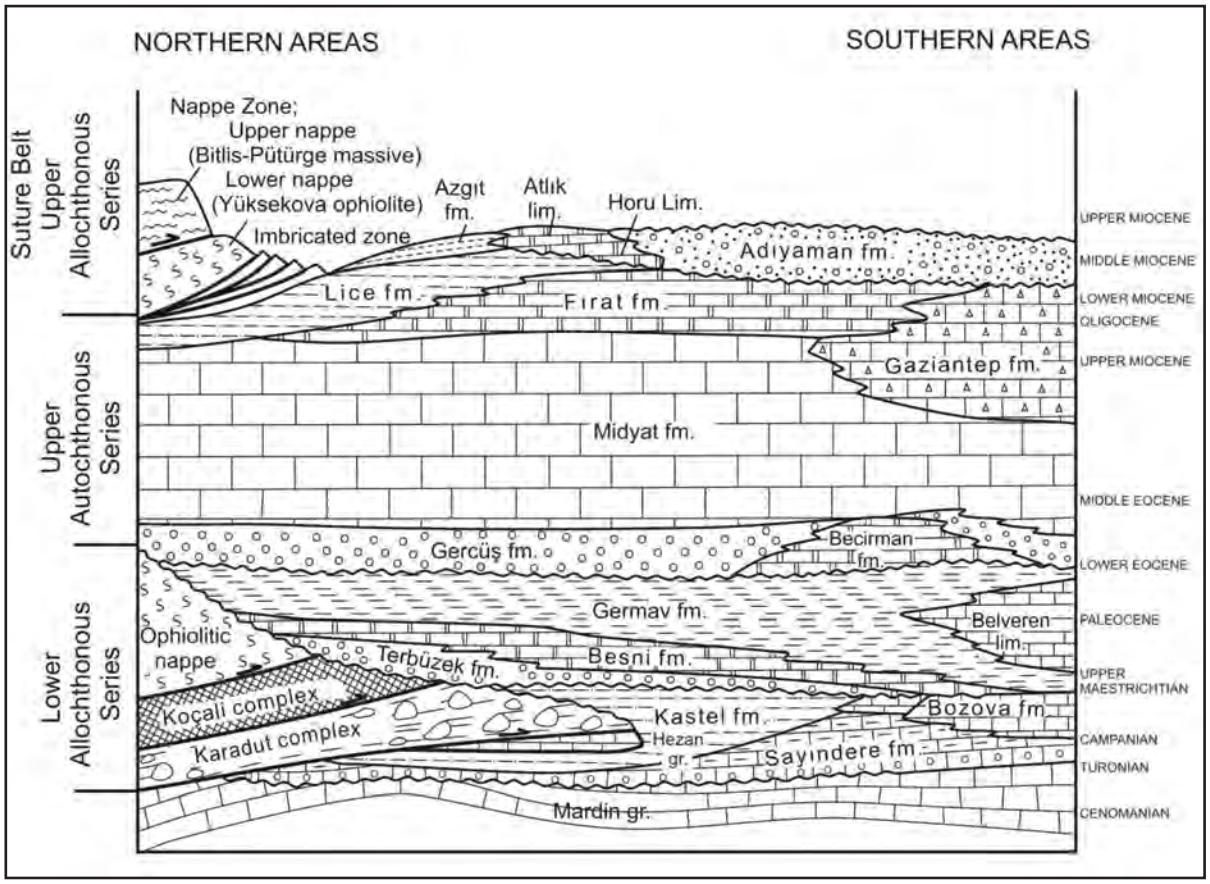

Figure 3- Generalized structural cross section of the Arabian Platform in SE Anatolia, from the suture zone at north to the north of Arabian Platform at south (modified from Yılmaz, 1993)

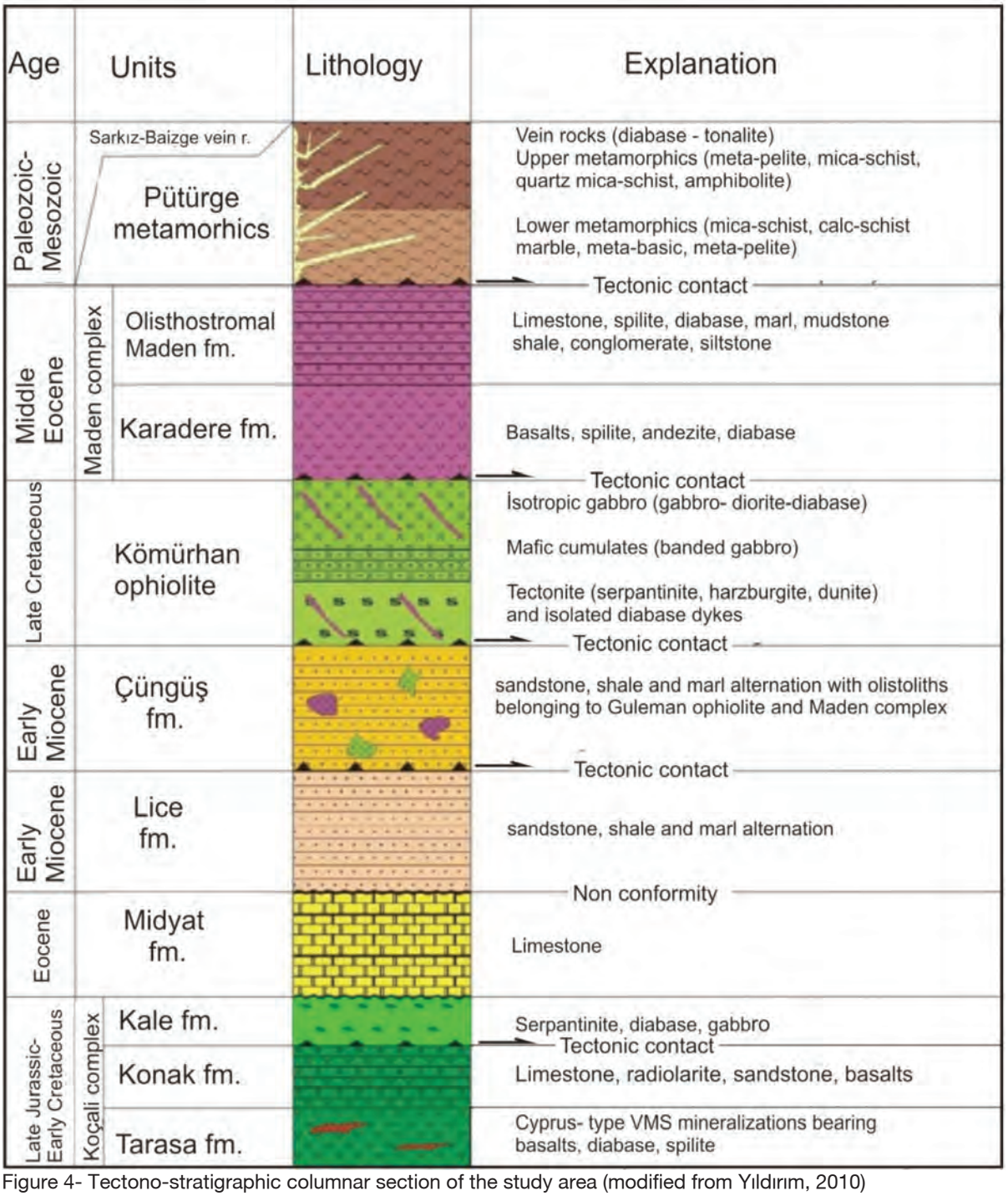

Figure 4- Tectono-stratigraphic columnar section of the study area (modified from Yıldırım, 2010)

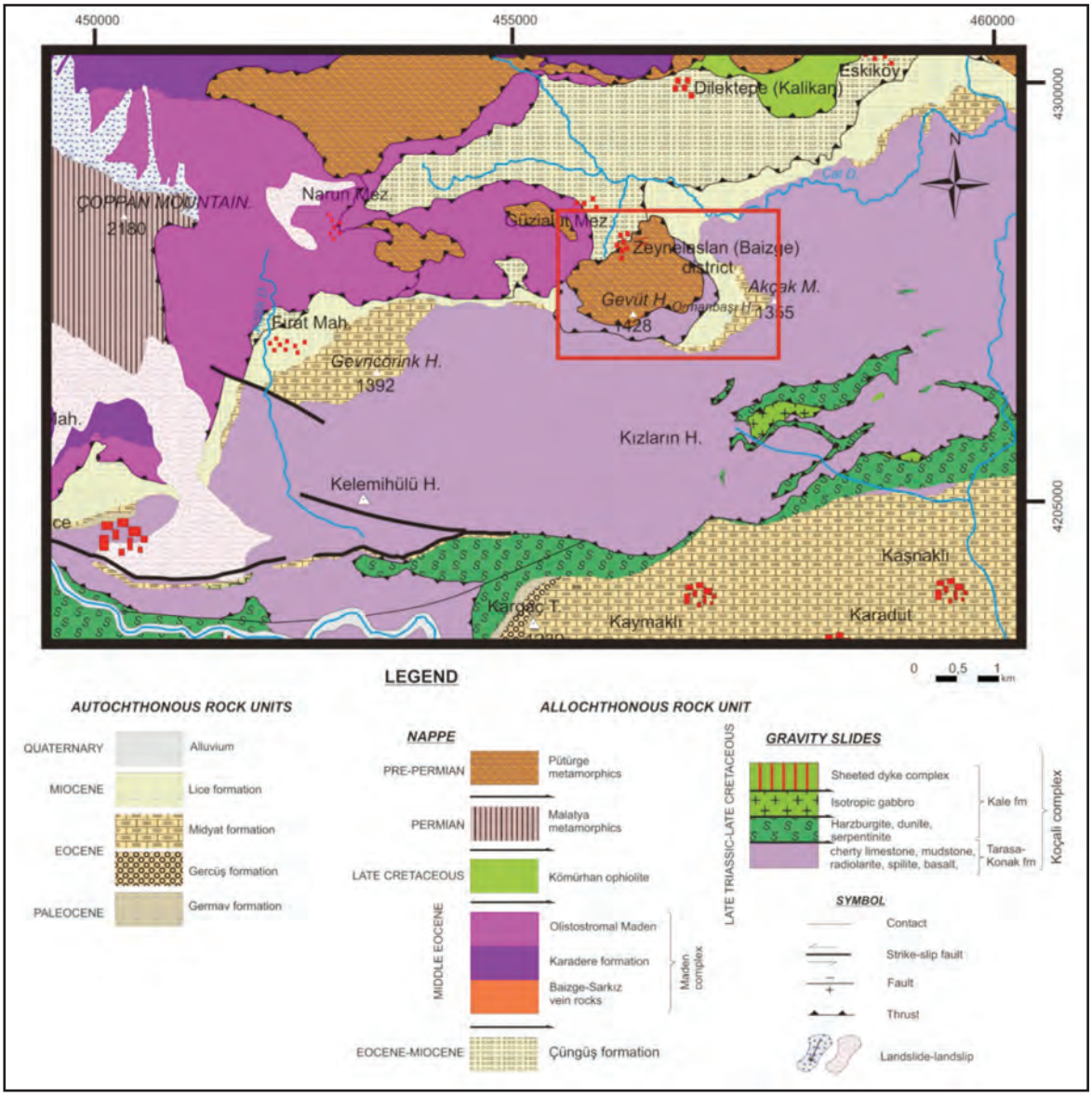

Figure 5- Geological map of the study area and its vicinity (modified from Perinçek, 1978, Herece, 2008)

ternation of sediments with volcanites and Kale formation is composed of serpentinite and diabase assemblages (Perinçek, 1978; Figure 4). The relations among these units are generally tectonics.

The age of the Koçali formation was given as Upper Jurassic – Lower Cretaceous by Sungurlu (1973). Koçali complex has been accepted as a part of Tethys Ocean which emplaced over the Arabian platform by gravity slides in Campanian–Maestrichtian (Rigo de Righi and Cortesini, 1964, Sungurlu, 1974; Perinçek, 1978). Yılmaz (1993) admits that Koçali complex was formed by ophiolitic melange and sedimentary blocks. He also accepts that the ophiolitic rocks which

formed under oceanic regime at north of the Arabian Platform and ensimatic island arc materials which developed due to the north dipping subduction were formed by block and tectonic slices which emplaced on the Arabian Platform in Upper Cretaceous. Bingöl (1993 *a, b*) states that Koçali complex was formed by an extensional zone over intra-oceanic subduction zone dipping north and by a submarine volcanism outside the extensional axis or by an arc volcanism which was then pushed over the northern edge of the Arabian Platform during Campanian – Maestrichtian. Uzunçimen et al. (2011) indicated that Koçali Complex consists of pelagic sediments (such as pelagic limestones and cherts) together with sediment derived platforms and oceanic crust based basic volcanic rocks in SE Turkey. The age of this unit was given as Late Jurassic – Early Cretaceous (Sungurlu, 1973; Perinçek, 1978) but the authors have stated that the age had risen from Middle Carnian to Raetian due to its radiolarian content.

The Koçali complex in the study area was tectonically overlain and imbricated by Pütürge metamorphics of the Çüngüş formation at Ormanbaşı Hill. However; this complex is observed as thrusted over Lice formation (Figure 5). The deposit which was traced in SE – NW trend right at the southern part of Akçak Hill is unconformably overlain by Midyat formation (Figures 4 and 5). The unit extending as a thin tectonical slice at Ormanbaşı Hill is represented by mudstone – volcanite, cherty limestone and shale consisting Tarasa – Konak formations and by the Kale formation which consists of serpentinites extending as a thin slice between these units (Figure 4).

ORE GEOLOGY

Several Cu mineralizations were detected in recent years by MTA within volcanites belonging to Koçali Complex cropping out in and around Adıyaman City (Yıldırım et al., 2008 *a, b*; 2009; 2010 *a, b*; Yıldırım, 2011). It was also revealed that these mineralizations showed similar features with Cyprus type VMS mineralizations. Ormanbaşı Hill location was considered as a promising area for Cyprus type volcanogenic massive sulfide mineralization and was investigated in terms of base and precious metals (Cu-Zn-Pb-Au-Ag).

FIELD STUDIES

Although there are several tectono-stratigraphic deposits, ore mineralizations were only observed in Koçali complex as a zone compatible with a thrust plane which is approximately in NE –SW trend.

The Koçali complex forming the basement in and around the study area is imbricated around Ormanbaşı Hill and tectonically overlies Çüngüş, Lice and Midyat (Fırat) formations. The complex is represented by spilite, diabase, radiolarite mudstone, claystone, shale and serpentinites in the study area (Tarasa formation) and sporadically consists of materials related to Çüngüş formation.

Mineralizations generally occur in severely altered, spilitized basic volcanites. These volcanites are sub marine volcanic rocks that corresponds to upper layers of the Koçali complex and was nomenclatured as Tarasa formation by Sungurlu (1973) (Figures 4 and 6).

Mineralizations took place in the form of reworked lensoidal and layer like shapes within mudstone, diabase, spilite and claystone – shales. Altered zones can easily be distinguished with their brownish and reddish colors and by excessively oxidized views at surface (Figures 7a, b and c). Besides; secondarily developed malachite – azurite coatings were also observed on the serpentinite slice as well that underlies this alteration zone (Figure 7 d). These zones show thicknesses varying between 10 to 100 meters and extend up to 300 meters.

Figure 6- Spilitized pillow lavas of the Koçali complex (100m. NE of Zeynelaslan settlement)

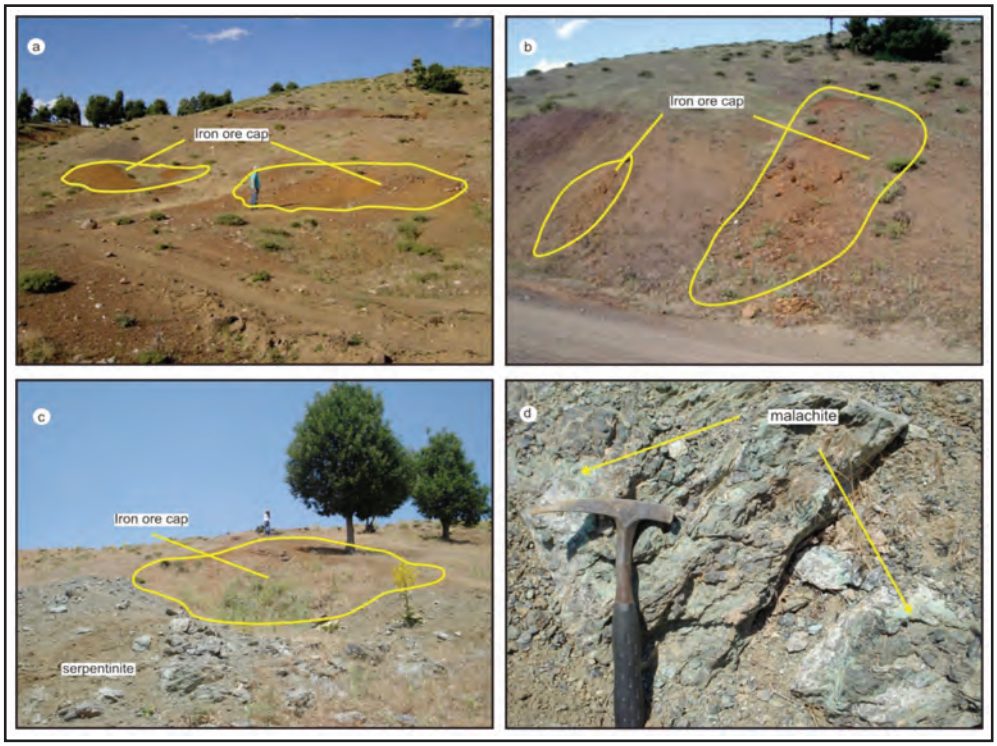

Figure 7- a-b; View from iron ore caps (gossan) in the mineralization area (looking towards NE) (Ormanbaşı Hill location, 100 m west of trench SY-6), c-d; Secondarily developed malachite and azurite occurrences within the iron ore cap at top and serpentinite slice at bottom (Ormanbaşı Hill location, trench SY- 6, looking towards NW)

Trenching

In Ormanbaşı Hill area where mineralizations generally crop out along thrust zones, six trenches were excavated perpendicular to zones where iron ore caps (gossan) occur in order the alteration zones to be traced better and to investigate their continuities (Figure 8). Trenches are maximum 65 m long, 1 m wide and 1.5 - 2 m deep. In some of them, silicious and pyritized zones were detected in which the stockwork structure was developed. However; in other

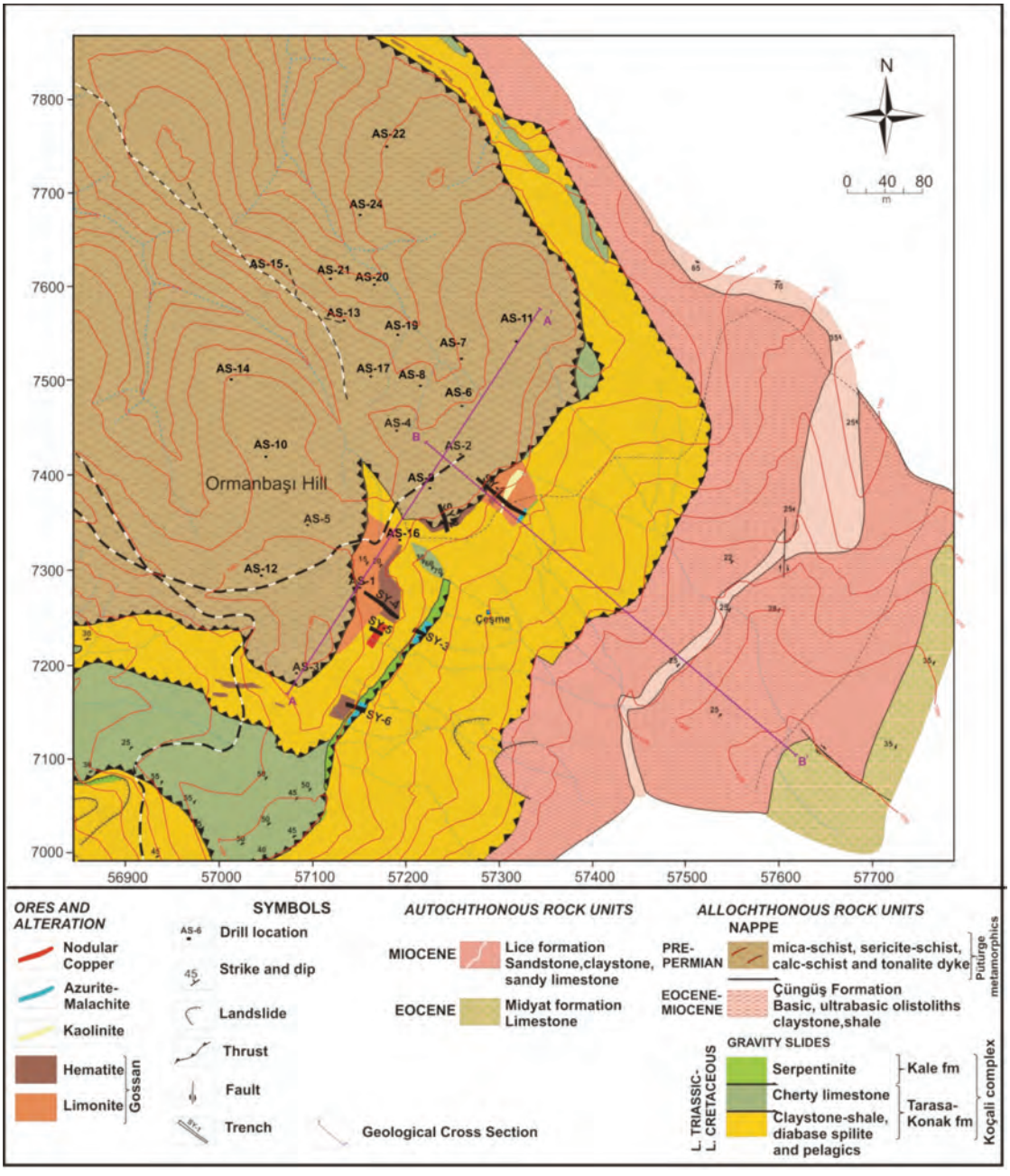

Figure 8- Ore geology map of the study area (Yıldırım, 2011)

trenches goethitic formations at levels which intense hematitization, limonitization within gossans and chalcozite - covellite bornite formations within layers of malachite and azurite were traced. Channel sampling from side walls of trenches were made to perform geochemical analyses. Maximum 3% Cu and 3480 ppb Au were obtained from samples taken in trenches.

Geophysical studies

As geophysical technique, the Induced Polarization (IP) method was performed in order both to determine the distribution of available mineralized zones within the study area and the location of deep-seated mineralizations. Within this purpose, profiles were drawn perpendicular to mineralization zones (SE–NW trending) (Figure 8 and 9). The sulphidization grade of geological structures, the geometry of these sulfidic structures and resistivity differences with respect to adjacent units were investigated in the study area (Bekar, 2010).

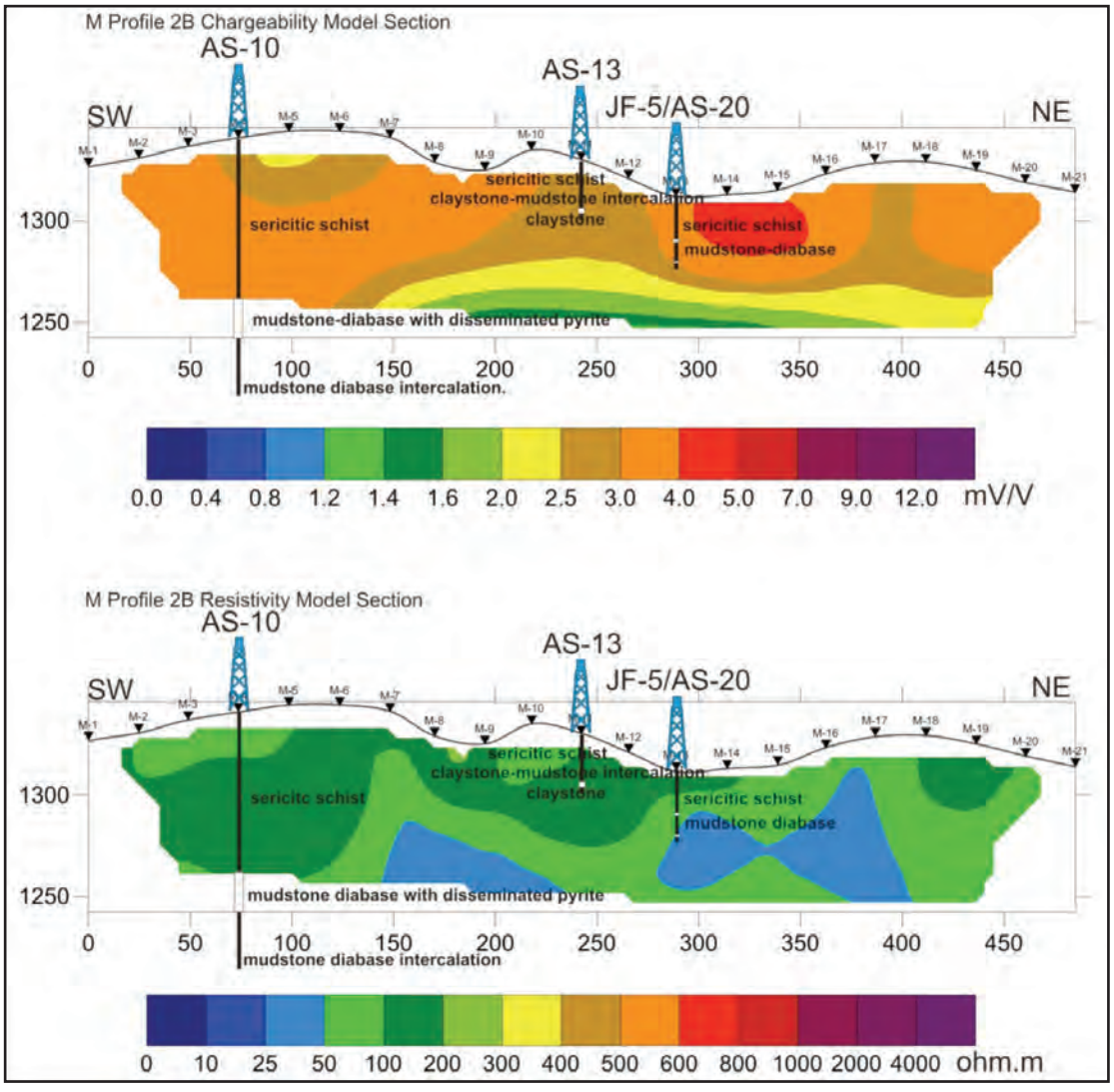

Figure 9- Back analysis of resistivity and chargeability for M- Y profiles (Bekar, 2010)

In Ormanbaşı Hill region, values from the area where mineralization was established by available drillings were obtained even less than the average chargeability values of the area (Figure 9). These low values were interpreted as these mineralizations represent an allochthonous view, do not show any continuity, thin out and thicken in places. These were also considered as units taking place within available mineralizations gave chargeability value (Bekar, 2010).

Drilling investigations

In Ormanbaşı Hill, Sincik (Adıyaman) investigation area, field studies and geophysical anomalies related to exploration and reservoir analyses were correlated and total length of 1933,25 m drilling were carried out in 25 wells. After determination studies had been completed, sample intervals according to the change in mineralization and alteration were determined bisecting core samples. The samples were prepared by quartering method then were submitted to analysis. In drillings; gossan, disseminated and veinlet chalcopyrite and sphalerite within massive pyrite, sporadically disseminated and stockwork levels, brecciated levels and pyrite and chalcopyrite levels were cut (Figures 10 and 11). Panel diagrams and geological cross sections made by the interpretation of well logs that had been obtained from

Figure 10- Massive ore mineral cut in drilling AS -2 and close up view from this bisected ore

Figure 11- Iron ore cap (gossan) that was cut in drilling AS-9 and view from cataclastic massive ore minerals in patches

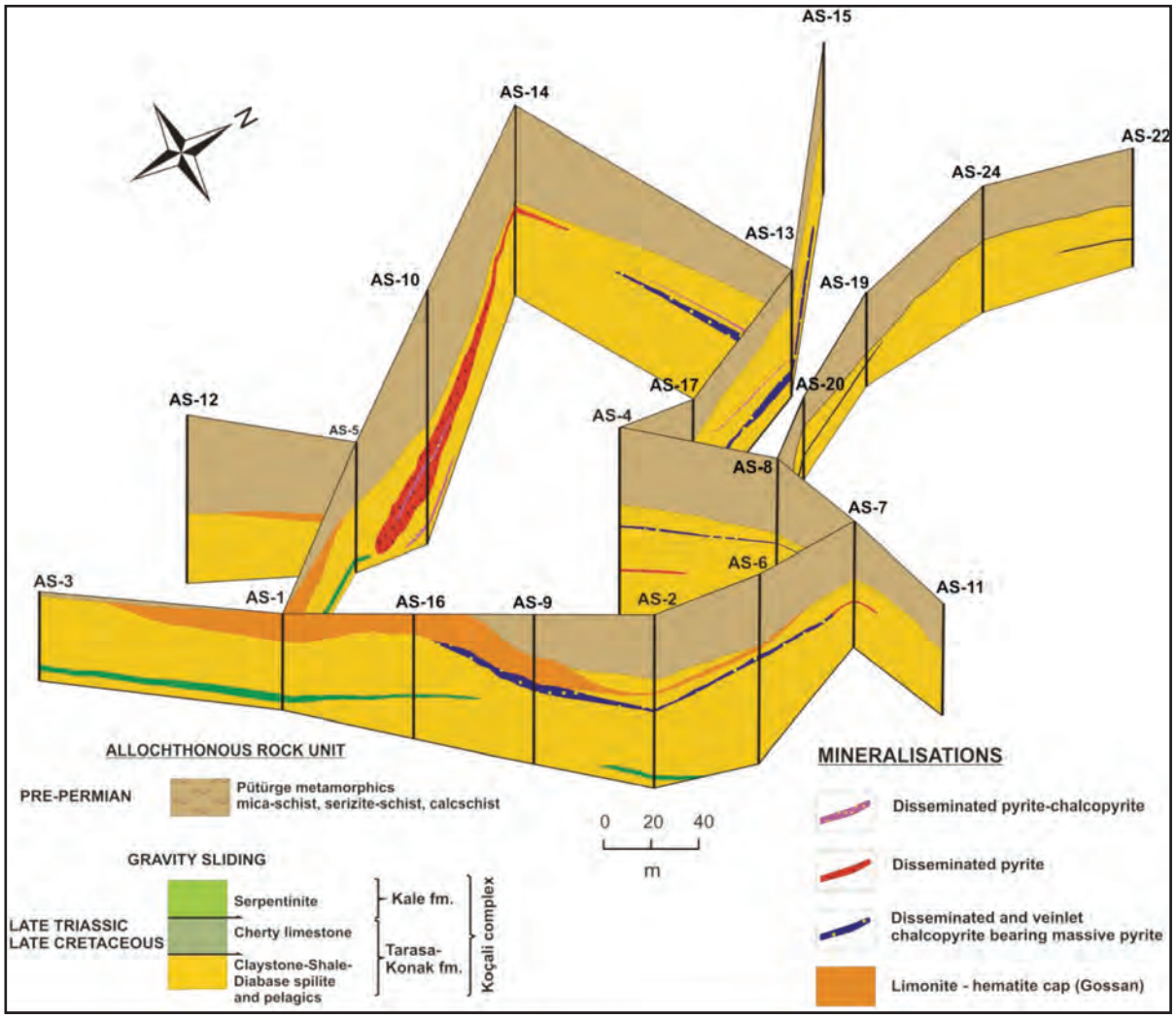

Figure 12- Panel diagram showing drillings in ore mineralization area (Yıldırım, 2011) (see Figure 8 for well locations)

drillings within study were given in Figures 12 and 13. The lateral and vertical variations of mineralized zones on panel diagram were obviously revealed. Mineralization is represented by massive pyrite towards deeper parts, however; it was formed by oxides at surface and at locations close to the surface (gossan). Mineralized sections sporadically show a thinning and thickening structure and this is clearly observed both in panel diagrams and in geological sections.

Alteration

Mineralizations which developed within volcanites of Koçali complex were generally formed from iron ore caps with limonite (also including pyrite), hematite and silica at the surface. Kaolinization was also observed in patches in these zones. However; alterations such as; chloritization, calcification, silicification, limonitization, hematitization, epidotization were generally observed on wall rocks surrounding mineralizations (Figure 14). Also, this type of alterations is frequently seen in sub marine volcanism.

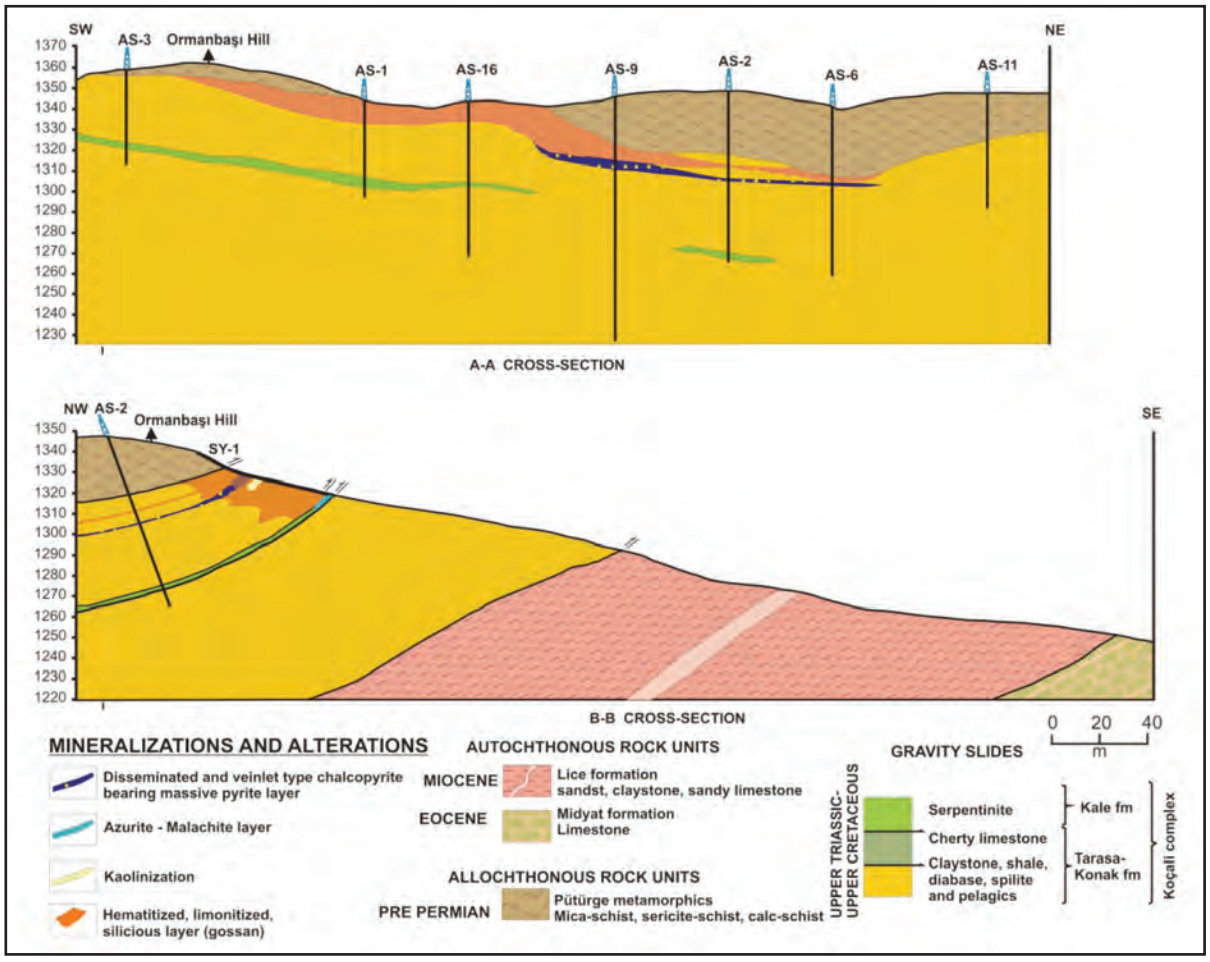

Figure 13- Geological cross sections passing through drillings in the ore mineralization area (Yıldırım, 2011) (see Figure 8 for well locations)

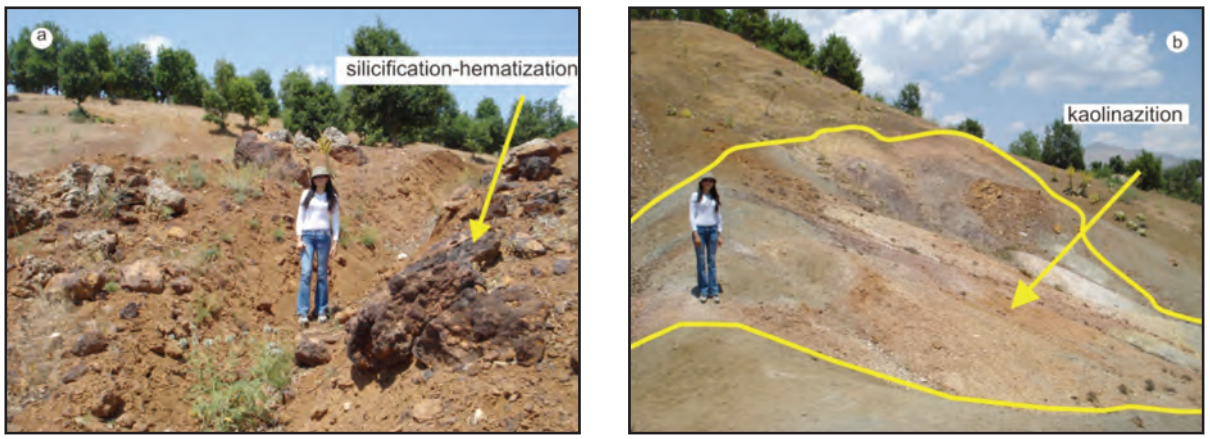

Figure 14- A view from alteration within mineralization zone (Ormanbaşı Hill location, SY-1 trench, looking towards NW)

LABORATORY STUDIES

Ore minerals and paragenesis

Pyrite, marcasite, chalcopyrite, sphalerite, bornite, chalcozine – covelline and native copper were detected as ore minerals due to macroscopic and microscopic studies for samples taken from mineralized zones at drillings and mineral exposures in the study area (Figure 15).

Geothite minerals with interstitial and colloidal textures were also encountered within iron ore cap at the surface. In sample with interstitial texture, Quartz and pyrite minerals were observed in veins or in such a way they had fulfilled voids (Figures 16 and 17).

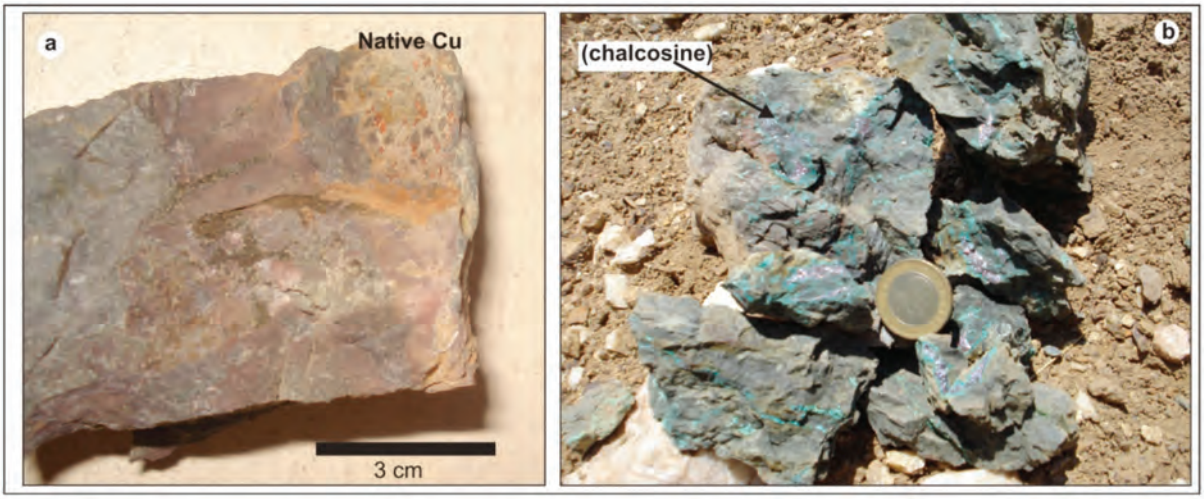

Figure 15- *a)* Native copper disseminations which developed on oxidation zone at surface (Trench SY-2), *b)* Malachite, azurite and chalcozine formations encountered in oxidation zone (Trench SY-1)

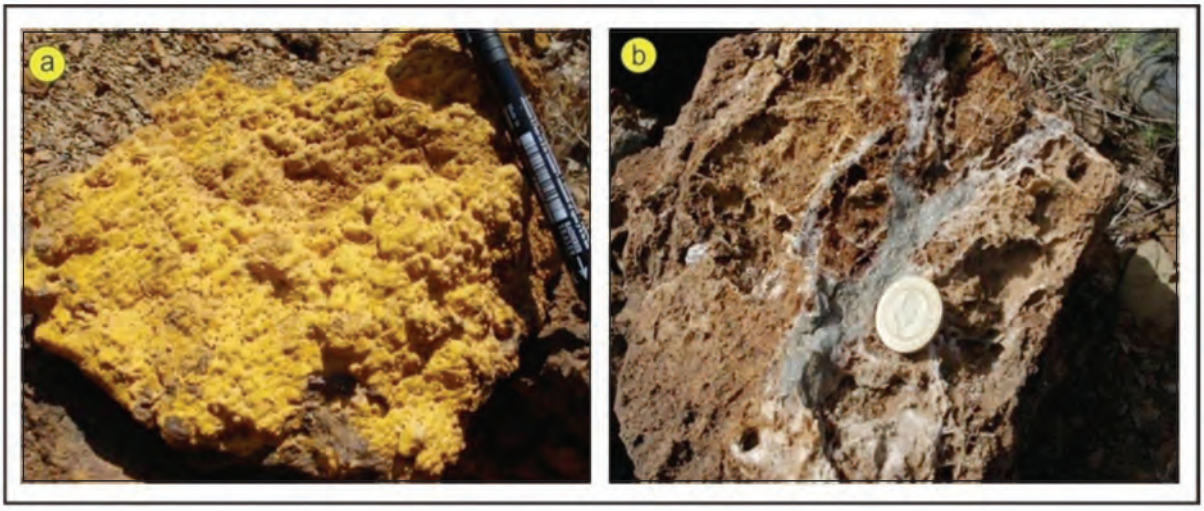

Figure 16- *a*) Colloidal texture developed in gossans (goethite), *b)* Pyrite – silica veins and interstitial texture developed in gossans

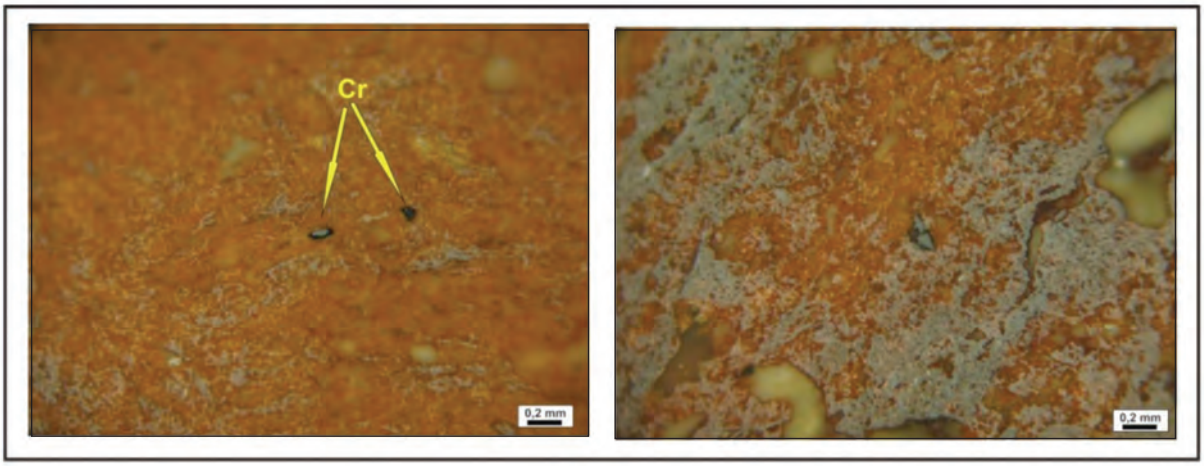

Figure 17- Limonite – hematite and goethite formations and microscope views of chromite granules encountered in gossans (Cr: chromite)

Limonite, hematite, goethite and chromite granules in them which had been reworked by tectonism were encountered in thin sections taken from gossans (Figure 17).

Pyrite is generally surrounded by sphalerite, chalcopyrite and gangue minerals (Figure 18) and is euhedral with smooth edges. However; chalcopyrite and sphalerite are encountered as matrix filling up pyrite granules. It indicates that, pyrite was formed earlier than sphalerite and chalcopyrite.

In paragenesis, pyrite is dominant mineral but chalcopyrite and sphalerite are present in fewer amounts. Chalcopyrite is the second most encountered ore mineral after pyrite and was formed after pyrite and sphalerite. Chalcopyrite has both confined pyrite and sphalerite and accumulated along cleavages and was encountered as irregular and amorphous granules. Besides; chalcopyrite has generally substituted pyrite and sphalerite (Figure 18). Chalcopyrite has turned into covelline and chalcozine along cleavages and edges in some thin sections (Figure 19).

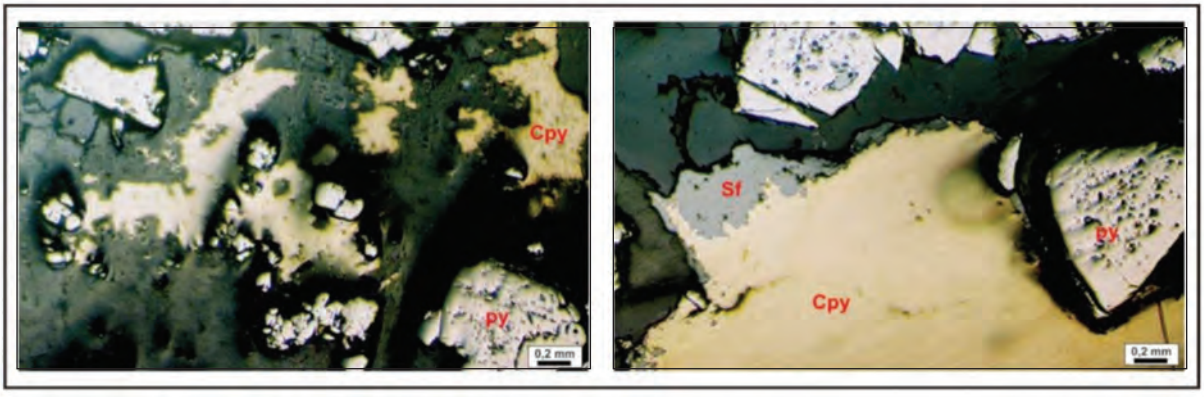

Figure 18- Euhedral pyrites, anhedral sphalerite and chalcopyrites encountered in massive pyrite ore mineral (Py: pyrite; Cpy: chalcopyrite; Sf: sphalerite) (core sample belonging to drilling AS-2)

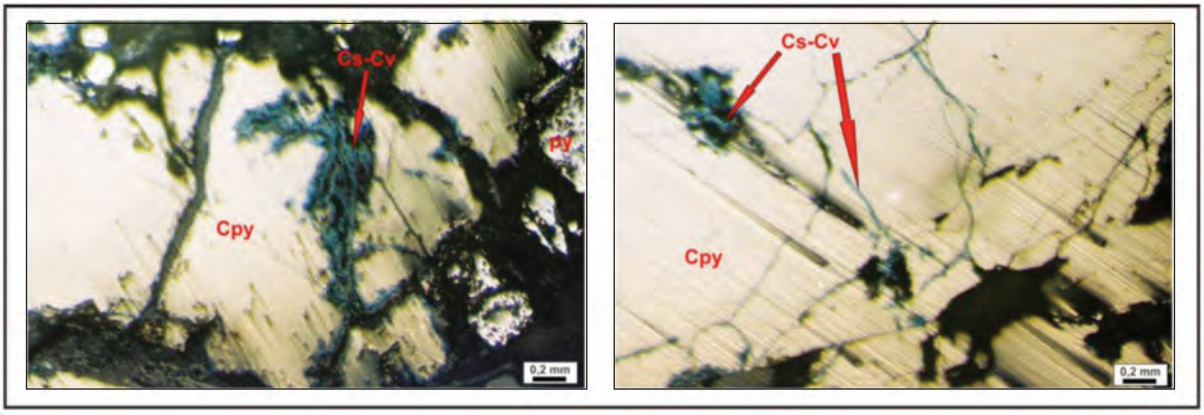

Figure 19- Secondarily developed chalcozine and covelline formations along fractures and cleavages of chalcopyrites within massive pyrite ore mineral (Cpy: chalcopyrite; Cs-Cv: chalcozine – covelline)

Sphalerite was less frequently encountered than pyrite and chalcopyrite. It was generally observed along cleavages and edges of pyrite, in the form of free granules and within chalcopyrite and seen in the form of anhedral granules.

Ore mineralizations present colloidal, zoned, euhedral to subhedral and cataclastic textures which is peculiar to massive sulfide deposits and were developed under low temperatures (Figure 20).

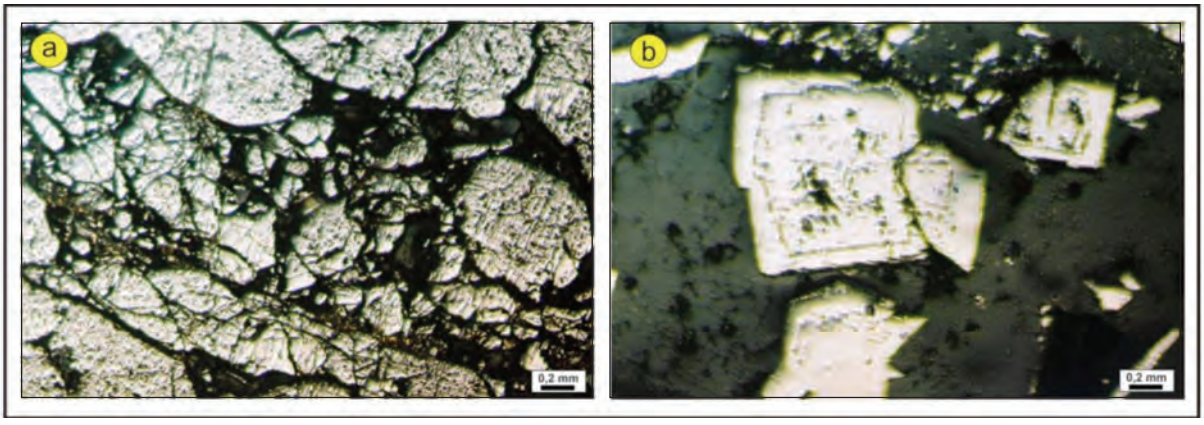

Figure 20- a) Cataclastic texture encountered in massive pyrite ore mineral, b) zoning developed in pyrites in massive ore

Cu mineralizations were only encountered in volcanites of Jurassic – Lower Cretaceous Koçali complex in the study area. Besides; manganese nodules with copper characterizing the oceanic environment were also observed within claystone – marls of the Koçali complex (Figure 21).

Mineralizations at surface were encountered in the form of limonitization, hematitization, argillitization and iron ore cap. However; the massive ore with pyrite were seen beneath the iron ore cap at surface. At deeper parts, disseminated – stockwork brecciated levels with pyrite and chalcopyrite takes place.

Figure 21- Manganese nodules with copper encountered in claystone and marl of the Koçali complex

Geochemical analyses and assessments

Among massive and stockwork ore samples within the study area, 15 of them were submitted to geochemical analysis to detect Cu, Pb, Zn, Ni Co, Mo, Sb, As, Bi Ag and Au contents (Table 1) by flame AAS/ICP-OES method at the Department of Mineral Analysis and Technologies of MTA. However; 8 ore/ore bearing rock samples collected at the surface were analyzed to detect major element oxide, trace and Rare Earth Elements (REE) by ICP-MS method in Activation Laboratories (ACTLABS) in Canada (Tables 2, 3 and 4).

Table 1- Base – precious metal contents of samples belonging to Sincik – Ormanbaşı Hill Mineralization (MTA- Ankara)

Sample No	Ore Type	Cu ppm	Pb ppm	Zn ppm	Ni ppm	Co ppm	Mo ppm	Sb ppm	As ppm	Bi ppm	Ag ppm	Au ppb	Depth (meters)
AS2-30	massive	18000	23	260	<10	_	30	<10	33	<10	4,3	250	41,70-42,70
AS6-18	massive	39000	457	23	<10	_	53	<10	<.20	<10	4,2	200	36,30-37,50
AS6-19	massive	28500	386	27	37	_	42	<10	<20	<10	3,9	140	37,50-38,30
AS8-20	massive	15250	30	445	20	_	38	<10	75	<10	6.9	170	39,55-40,25
AS9-15	massive	13100	49	4330	65	_	30	<10	28	<10	4.8	180	30,60-31,40
AS9-16	massive	22100	44	14200	<10	_	35	<10	<20	<10	4.5	160	31,40-32,60
AS9-17	massive	36120	100	27000	<10	_	30	<10	31	<10	7.8	300	32,60-34,00
AS9-18	massive	27900	31	2380	<10	_	124	<10	<20	<10	4.5	40	34,00-35,50
AS10-33	stockwork	10690	52	20360	<10	401	33	<10	23	<10	6	260	83,90-85,00
AS10-43	stockwork	33520	100	28230	<10	240	31	<10	56	<10	10.7	290	111,50-114,50
AS13-23	massive	34160	139	23400	<10	235	22	<10	22	<10	9.6	420	50,00-51,50
AS13-24	massive	19010	56	26900	<10	283	34	<10	33	<10	7.3	260	51,50-53,00
AS13-25	massive	16170	98	16330	<10	354	38	<10	<20	<10	5.8	300	53,00-54,15
AS-19-3	massive	15500	<10	295	<10	140	13	<10	20	<10	4.7	150	34,40-34,85
AS-20-9	massive	9470	31	91	135	105	11	<10	<20	<10	1.9	50	29,30-29,40

Table 2- Major oxide, trace element and REE contents of samples belonging to Sincik – Ormanbaşı Hill Mineralization

Sample No	Ore Type	SiO_2 %	Al_2O_3 %	Fe_2O_3(T) %	MnO %	MgO %	CaO %	Na_2O %	K_2O %	TiO_2 %	P_2O_5 %	Loss in fire %	Total %
S-2	Gossan,limonite hematite	33.68	0.70	52.32	0.05	0.17	0.15	0.06	0.06	0.10	0.04	11.22	98.57
S-7	Gossan,limonite, hematite	54.10	6.27	22.33	0.13	1.08	0.61	2.44	0.33	2.73	0.26	8.81	99.10
S-10	Gossan, pyrite	64.68	0.86	23.95	0.02	0.10	0.08	0.13	0.12	0.03	0.02	9.22	99.22
S-11	Serpantinites including malachite	37.72	2.51	8.13	0.35	30.18	0.25	0.04	0.03	0.005	0.04	15.21	94.46
S-15	Gossan, hematite, pyrite	75.64	1.09	17.79	0.01	0.08	0.06	0.11	0.10	0.56	0.01	3.07	98.53
S-13	Manganese nodule including malachite	17.89	3.87	39.18	0.02	0.80	0.12	0.43	0.45	0.24	0.58	1.90	65.49
S-18	Gossan, pyrite	69.48	1.7o	19.38	0.02	0.09	0.06	0.12	0.23	0.28	0.01	7.15	98.52
S-21	Gossan, malachite, limonite	83.01	2.63	6.55	0.02	0.08	1.21	0.13	0.08	0.01	0.05	3.66	97.43

Table 3- Trace element contents of samples belonging to Sincik – Ormanbaşı Hill Mineralization (ACTLABS – Canada)

Sample No	Sc ppm	Be ppm	V ppm	Ba ppm	Sr ppm	Y ppm	Zr ppm	Cr ppm	Co ppm	Ni ppm	Cu ppm	Zn ppm	Ga ppm	Ge ppm	As ppm	Rb ppm	Nb ppm	Mo ppm	Ag ppm	In ppm	Sn ppm	Sb ppm	Cs ppm
S-2	2	< 1	143	8	4	< 2	27	60	14	< 20	1710	310	9	2	190	< 2	2	> 100	> 100	< 0.2	13	10.6	< 0.5
S-7	22	< 1	496	154	63	< 2	175	250	54	30	2440	710	68	3	87	8	4	28	8.1	1.9	3	1.3	< 0.5
S-10	< 1	< 1	16	67	6	< 2	5	30	473	< 20	460	150	4	< 1	18	3	< 1	78	16.7	< 0.2	1	1.5	< 0.5
S-11	9	1	33	52	6	5	< 4	3110	394	2420	27900	770	< 1	1	6	< 2	< 1	8	< 0.5	< 0.2	< 1	< 0.5	< 0.5
S-15	5	< 1	42	101	9	5	40	40	75	< 20	260	40	3	2	31	2	< 1	83	3.7	< 0.2	4	2.8	< 0.5
S-13	12	1	216	49	16	4	35	260	36	50	28000	100	4	< 1	32	16	2	4	< 0.5	< 0.2	< 1	< 0.5	1.3
S-18	3	< 1	51	720	17	< 2	26	50	89	< 20	430	90	10	1	20	4	< 1	41	8	< 0.2	4	3.4	< 0.5
S-21	2	< 1	41	81	32	5	5	40	61	30	19800	360	< 1	< 1	6	< 2	< 1	11	< 0.5	< 0.2	< 1	1	< 0.5

Table 4- REE contents of samples belonging to Sincik – Ormanbaşı Hill Mineralization (ACTLABS – Canada)

Sample No	La ppm	Ce ppm	Pr ppm	Nd ppm	Sm ppm	Eu ppm	Gd ppm	Tb ppm	Dy ppm	Ho ppm	Er ppm	Tm ppm	Yb ppm	Lu ppm	Hf ppm	Ta ppm	W ppm	Tl ppm	Pb ppm	Bi ppm	Th ppm	U ppm
S-2	2.2	2.6	0.36	1.4	0.3	0.09	0.3	< 0.1	0.4	0.1	0.3	0.06	0.4	0.08	0.4	0.1	4	2.7	177	0.5	0.7	2.2
S-7	3	4.9	0.36	1	0.2	0.06	0.3	< 0.1	0.5	0.1	0.5	0.09	0.7	0.12	4.1	0.3	1	1.8	142	< 0.4	0.6	0.4
S-10	1	1.5	0.19	0.6	0.1	< 0.05	< 0.1	< 0.1	0.1	< 0.1	< 0.1	< 0.05	< 0.1	< 0.04	< 0.2	< 0.1	12	< 0.1	12	1.1	0.3	0.6
S-11	3	25.1	1.43	6.8	2	0.51	1.7	0.3	1.4	0.2	0.6	0.09	0.6	0.09	< 0.2	< 0.1	3	0.2	< 5	< 0.4	< 0.1	0.5
S-15	5.3	11.9	1.61	7.3	1.4	0.41	0.9	0.2	0.9	0.2	0.7	0.11	0.8	0.13	0.9	< 0.1	6	< 0.1	< 5	1.6	0.2	2.2
S-13	7.2	19.2	2.51	10.5	3	0.84	2.6	0.5	2.6	0.5	1.2	0.17	1.1	0.17	1	0.2	2	0.6	22	< 0.4	2.6	2.4
S-18	1.1	2.3	0.31	1.3	0.4	0.18	0.4	< 0.1	0.6	0.1	0.4	0.06	0.4	0.07	0.4	< 0.1	3	0.2	25	< 0.4	0.3	3
S-21	3.2	6.8	1.13	5.3	1.4	0.39	1.3	0.2	1.2	0.2	0.6	0.09	0.5	0.08	< 0.2	< 0.1	2	0.2	< 5	< 0.4	0.2	2

The classification of VMS deposits in terms of base metals in the world is seen in figures 22a and b. Although Pb content is low, Cu and Zn contents are high in mineralization at Ormanbaşı Hill location. This is one of the typical characteristics of VMS deposits associated with ophiolites (Galley and Koski, 1999). According to this classification, it is seen that samples plot into Cyprus type volcanogenic massive sulfide deposits area (Figures 22 a, b).

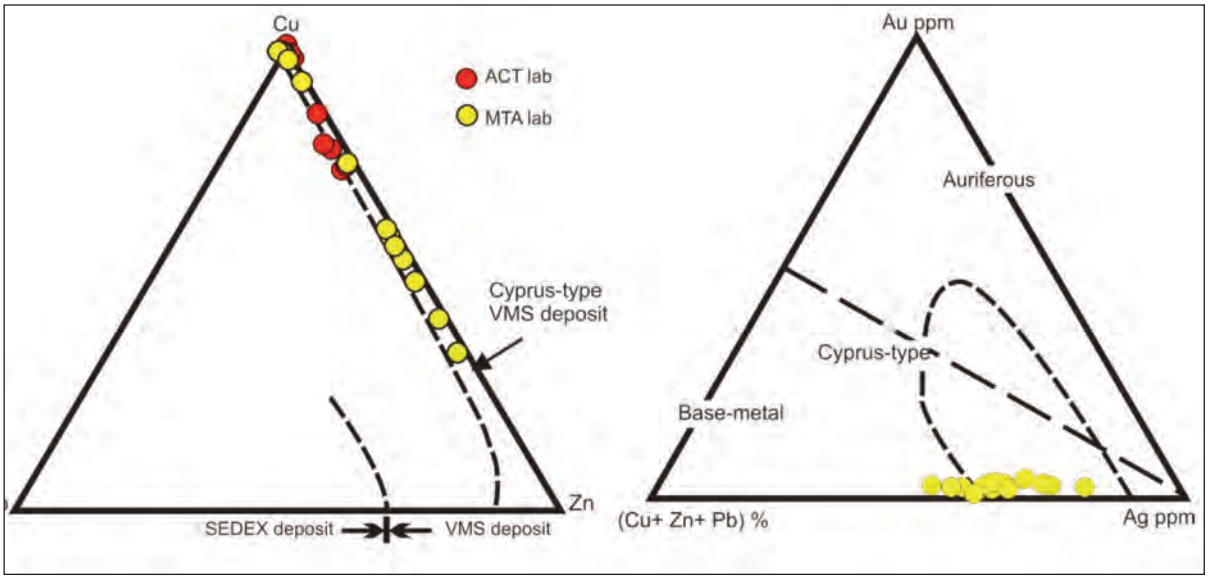

Figure 22- The distribution of samples belonging to Sincik – Ormanbaşı Hill Mineralization using; a) Cu–Pb–Zn discrimination diagram (from Galley and Koski, 1999) and b) Au-(Cu+Zn+Pb)+Ag discrimination diagram (Barrie and Hannington, 1999) (according to Galley and Koski, 1999)

Trace element and REE contents in pyrites are important to understand the origin of mineralizations. It is seen that REE contents of pyritic ore samples in Ormanbaşı Hill present a trend close to chondrite values in chondrite normalized diagram and there is not observed a high enrichment (Figure 23). This shows that, the source of metals forming the mineralization are not marine sedimentary but are associated with magmatic rocks.

The low Pb contents (Galley and Koski, 1999) of Pb, Cu, Ag, Au, Zn element contents in samples belonging to Ormanbaşı Hill mineralizations in primitive mantle normalized spider diagrams show a resemblance to Cyprus type VMS deposits (Figure 24).

Co/Ni ratio is used as a potential discriminator between magmatic – hydrothermal and sedimentary environments. Co/Ni ratios are less than 1, although high Co and Ni contents are encountered in pyrite and pyrrhotine in sedimentary, volcanogenic or diagenetic source materials (Cambel and Jarkovsky, 1967). Co and Ni contents are generally low in hydrothermal source sulfides (less than 100 ppm) and the ratio of Co/Ni is much higher than 1 (Cambel and Jarkovsky, 1967). Although the amount of Ni is higher than Co element on earth crust, Co/Ni ratios in hydrothermal pyrites are above 1. Co element is leached from wall rocks easier than Ni, then is taken into solution and diluted in deposits (Güleç and Erler, 1983). During analyses carried out in massive pyrites belonging to Ormanbaşı

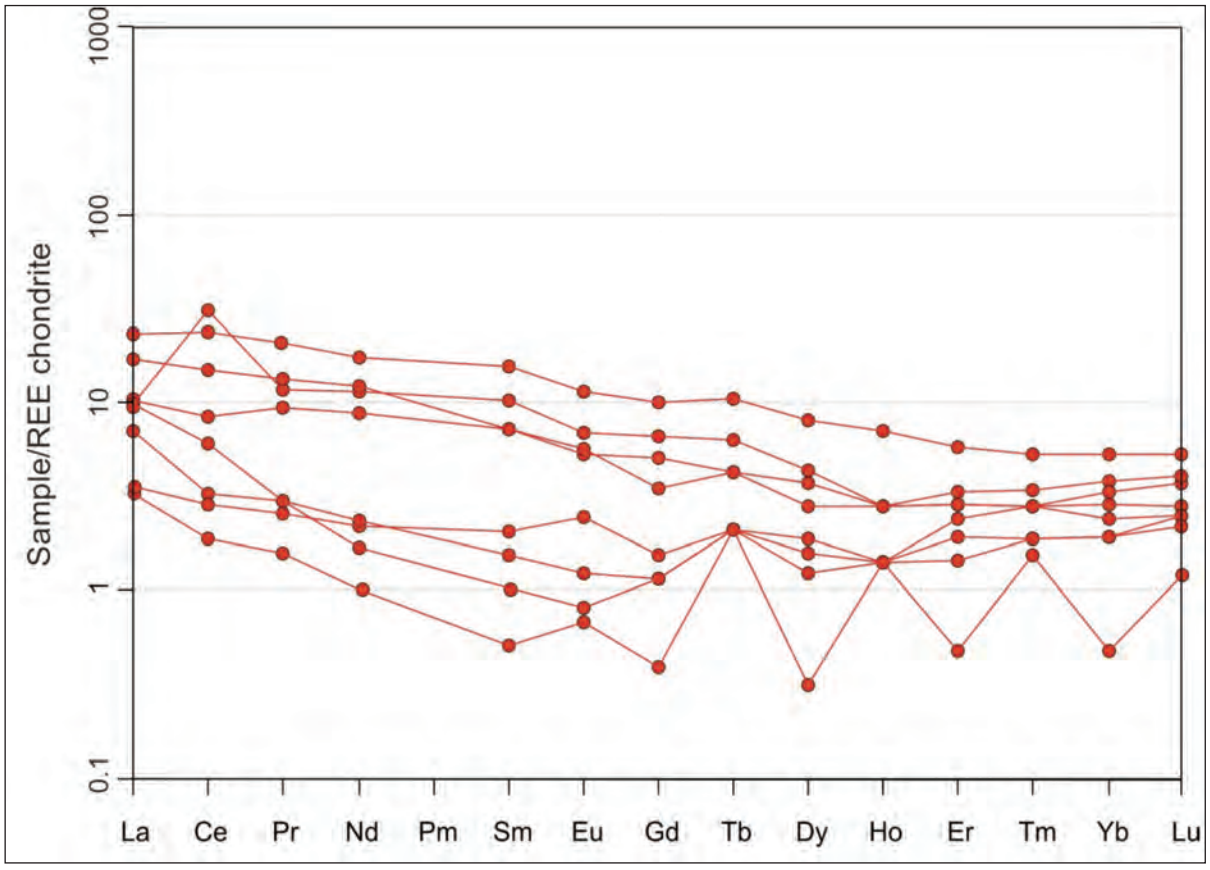

Figure 23- Chondrite normalized (Boynton, 1984) REE multi element distributions for samples belonging to Ormanbaşı Hill mineralizations

Hill mineralizations, Co/Ni ratios were seen higher than 1 and the content of Ni is low. This phenomenon was interpreted as the hydrothermal processes had been effective in mineralizations.

SOTOPE STUDIES

δ ^{34}S analysis were carried out in laboratory of the Lausanne University (Switzerland) in 2 samples which had been selected from ore minerals in the study area. In sulphur isotope studies; it is considered that, if the average ^{34}S for the deposit is 0, then it is deep and is homogenous source, if S is negative then it indicates a bacteriological activity and sedimentary deposition (Rollinson, 1993). For magmatic rocks ^{34}S is 0, for hydrothermal solutions associated with volcanism ^{34}S is (+) and in sedimentary rocks ^{34}S ranges in between -10 and -40 (Rollinson, 1993).

In pyrite and chalcopyrite samples within the study area ^{32}S/^{34}S ratios were found as 6.9 and 7.6 (Table 5).

Sample No Explanation δ ^{34}S‰ S-19 Pyrite- Chalcopyrite (surface) 7.6

S-32 Pyrite- Chalcopyrite (drilling) 6.9

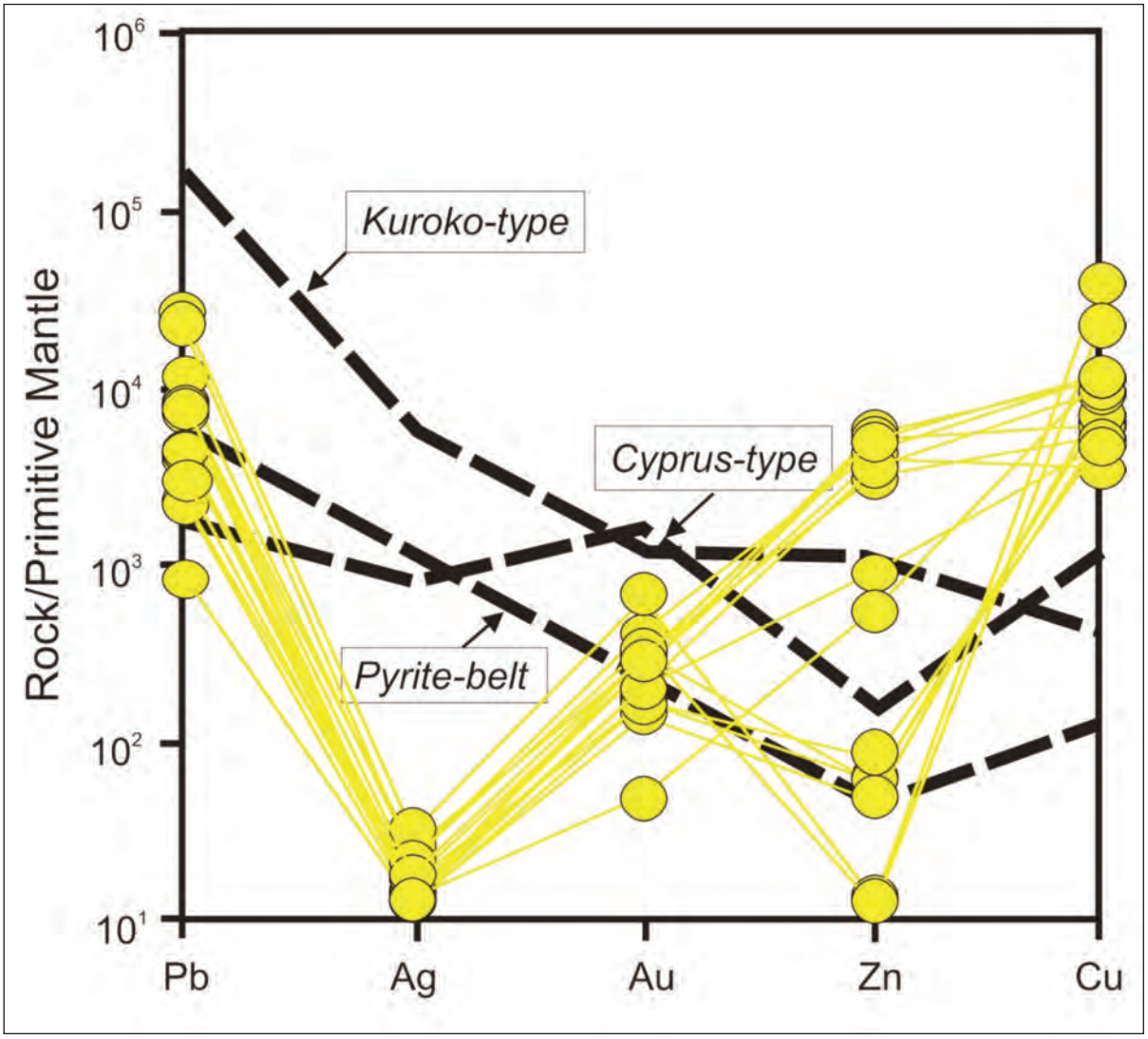

Figure 24- Spider diagram (primitive mantle normalized) of Pb, Ag, Au, Zn and Cu contents for samples belonging to Ormanbaşı Hill mineralizations (Galley and Koski, 1999)

Table 5- $^{32}S/^{34}S$ values of two samples belonging to Ormanbaşı Hill mineralization (Lausanne University, Switzerland)

Sample No	Explanation	$\delta\ ^{34}S‰$
S-19	Pyrite- Chalcopyrite (surface)	7.6
S-32	Pyrite- Chalcopyrite (drilling)	6.9

When minerals in Sincik and Torodos volcanogenic massive sulfide deposits were compared with each other, it was seen that these exhibited similar sulfur isotope values. These values are both compatible with sulfur ratios in hydrothermal solutions associated with volcanism and with Cyprus type VMS deposits on the world (Figure 25) (Rollinson, 1993).

$\delta^{34}S$ values of pyrites taken from massive sulfide deposits which was observed in Torodos ophiolites range between -1.1 and 7.5 ‰. However; these values were restricted to +4 and +7 ‰ (Clark, 1971; Hutchinson and Searle, 1970; Jamieson and Lydon, 1987). Variations within this interval can be observed even in the same deposit, but it is clear that sulfurs in this sulfide deposit were mainly derived from magmatic rocks.

RESULTS AND DISCUSSIONS

The ophiolites originated within layers of oceanic crust but these were then placed on the continental crust. Therefore; these were considered as closely being associated with sea water since these had remained at the sea bottom throughout long geological history. The interaction of rocks with sea water is inevitable especially for basalts located at the uppermost part of the ophiolitic series and plate dike complex underneath the basalts and even partly for gabbroic

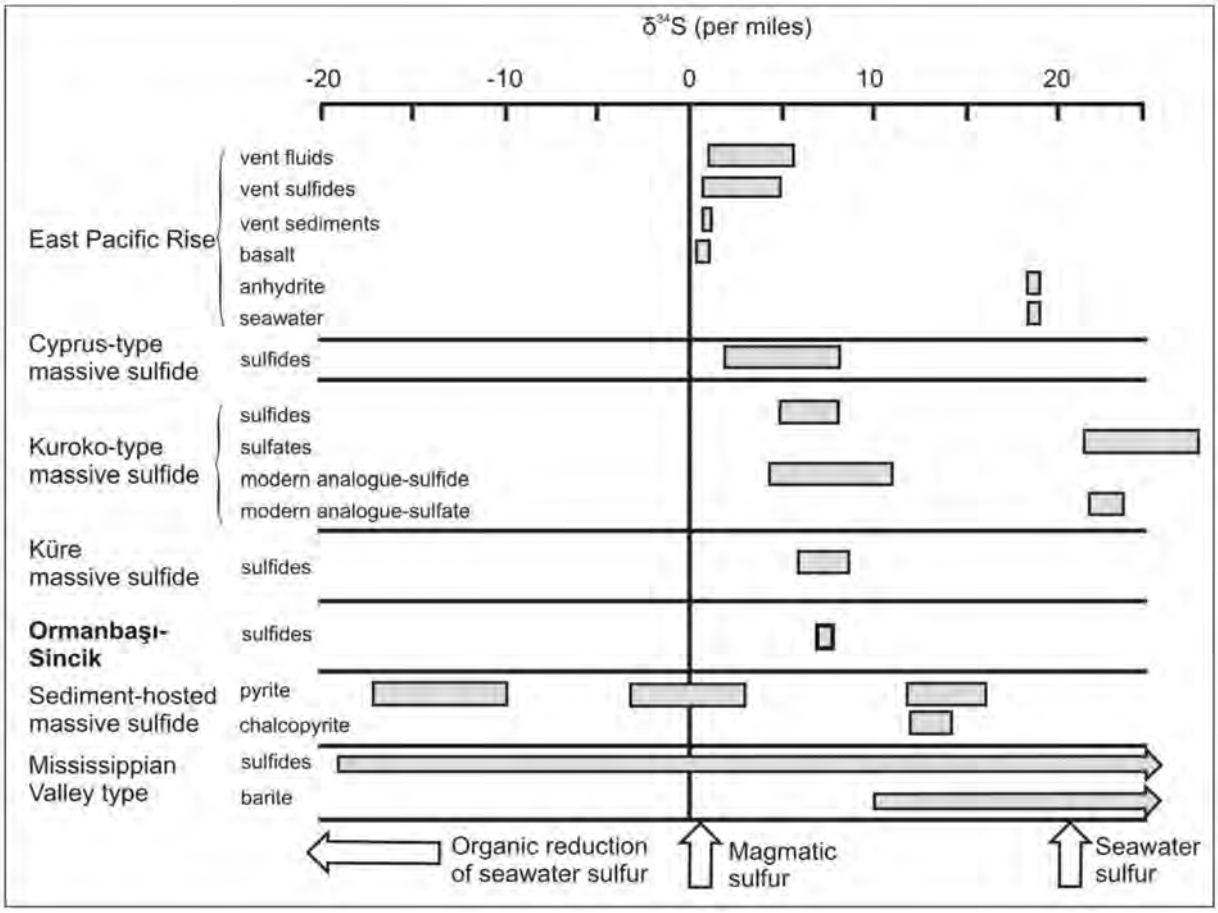

Figure 25- $\delta^{34}S$ isotope values in the study area and in some massive sulfide deposits (Rollinson, 1993)

sections. This interaction in many cases creates great mineralogical and geochemical changes. The cycling fluid penetrates rock units intruding into oceanic crust and causes significant changes in chemical compositional with the effect of high temperature (İmer, 2006). These fluids which have become hydrothermal solution reach the sea bottom and spreads over the bottom rising up by the effect of adiabatic pressures through tectonic fracture and fissures together with other volcanic materials in active volcanic systems.

Metal sulfides suddenly precipitate in situ or at short distances due to rapid cooling, sudden change in pH and Eh and by the effect of sea water in this medium. The spread of mineralized solutions over the sea bottom through fracture and fissure lines corresponds to the periods which the rate of magma development with silica composition is minimum. Fumeroles which occur towards the end of sea bottom volcanic activity could also form mineralization in such ore formations. Some investigations in Japan revealed that fumeroles had formed massive sulfide deposits due to their repetitive activities (Tatsumi, 1970; Sato, 1974).

In previous studies, Gültekin (2004) has stated that Ormanbaşı Hill mineralizations had been traced along tectonical lines and mineralizations in this area were suitable to epithermal type of mineralization due to the presence of minerals showing low temperature conditions and structural – textural features. Not only the presence of mineralization to be only in Koçali complex or being deposited over thrust plane but also the mineral paragenesis, textural features, alteration types, chemical and isotopic findings all indicate that these mineralizations are Cyprus type VMS mineralization in this study. Besides; low temperature minerals which were encountered at the surface could extensively be found at gossan levels of Cyprus type VMS mineralizations (Savkins, 1990).

Mineralizations in the region are available in Koçali complex and are compatible with the general lineation of the Southeast Anatolian Thrust Belt. Mineralizations are observed in mudstone, diabase, spilite, claystone and shales, allochthonous and are in the form of lenses and layers. It is therefore similar to Çüngüş (Derdere) mineralization with these features (Şaşmaz et al., 1999). Mineralizations are generally massive in character and are sporadically observed as stockwork and disseminated. However; there are pyrite, chalcopyrite, sphalerite, pyrrhotine, chalcosine and covelline in mineral paragenesis. While this is seen as an iron ore cap especially at the surface, it passes into massive ore at depths. Colloidal, euhedral to subhedral, cataclastic and zoning textures peculiar to massive sulfide deposits that had developed at low temperatures were encountered.

It is seen that hydrothermal alterations observed in Koçali complex widely bear the traces of low graded oceanic bottom metamorphism. Hence; the metamorphic paragenesis prevailing in the study area is represented by the metamorphic mineral assemblage as quartz + albite + chlorite + epidote. These minerals which are typically observed in altered ophiolitic rocks present pressure and temperature conditions belonging to green schist facies.

The base metal association in Sincik mineralization is Fe – Cu – Zn which originated in sulfide forms. The metals which were found in mineralized zones should have been taken into solution mainly by being leached from the base rock as a result of the hydrothermal fluid cycle. Later on; these should have been occupied in the form of sulfur compounds in hydrothermal solutions and precipitated at the sea bottom and/or shallow depth conditions in the form of sulfuric compounds in upper zones due to temperature decrease, sudden Eh/pH change and rapid geochemical variations in the sea water.

Looking at the metallic composition in Sincik mineralization, it was easily seen that Cu had

higher concentration compared to Zn and Pb. As a result of analyses carried out in MTA and ACT-LAB, the average Cu concentrations in these mineralizations were obtained as 2.2 and 1.0 %, respectively. These Cu values show resemblance with Torodos massive sulfide mineralization (average Cu: 2.78 %) (Constantinou and Govet,1973; Hanington et al., 1998).

When the sulfur isotope values of pyrites taken from the study area was correlated with the isotope values in Torodos massive sulfide deposits, there was observed a similarity between these mineralizations.

As a result; it was concluded that mineralizations exhibited the general features of Cyprus type volcanogenic massive sulfide deposits and had no relation with the epithermal type mineralization which had been defined in previous studies. Future studies should be focused on the establishment of conjugates of these formations along the belt and on the correlation of these formations with other formations. In doing so; a new Cyprus type VMS metallogenic belt could be established along the Southeast Anatolian Thrust Belt.

ACKNOWLEDGEMENT

This study has been carried out within the framework of the project namely the “Investigation of Cyprus type VMS mineralizations within Koçali complex” by the Mine Research and Exploration Department of the General Directorate of Mineral Research and Exploration (MTA) Ankara, Turkey. We would express our indebted appreciation to Ali Aydın (Geo. Eng, Ms.), Yunus Ay (Geo. Eng, Ms.), Bülent Kalı (Geo. Eng, Ms.), Muhittin Yığmatepe (Geo. Eng), and to Kürşad Beker (Geophy. Eng., Ms.) for their supports during field studies. We also would like to express our special thanks to Dr. Yahya Çiftçi for his critics and supports he made during this study.

Manuscript received January 10, 2012

REFERENCES

Altınlı, İ. E., 1966. Doğu ve Güneydoğu Anadolu’nun jeolojisi. MTA Bulletin, 66, 35-74.

Barrie, C. T. and Hannington, M. D., 1999. Classification of volcanic-associated massive sulfide deposits based on host-rock composition. Reviews in Economic Geology, v. 8, 1-11.

Bekar, K., 2010. Adıyaman – Sincik – Ormanbaşı Tepe Sahasının IP Yöntemi ile Araştırılması. 3. Yer Elektrik Çalıştayı, Genişletilmiş Özet Kitabı, Ankara Üniversitesi Ilgaz ÖRSEM Tesisleri, Çankırı, 24-26 Mayıs 2010.

Beyarslan, M., Bingöl, A. F. and Yıldırım, N., 2009. Koçali Ofiyolitik Karmaşığının petrolojik ve tektono-magmatik özellikleri (Adıyaman). Tübitak Project (107Y344). (unpublished).

Bingöl, A.F., 1993 *a.* Çermik-Çüngüş ve Dicle Yöresi Magmatik Kayaçlarının Petrografik Özellikleri. F.Ü. Fen Bilimleri Enstitüsü Fen ve Müh. Bilimleri Dergisi, 5/1, 1-9.

————, 1993 *b.* Çermik Yöresinde Koçali Karmaşığı’nın Jeokimyası. Doğa ve Yer Bilimleri Dergisi, 55-61.

Boynton, W.V., 1984. Cosmochemistry of the rare earth elements: meteorite studies. In: Henderson, P. (Ed.), Rare Earth Element Geochemistry. Elsevier, Amsterdam, 63–114.

Campel, B. and Jorkovsky, J., 1967. Geochemie der Pyrite einiger Lagerstätten der Tschechoslowakei. VSAV Bratislava, 493p.

Cengiz, R., 1991. Doğanşehir Malatya Yöresinin Jeolojisi Maden Jeolojisi ve Jeokimyası. Maden Tetkik ve Arama Genel Müdürlüğü, Report No: 10317, Ankara (unpublished).

Clark, L.A., 1971. Volcanogenic ores: comparison of cupriferous pyrite deposits of Cyprus and Japanese Kuroko deposits. Soc. Mining Geologists Japan, Special Issue 3, 206-215.

Constantinou, G. and Govett, G.J.S., 1973. Geology, geochemistry and genesis of Cyprus sulfide deposits. Economic Geology 68, 843-858.

Galley A.G. and Koski, R.A., 1999. Setting and characteristics of ophiolite-hosted volcanogenic massive sulphide deposits in Barrie, C.T., and Hannington, M.D., eds., Volcanic-Associated Massive Sulphide Deposits: Processes and Examples in Modern and Ancient Settings: Reviews in Economic Geology, v. 8, 215-236.

Güleç, N. and Erler, A., 1983. Masif sülfit yataklarındaki piritlerin karakteristik iz element içerikleri. TJK Bulletin, 26, 2, 145-152.

Gültekin, B., 2004. Sincik (Adıyaman) yöresi bakır ve altın içeren kuvars damarlarının oluşumu ve kökeni. Yüksek Lisans Tezi, Hacettepe Üniversitesi Fen Bilimleri Enstitüsü, Ankara (unpublished).

Hannington, M.D., Galley, A.G., Herzig, P.M. and Petersen, S., 1998. Comparison of the TAG mound and stockwork complex with Cyprus-type massive sulfide deposits, In: Herzig, P.M., Humphris, S.E., Miller, D.J., and Zierenberg, R.A., (eds.), 1998. Proceedings of the Ocean Drilling Program, Scientific Results 158, 389-415.

Herece, E., 2008. Doğu Anadolu Fayı (DAF) Atlası. MTA Special Issue, 13, Ankara.

Hutchinson, R.W. and Searle, D.L., 1970. Strata bound pyrite deposits in Cyprus and relations to other sulfide ores. Soc. Min. Geol. Jpn. Spec. Iss. 3, 198-205.

İmer, A., 2006, Genesis Of The Karaali (Ankara, Turkey) Fe-Cu Sulfide Mineralization, A thesis submitted to the Graduate School of Natural and Applied Sciences of the Middle East Technical University, Ankara, 175.

Jamieson, H. E. and Lydon, J. W., 1987. Geo chemistry of a fossil ore-solution aquifer: chemical exchange between rock and hydrothermal fluid recorded in the lower portion of research drill hole CY-2a, Agrokipia, Cyprus. In: Robinson, P. T., Gibson, I. L. and Panayiotou, A., (eds.), Cyprus Crustal Study Project: Initial Report, Holes CY-2 and 2a. Ottawa, Ontario, Canada, Geological Survey of Canada, 139-152.

Ketin, İ., 1966. Anadolu'nun tektonik birlikleri. Mineral Research and Expolaration Bulletin, 66, Ankara, 20-34.

Kovenko, V., 1943. Visite de la region de Pütürge, vilayet de Malatya. MTA Rep. No: 1393, Ankara.

Özçelik, M., 1985, Malatya güneydoğusundaki magmatik kayaçların jeolojisi ve tektonik ortamına jeokimyasal bir yaklaşım. TJK Bulletin, 28, 1, Ankara, 19-35.

Parlak, O., 2006. Geodynamic significance of granitoid magmatism in southeast Anatolia: Geochemical and geochronogical evidence from Göksun-Afşin (Kahramanmaraş, Turkey) region. International Journal of Earth Sciences, 95, 609-627.

————, Höck, V., Kozlu, H. and Delaloye, M., 2004. Oceanic Crust Generation in an Island Arc Tectonic Setting, SE Anatolian Orogenic Belt (Turkey). Geological Magazine, 141, 583-603.

————, Rızaoğlu, T., Bağcı U., Karaoğlan F. and Höck V., 2009. Tectonic significance of the geochemistry and petrology of ophiolites in southeast Anatolia, Turkey. Tectonophysics, 473, 1-2, 173-187.

Perinçek, D.,1978. Çelikhan- Sincik- Koçali (Adıyaman ili) alanının jeolojisi ve petrol olanaklarının araştırılması. Ph.D. Thesis, İstanbul Üniv. Fen Fak. Tatbiki Jeol. Kürsüsü, 212.

————, 1979. Geological Investigation of the Çelikhan-Sincik- Koçali Area (Adıyaman Province). İst. Üniv. Fen. Ed. Mec. Seri: B, 127-147.

———— and Kozlu, H., 1984. Stratigraphy and structural relations of the units in the Afşin – Elbistan - Doğanşehir region (Eastern Taurus). Tekeli, O. and Güncüoğlu, M.C. eds. Int. Symp. on the geology of the Taurus Belt, proceedings, 181-198.

Pişkin, Ö., 1972. Etude mineralogique de la region situee a L'Est de Çelikhan (Taurus ori-Adıyaman –Türkiye). TJK Bulletin,21/2, 107-111.

Rigo de Righi, M. and Cortesini, A., 1964. Gravity tectonics in foothills Structure belt of Southeast Turkey. Bulletin American American Association of Petroleum Geologists, v.48, 1911-1937.

Rollinson H.R., 1993. Using Geochemical Data: Evaluation, Presentation, Interpretation, Longman. UK. 352.

Sato, T., 1974. Distribution and geological setting of the kuroko deposits. Society of Mining Geologists of Japan, Special Issue 6: 1-10.

Sawkins, F.J., 1990. Metal Deposits in Relation to Plate tectonics. 2nd ed., Springer, Verlag, New York, 461p.

Sungurlu, O., 1973. VI. Bölge Gölbaşı – Gerger arasındaki sahanın jeolojisi. TPAO Report No: 80, Ankara (unpublished).

————, 1974. VI. Bölge Kuzey sahalarının jeolojisi. TPAO Report no: 871, Ankara.

Şaşmaz, A., Gülenay, G. and Sağıroğlu, A., 1999. Taşınmış Kıbrıs tipi bakır cevherleşmelerine tipik bir örnek: Derdere (Çüngüş-Diyarbakır) cevherleşmeleri. TJK Bull. 42, 1, 105-117.

Tatsumi, T., 1970. Volcanism and ore genesis. University of Tokyo Press, Tokyo, 448p.

Tolun, N., 1955. Besni, Adıyaman, Samsat arası bölgelerin jeolojik etüdü. MTA Report No: 2251, Ankara (unpublished).

Turgay, I., 1968. Adıyaman-Kahta ilçesi Sincek Nahiyesi Siltikuş Tepe Bakır Aramaları PS Etüdü. MTA Report No: 4320, Ankara (unpublished).

Türkyılmaz, B., 2004. Çelikhan-Sincik Arasında Yüzeyleyen Magmatik Kayaçların Petrografisi ve Petrolojisi, Ph. D. Thesis, Fırat Üniversitesi Fen Bilimleri Enstitüsü, Elazığ (unpublished).

Uzunçimen, S., Tekin, U.K., Bedi Y., Perincek D., Varol E. and Soycan H., 2011. Discovery of the Late Triassic (Middle Carnian–Rhaetian) radiolarians in the volcano-sedimentary sequences of the Kocali Complex, SE Turkey: Correlation with the other Tauride units. Journal of Asian Earth Science, 40, 1-4, 180-200.

Yalçın, N., 1976. Narince-Gerger (Adıyaman ili) alanının jeoloji incelemesi ve petrol olanaklarının araştırılması. Ph. D. Thesis, İ.Ü. Tatbiki Jeoloji Kürsüsü.

Yazgan, E., 1972. Etude geologique et petro graphique du complexe ophiolitique de la region situee au sud-est de Malatya (Taurus oriental, Turquie) et de sa couverture volcanosedimentaire. These no: 1575, Univ. Geneve, 236p.

———— and Asutay, H.J., 1987. Malatya Güneydoğusunun Jeolojisi ve Doğu Toroslar'ın Jeodinamik Evrimi. MTA Report No: 8272, Ankara (unpublished).

Yıldırım, E., 2010. Çelikhan-Sincik Arasında Yüzeyleyen Magmatik Kayaçların Petrografisi ve Petrolojisi. Doktora Tezi, Fırat Üni. Fen Bilimleri Ens., Elazığ, 244. (unpublished).

Yıldırım, M. and Yılmaz, Y., 1991. Güneydoğu Anadolu orojenik kuşağının ekaylı zonu. Türkiye Petrol Jeologları Derneği Bülteni, 3, 57-73.

Yıldırım, N., 2011. Ormanbaşı Tepe (Sincik-Adıyaman) Bakır Cevherleşmesinin Maden Jeolojisi Raporu. MTA Report No: 3301, Ankara (unpublished).

————, Ay, Y., Aydın, A., Yığmatepe, M., Kalı, B. and Yıldırım, E., 2008 *a*. Koçali Karmaşığı İçerisindeki Taşınmış Kıbrıs Tipi Masif-Sülfit (Cu) Cevherleşmelerine Yeni Bir Örnek, Ormanbaşı Tepe (Sincik-Adıyaman) Cevherleşmeleri. 61. TJK Abstracts.

————, Aydın, A., Ay, Y., Yığmatepe, M. and Yıldırım, E, 2008 *b*. Ormanbaşı Tepe (Sincik-Adıyaman) Cevherleşmelerinin Kıbrıs Tipi Masif-Sülfid (Cu) Cevherleşmesi Olduğuna Dair Bulgular. Prof. Dr. Servet YAMAN Maden Yatakları-Jeokimya Çalıştayı, Ç. Ü. Jeoloji Mühendisliği Bölümü (Adana).

————, ————, Yığmatepe, M., Akgül, M. and Yıldırım, E., 2009. Levha dayk karmaşığı içerisindeki Kıbrıs tipi masif sülfid cevherleşmelerine Türkiye'den bir örnek: İncekoz (Adıyaman) Cu cevherleşmesi. 62. TJK Abstracts, 220-221.

————, Ay, Y., Çakır, C., İlhan, S., Dönmez, C. and Yıldırım, E., 2010 *a*. Koçali Ofiyolitik Karmaşığı'nın Metalojenik (Cu-Au) Önemi, IV. Ulusal Jeokimya Sempozyum Bildirileri, Elazığ, 79-80.

————, İlhan, S., Akyıldız, M., Yıldırım, E., and Dönmez, C., 2010 *b*. The Importance of the Ophiolites of the Southern Branch of the Neotethys (Koçali Ophiolitic Complex), in Terms of the Cyprus type VMS Deposits. 7. Uluslararası Doğu Akdeniz Jeolojisi Sempozyumu, Çukurova Üniversitesi, Jeoloji bölümü, Adana.

Yılmaz, Y., 1990. Comparisons of young volcanic association of western and eastern Anatolia formed under a compressional regime: a review. Journal of Volcanology and Geothermal Research, 44, 69-87.

————, 1993. New evidence and model on the evolution of the southeast Anatolian orogeny. Geological Society of American Bulletin, 105, 251-271.

————, Yiğitbaş, E., Yıldırım, M. and Genç, Ş.C., 1992. Güneydoğu Anadolu metamorfik masiflerinin kökeni. Türkiye 9. Petrol Kong., Proceedings, Ankara, 296-306.

Yıldırım, Y., Yiğitbaş, E. and Genç, C. 1993. Ophiolitic and metamorphic assemblages of Southeast Anatolia and their significance in the geological evolution of the orogenic belt. Tectonics, 12, 1280–1297.

Yiğitbaş, E., Yılmaz, Y. and Genç, Ş. C., 1992. Güneydoğu Anadolu orojenik kuşağında Eosen nap yerleşmesi. Türkiye 9. Petrol Kongresi, Proceedings, 307-318.

————, Genç, Ş. C. and Yılmaz, Y., 1993. Güneydoğu Anadolu orojenik kuşağında Maden grubunun tektonik konumu ve jeolojik önemi. A. Suat Erk Sempozyumu, Bildirileri, Ankara Üniversitesi Fen Fakültesi, 251-264.